Sedimentological facies analysis of the mid-Jurassic Garn Formation in Halten Terrace area, Mid-Norway Continental Shelf

Kay Sørbø

Thesis for Master degree

in Petroleum Geology/Sedimentology

ABSTRACT

The mid-Jurassic Garn Formation in the Halten Terrace area, Mid-Norway Continental Shelf, has been studied on the basis of ~500 m of well-core samples from 9 selected wells, geophysical wireline logs from nearly 30 wide-spread wells and two selected seismic cross-sections. The aim of this sedimentological study was to improve the existing general understanding of the Garn Fm. sedimentary environment and also to assess the role of contemporaneous fault tectonics in its deposition.

The Garn Formation consists of sandstones, but varies laterally in thickness and only locally reaches >100 m. On the basis of detailed sedimentological analysis, the following facies associations are recognized as the main components of the Garn Fm.: deposits of tidal sand ridges (longitudinal tidal bars), deposits of sheltered (heavily bioturbated) and non-sheltered (little- or non-bioturbated) inter-ridge swales, deposits of shoal-water subtidal sandflats and subordinate deposits of wave-worked littoral shoals. Tidal sand-ridge deposits volumetrically predominate in the studied well-core profiles. The study thus supports the palaeogeographic notion of the mid-Jurassic Halten Terrace being a tidally-dominated seaway linking the Boreal Ocean to the north with the Tethys Ocean to the south.

The present study also supports the notion that the mid-Jurassic sedimentation in the Halten Terrace area was controlled by active extensional fault tectonics, which bathymetrically compartmentalized the area into an array of NE-trending incipient grabens and half-grabens. The resulting topographic configuration is thought to have greatly enhanced the action of tidal currents and controlled spatial sand dispersal.

The study confirms further the general notion that the Garn Formation is a transgressive succession composed of a transgressive parasequence set. The thickness and number of the vertically stacked transgressive to normal-regressive parasequences appears to vary laterally across the Halten Terrace, depending on the local fault activity. Only 3 to 5 transgressive–regressive parasequences, ~7–58 m thick, have been recognized in the main axial zone of the Halten Terrace seaway, but up to 16 thinner coeval parasequences were recognized at the outer (NW) margin of the Halten Terrace. The marginal flank of the synclinal Halten seaway was apparently much more sensitive to the interplay of bathymetric changes and pulses of lateral sand supply.

The study as a whole considerably improves our general understanding of the origin of the Garn Fm. and also bears important implications for this formation's geo-model as a petroleum reservoir.

II

TABLE OF CONTENTS

1 INTRODUCTION

This study in sedimentary geology concerns the Garn Formation (Bajocian–Bathonian) of the Middle Jurassic Fangst Group in the Halten Terrace area, Mid-Norway Continental Shelf, with a regional focus on the formation's depositional environments and possible tectonic control on its sedimentation. The Halten Terrace, as defined by Dalland et al. (1988), is a rhomboidal-shaped terrace extending between 64°N and 65°30'N as a major structural element of the Mid-Norway Continental Shelf. It is bordered by the Trøndelag Platform to the east and by the Vøring and Møre basins to the west and southwest. Well cores and geophysical wireline well-logs from the Ragnfrid, Tyrihans, Fogelberg, Åsgard/Smørbukk South, Yttergryta fields and a structure southeast of the Ragnfrid discovery (Fig. 1.1) have been used to conduct this sedimentological study. Two regional seismic cross-sections oriented W–E and NW–SE have also been interpreted to aid the results derived from the sedimentological facies analysis.
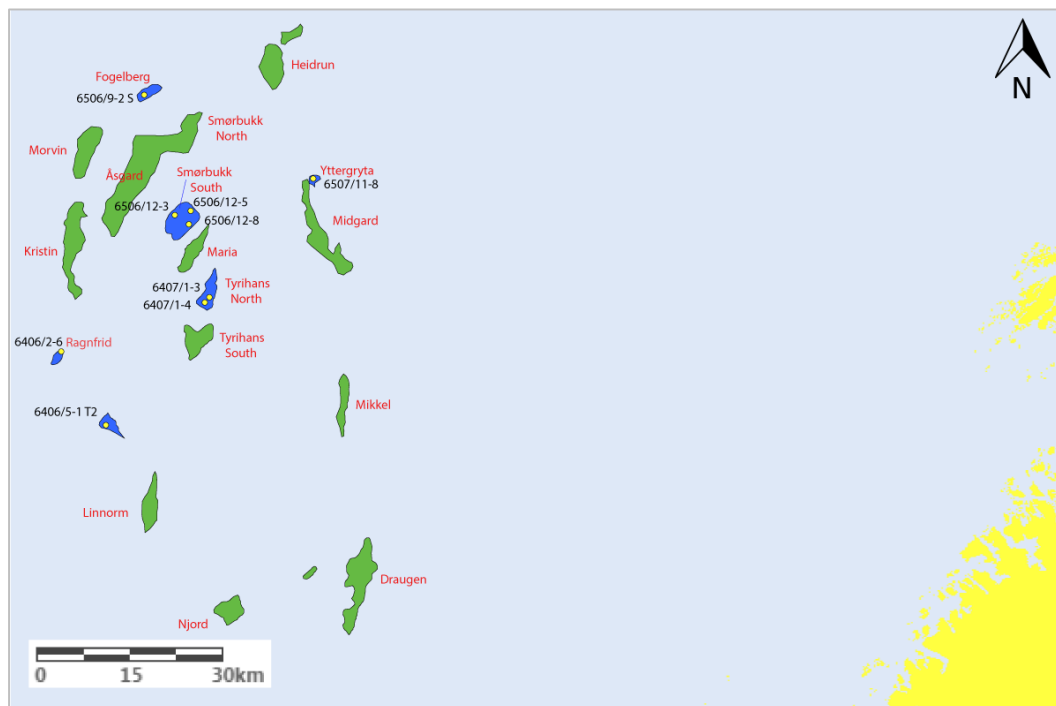
Figure 1.1: Location map of the main oil/gas fields and prospects in the Halten Terrace. The blue colour indicates fields/prospects where well cores and wireline logs have been used in this study, while green colour indicates other major fields/prospects. The yellow colour on the right indicates the Norwegian shoreline. Modified from NPD (2017).

The Halten Terrace is a highly block-faulted structural element, bounded to the east and northeast by the Vingleia and Bremstein fault complexes and to the west and southwest by the Klakk Fault Complex. Main petroleum reservoirs in the Halten Terrace (Fig. 1.1) are in the Early to Middle Jurassic siliciclastic succession deposited in sedimentary environments ranging

from fluvial/paralic to shallow marine (Dalland et al., 1988; Swiecicki et al., 1998), within a narrow epicontinental Jurassic seaway linking the Boreal Ocean to the north with the Tethyan Ocean to the south (Doré, 1991, 1992).

The Garn Formation is a thick (>100 m) sandstone succession that contains hydrocarbons in several fields and is an attractive regional exploration target (Koch and Heum, 1995). The sandstones have been studied by many authors, including Gjelberg et al. (1987), Dalland et al. (1988), Ehrenberg et al. (1992, 1998), Corfield and Sharp (2000), Chuhan et al. (2001), Corfield et al. (2001), Elfenbein et al. (2005), Marsh et al. (2010), Quin et al. (2010), Bell et al. (2014) and Messina et al. (2014). These deposits have long been recognized to be of shallow-marine origin, but the exact nature of their sedimentary environment is rather controversial. Over a quarter century (1987–2001), the sandstones were interpreted to represent fluvio-deltaic and shoreface environments – an opinion summarized also in the benchmark volume edited by Ramberg et al. (2013). However, a major role of tidal currents in the deposition of the Garn Fm. has been increasingly postulated in more recent publications (Corfield et al., 2001; Elfenbein et al., 2005; Quin et al., 2010; Messina et al., 2014). As pointed out and discussed by Messina et al. (2014) with respect to the Kristin Field, a tidal palaeoenvironmental interpretation would mean a different understanding of the geometry, facies architecture and primary heterogeneity of sandstone bodies – with major further implications for reservoir geo-models.

Another contentious issue is the impact of syndepositional tectonics on the spatial development and thickness distribution of the Garn Formation. Syndepositional fault activity has been recognized or postulated in several local, field-scale studies (e.g., Gjelberg et al., 1987; Dalland et al., 1988; Corfield and Sharp, 2000; Brekke et al., 2001; Quin et al., 2010; Messina et al., 2014). Messina et al. (2014) have suggested that the Halten Terrace at the time of the Garn Fm. sedimentation probably consisted of a complex array of NE-trending incipient grabens and half-grabens, whose bathymetric and structural configuration would have considerably enhanced the action of tidal currents and control of spatial sand dispersal.

The aim of the present study is to address these two crucial issues on a broader regional scale by contributing to a better understanding of the sedimentary environment of the Garn Fm. and by assessing whether the deposition of this sandstone formation was indeed governed by contemporaneous fault-block tectonics of the Halten Terrace.

2 GEOLOGICAL SETTING

2.1 Study area

The study area for the present thesis is the Halten Terrace (Haltenbanken), located between 64°N and 65°30'N on the Mid-Norway Continental Shelf (Fig. 2.1). Together with the Trøndelag Platform to the east, it forms the eastern margin of the Vøring Basin (Bell et al., 2014). It is regarded as the most prolific hydrocarbon province in offshore mid-Norway, with more than a dozen gas and oil fields in the Early to Middle Jurassic siliciclastic sedimentary rocks (Spencer et al., 1993; Koch and Heum, 1995). These reservoir rocks were deposited in sedimentary environments ranging from fluvial/paralic to shallow marine (Dalland et al., 1988; Swiecicki et al., 1998), within a narrow epicontinental Jurassic seaway separating the Boreal and Tethyan oceans (Doré, 1991, 1992).
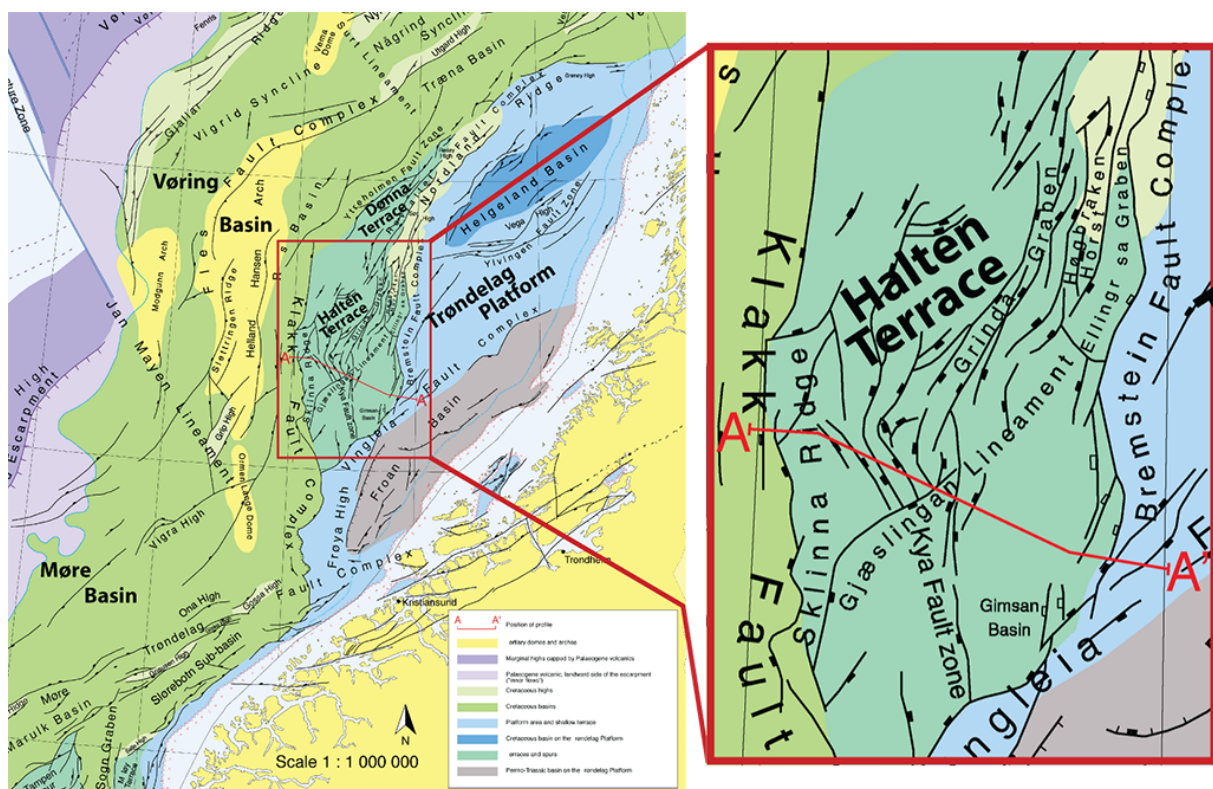
Figure 2.1: Structural elements of Mid-Norway Continental Shelf. Geological profile A–A' is shown in Fig. 2.2. Modified from Blystad et al. (1995).

The Halten Terrace is a highly block-faulted terrace (Bell et al., 2014) bounded to the east and northeast by the Vingleia and Bremstein fault complexes, which separate the terrace from the largely unfaulted Trøndelag Platform, and to the west and southwest by the Klakk Fault Complex separating the terrace from the deep Vøring and Møre basins (Figs. 2.1 and 2.2). The

Halten Terrace has a rhombic shape, which is due to a complex pattern of normal faults of different ages, with the two dominating trends as N–S and NNE–SSW (Blystad et al., 1995). The terrace is about 80 km wide and 130 km long, with an area of around 10,400 km^2 (Blystad et al., 1995; Marsh et al., 2010). The eastern part of the terrace is dominated by large, gently tilted fault blocks, whereas the western part is dominated by smaller and more rotated fault blocks (Koch and Heum, 1995). The Dønna Terrace is the continuation of the Halten Terrace to the north and is separated from the Trøndelag Platform by the Nordland Ridge (Fig. 2.1).
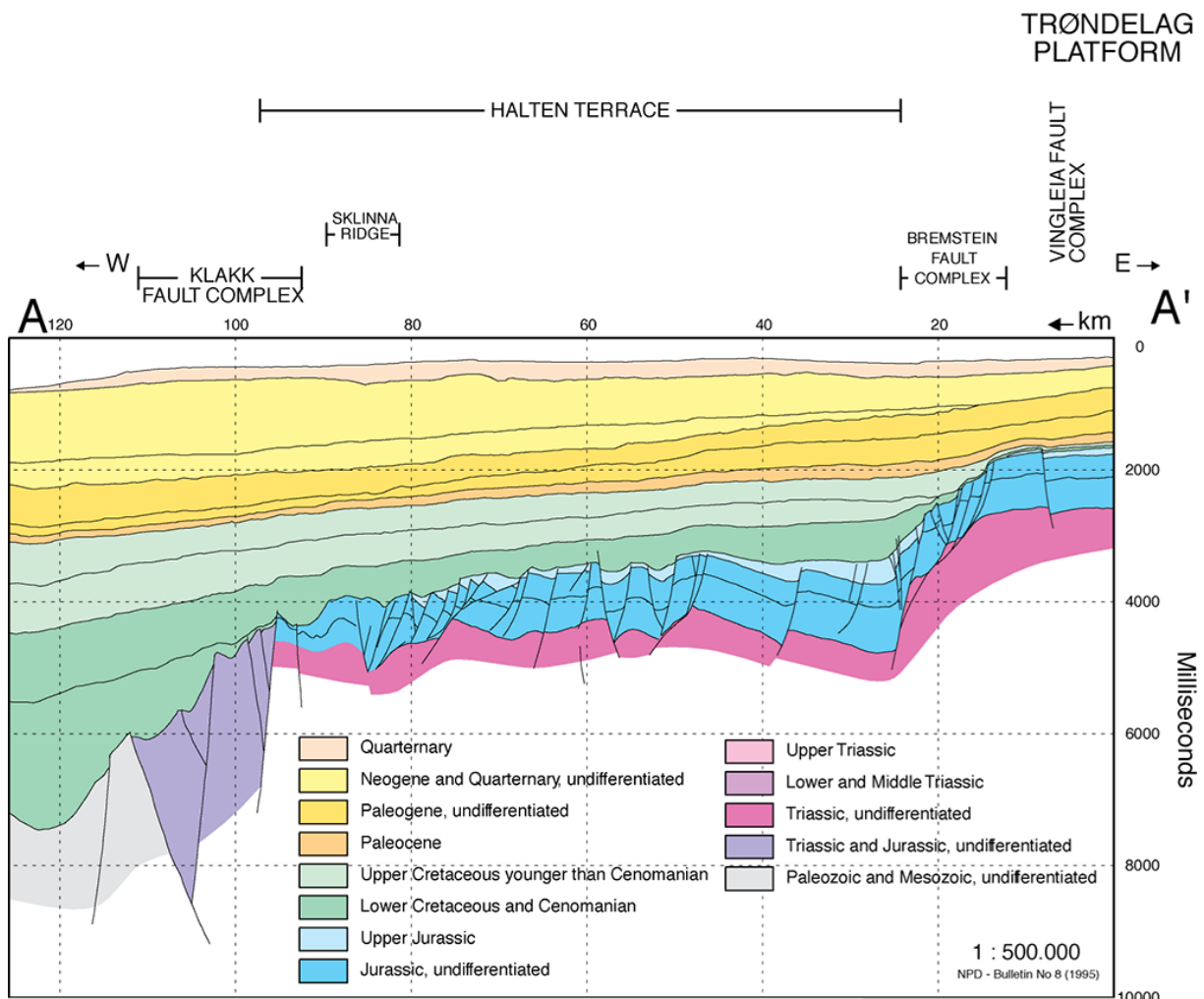
Figure 2.2: Geological profile through Halten Terrace area. Note the highly block-faulted nature of the Halten Terrace. The transect line A–A' is indicated in the map in Fig. 2.1. Modified from Blystad et al. (1995).

The Jurassic deposits, particularly the mid-Jurassic sandy Garn Formation as the focus of this study, are present in all parts of the terrace except for the western part of the Sklinna Ridge along the Klakk Fault Complex, where the Jurassic is eroded and older strata generally dip steeply towards the east (Fig. 2.2; Blystad et al., 1995). The following review sub-chapter gives a brief tectonic history of the area that evolved into the present-day Mid-Norway Continental

Shelf, with a focus on the tectonic and stratigraphic development that took place prior to the Palaeogene continental breakup of Baltica and Laurentia and the opening of North Atlantic.

2.2 Regional tectonic development

Palaeozoic

Located in the Norwegian Sea area, the Halten Terrace is part of a long and complex tectonic history starting with the closure of the Iapetus Ocean and culmination of the Caledonian orogeny in the Late Silurian to Early Devonian and the subsequent initiation of the orogen extensional collapse (Swiecicki et al., 1998; Braathen et al., 2002; Skilbrei et al., 2002). Complex sinistral fault movements occurred along the axis of the Arctic–North Atlantic Caledonides in the Mid-Devonian to Early Carboniferous (Bukovics et al., 1984; Swiecicki et al., 1998) because the plate collision was transpressional, rather than head-on in style. This movement therefore weakened a broad zone of the crust in the orogen, creating deep fractures that were later reactivated when wrenching ceased and was replaced by crustal extension in the Norwegian–Greenland Sea rift system in the Late Carboniferous (Bukovics et al., 1984). In the period of earliest Carboniferous to Late Permian, the region of the present-day North Atlantic was in the northern part of the Pangean supercontinent (Brekke et al., 2001). The extensional forces that started to act in the Mid-Devonian to Early Carboniferous would eventually lead to the opening of the Norwegian–Greenland Sea segment of the North Atlantic around the Palaeocene–Eocene transition (Doré et al., 1999).

According to Marsh et al. (2010), five regional episodes of tectonic extension had influenced the structural development of the Halten Terrace. These rifting events occurred in the Early to Middle Devonian, Carboniferous, Late Permian to Early Triassic, late Middle Jurassic to Early Cretaceous and Late Cretaceous to Early Eocene. However, other authors (e.g., Brekke et al., 2001) consider only three main rifting episodes for the tectonic evolution of the Norwegian Continental Shelf, which occurred from Early Carboniferous to Middle Triassic, Middle Jurassic to Early Cretaceous and Late Cretaceous to Early Palaeogene.

The initiation of rifting in Carboniferous is evidenced by the great thicknesses of sediment, including the Early Permian red conglomerates, that accumulated in large half-grabens in East Greenland (Surlyk, 1990). However, there is no similar compelling evidence on the Mid-Norway Continental Shelf, although the presence of clastic Upper Palaeozoic rocks was inferred in the early studies of the Trøndelag Platform (Ziegler, 1988).

Triassic

At the beginning of Triassic, Norway was located in the sub-tropical zone between 25°N and 40°N (Nøttvedt et al., 2008). At this time, Norway and Greenland were separated by a low-lying basinal area around 300–500 km in length (Ramberg et al., 2013). The Triassic deposits in the present-day Norwegian Sea and East Greenland represent mainly continental alluvial environments with short-lived marine incursions from the north (Brekke et al., 2001). Syndepositional rift and strike-slip tectonics governed the accumulation of Triassic deposits in this basin (Ziegler, 1988). The area between Norway and Greenland was affected by thermal subsidence and accelerated crustal extension with a SW–NE rift trend (Bukovics et al., 1984; Ziegler, 1988; Martinius et al., 2001). The Late Permian to Early Triassic rifting event produced large rotational fault blocks in the Norwegian Sea basin, and the rift system eventually propagated southwards into the North Sea region where the Viking and Central grabens were formed (Ziegler, 1988). The Late Permian to Early Triassic rift episode marks the onset of the break-up of the Pangean supercontinent (Brekke et al., 2001).

According to Marsh et al. (2010), there is currently little consensus as to the possible duration and extent of Permo–Triassic rifting on the Halten Terrace. The rifting is most evident in onshore East Greenland, where a major phase of normal faulting ended in the Middle Permian and subsequent rotational block faulting occurred in the Early Triassic (Surlyk, 1990; Seidler et al., 2004).

By the Late Triassic, Norway and the whole NW Europe came into the temperate climate zone (Ramberg et al., 2013), with the mid-Norway area located at approximately 45°N (Torsvik et al., 2002). Except for some minor uplifts and faulting along the Nordland Ridge and Frøya High, relative tectonic quiescence prevailed from the earliest Middle Triassic (Nøttvedt et al., 2008) until the Late Triassic (Ehrenberg et al., 1992). The bounding fault zones of the Halten Terrace might have started developing already at this stage (Gabrielsen and Robinson, 1984) and syndepositional Triassic faulting has also been documented in the Trøndelag Platform (Bukovics et al., 1984).

Early Jurassic

A change in rift tectonics associated with incipient ocean-floor spreading in the Tethys to the southeast and in the proto-central Atlantic to the southwest occurred at the Triassic–Jurassic transition (Doré et al., 1999). Contemporaneous with the change in rift tectonics was a continuous sea-level rise through the Jurassic, leading to the development of a permanent

seaway between Greenland and Norway, connecting the Boreal Sea in the north with the Tethys Ocean in the south (Nøttvedt et al., 2008).

The post-Triassic structural evolution in the northern part of the Halten Terrace was highly influenced by a thick succession of Triassic salts, which resulted in development of a complex range of fault and halokinetic structures (Pascoe et al., 1999; Corfield and Sharp, 2000; Marsh et al., 2010; Elliott et al., 2012). However, the Triassic salts were thin and little mobile in the southern part of the Halten Terrace, where basement-involving faults dominated the structural style of tectonic deformation and thereby resulted in the formation of a large, east-dipping half-graben (Bell et al., 2014).

Middle Jurassic

By the Middle Jurassic, Norway had drifted to between 45°N and 60°N, but a change in the pole of rotation caused it to rotate slightly southwards, to between 40°N and 55°N (Nøttvedt et al., 2008). The rifting phase that commenced in the Middle Jurassic and extended into Early Cretaceous affected the interior parts of the Trøndelag Platform, which became subject to minor faulting by partial reactivation of older faults in the Vingleia Fault Complex and to a more intense rifting activity initiated along the platform edges in the future terrace areas of Halten and Dønna (Brekke, 2000).
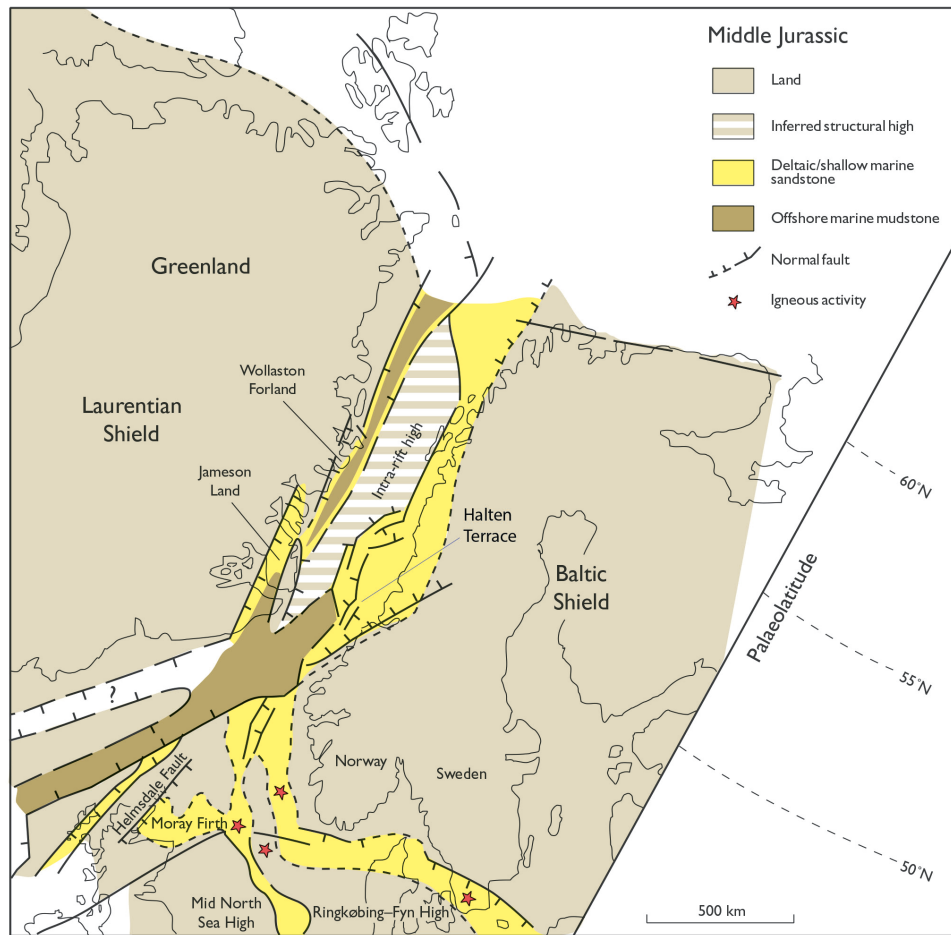
Figure 2.3: Middle Jurassic schematic pre-drift reconstruction of the seaway between Norway and Greenland. Note the narrow seaways that existed on both sides of the inferred intra-rift high which likely contributed to supply of sediments to the Mid-Jurassic basins. Slightly modified from Surlyk (2003).

The Garn Formation is part of the Middle Jurassic Fangst Group that was deposited during the late Toarcian to early Bathonian. Evidence presented by Ehrenberg et al. (1998) might indicate that a large landmass west of the Halten Terrace was supplying sediment to the basin through most of the Jurassic. The source of local clastic supply might have been the leading edges of some of the major fault blocks that became uplifted by syndepositional faulting (Bukovics and Ziegler, 1985) or thermal doming of the Møre and Vøring areas, creating a western hinterland as postulated by Brekke et al. (2001). The basin of the Jameson Land area in East Greenland, which co-existed in the Early to Middle Jurassic, also shows evidence of sediment supply from the east and north (Surlyk, 1990), which supports the notion of an emergent landmass between Norway and Greenland (Fig. 2.3). Although Ehrenberg et al. (1992) have suggested a nearly total tectonic quiescence in the Halten Terrace area at that time, there is evidence of active rifting in East Greenland from the late Bajocian (Price and Whitham, 1997), and similar activity

in the Halten Terrace area has been inferred by Pedersen et al. (1989) for the Toarcian and confirmed by Corfield et al. (2001) for the time from early Bajocian onwards.

Late Jurassic

The rifting episode continued through the Late Jurassic, when faulting made the Halten and Dønna terraces evolve into individual structural elements. However, the terraces stayed close to the same elevation as the Trøndelag Platform to the east, relative to the basins to the west, throughout the Mid-Jurassic to Early Cretaceous rifting phase (Brekke, 2000). The Halten Terrace became subject to both E–W and NW–SE tectonic extension, which resulted in the formation of a conjugate system of normal faults trending NE–SW and NW–SE, in addition to the dominant faults trending N–S (Koch and Heum, 1995). A result of this faulting in the Late Jurassic was an expanded Upper Jurassic succession along the Vingleia, Bremstein and Revfallet fault complexes at the eastern margin of the terraces (Figs. 2.1 and 2.2; Brekke, 2000). Active rifting from the Late Jurassic to Early Cretaceous has been documented across the rift in East Greenland (Surlyk, 1990) and in the Mid-Norway Shelf (Swiecicki et al., 1998; Doré et al., 1999).

Cretaceous to Pliocene

In the Early Cretaceous, Norway was located approximately between 45°N and 60°N (Torsvik et al., 2002). During this time rifting in the Mid-Norway Shelf transferred from the Halten and Dønna terraces out into the Møre and Vøring basins to the west (Fig. 2.1; Nøttvedt et al., 2008). The rifts in the basins subsided rapidly while their flanks remained generally high (Bukovics and Ziegler, 1985). That an onset of sea-floor spreading in the North Atlantic was imminent can be seen from the fact that the crystalline crust in these basins was reduced by 20–25 % from its original thickness, leaving it only a few kilometres thick (Brekke, 2000; Skogseid et al., 2000).

Several rifting events during Early Cretaceous have been identified in East Greenland (Whitham et al., 1999), but are less well documented in the Mid-Norway Shelf. The final separation of the Halten and Dønna terraces from the Trøndelag platform occurred in two rifting phases of subsidence: one in the Early Cretaceous and another in post-Cenomanian time, which is evident from the expansion of the Cretaceous succession across the Vingleia, Bremstein and Revfallet fault complexes that stretch along the boundary between the terraces and the platform (Brekke, 2000). The Late Cretaceous (post-Cenomanian) rifting was apparently more pronounced (Brekke et al., 1999).

The onset of volcanic activity and seafloor spreading due to the opening of the North-East Atlantic Ocean at the Palaeocene/Eocene transition marked the culmination of a ca. 340 Ma history of complex extensional tectonics and sedimentary basin formation that started with the extensional collapse of the Caledonian orogen in the Late Silurian to Devonian time (Doré et al., 1999; Braathen et al., 2002; Skilbrei et al., 2002).

2.3 The Halten Terrace Jurassic stratigraphy

The Jurassic stratigraphy of the Mid-Norway Continental Shelf comprises the Early Jurassic Båt Group, Middle Jurassic Fangst Group and Middle to Late Jurassic Viking Group (Fig. 2.4; Dalland et al., 1988). Each group is subdivided into formations, where the Båt Group in ascending order consists of the Åre, Tilje, Ror and Tofte formations; the Fangst Group consists of the Ile, Not and Garn formations; and the Viking Group consists of the Melke, Rogn and Spekk formations.

The continuation of the northward drift of Baltica during Late Triassic led to an increasingly humid climate that brought about the change from 'red-beds' to 'grey-beds' sedimentary conditions (Swiecicki et al., 1998) and initiated an environmental trend that culminated in the deposition of the paralic, coal-bearing sediments of the Early Jurassic Åre Formation (Dalland et al., 1988). The Hettangian to early Pliensbachian Åre Fm. (Fig. 2.4) is composed of a series of sandstones, mudstones and coals interpreted to have been deposited in a fluvial to deltaic environment (Dalland et al., 1988). In terms of its facies, the Åre Fm. is divided into two informal units (Svela, 2001). The lower unit is entirely non-marine and consists of fluvial to lower delta-plain sediments with thick coal-bearing floodplain deposits. The upper unit is considered to have been deposited in coastal plain and delta-plain environments, but later in a marginal marine setting (Kjærefjord, 1999).
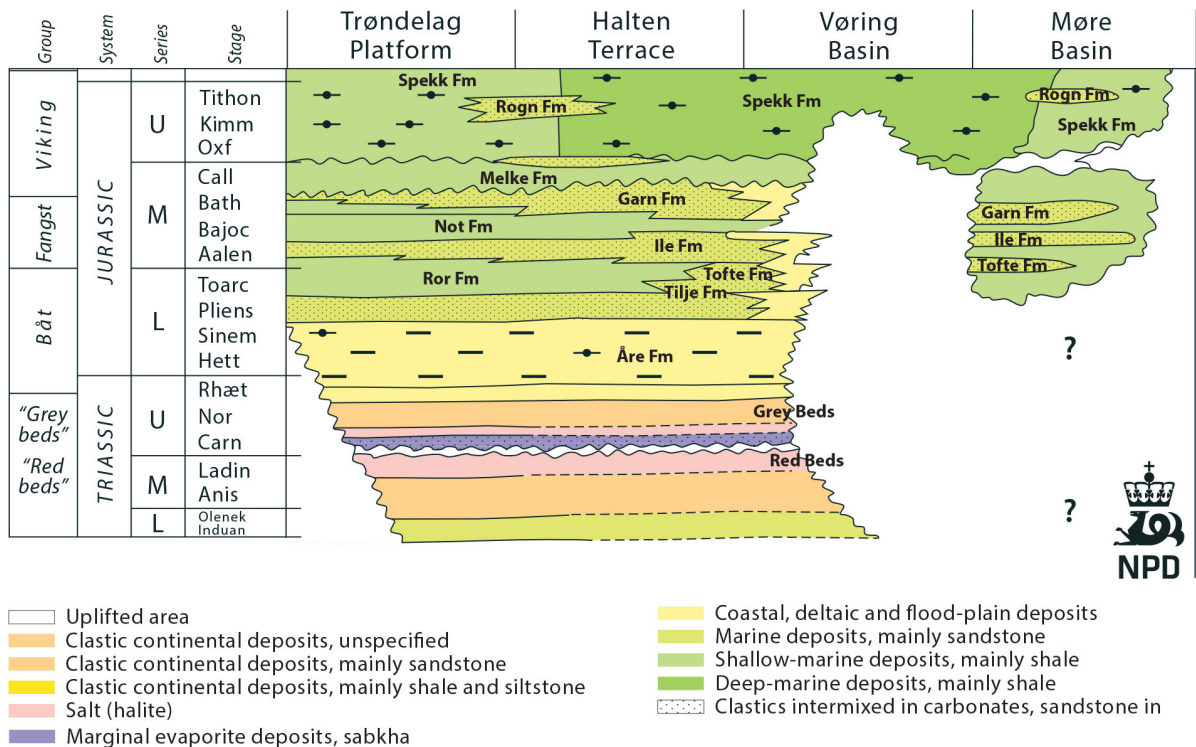
Figure 2.4: Lithostratigraphic chart of the Triassic and Jurassic of the Norwegian Sea. Slightly modified from NPD (2014).

The Åre Formation is overlain by the Tilje Formation of late Pliensbachian to early Toarcian age (Fig. 2.4). This formation is highly heterolithic, composed of thinly interbedded mudstones, siltstones and fine-grained sandstones interpreted to have been deposited in a deltaic to shallow marine setting (Dalland et al., 1988), possibly with tidal influences (Koch and Heum, 1995). Detailed study of the Tilje Fm. in the Heidrun and Smørbukk fields by Martinius et al. (2001) indicates that the formation consists of a lower estuarine unit and an upper tide- and wave-dominated deltaic unit.

The overlying Ror Formation of Toarcian age (Fig. 2.4) consists of open-marine shelf deposits comprising heterolithic sandy mudstones with coarsening-upwards sandier units (Dalland et al., 1988) and with local intercalations of the westerly deltaic sandstone wedges of the Tofte Formation. The coeval Tofte Fm. of Toarcian age (Fig. 2.4) is interpreted to be a local fan delta with a western sediment supply (Koch and Heum, 1995).

These deposits are overlain by the Ile Formation of Aalenian age (Fig. 2.4). It consists of fine- to medium-grained and subordinate coarse-grained sandstones with interbeds of thinly laminated siltstones and shales (Dalland et al., 1988). The Ile Fm. represents mainly tidal-channel and tidal-flat environments, but has also been interpreted as a tide-dominated deltaic complex in the Kristin Field (McIlroy, 2004a). The Ile Fm. would then appear to have recorded

11

the beginning of the Mid-Jurassic predominance of tidal sedimentation in the Halten Terrace area, which probably acted as a narrow seaway between the Boreal and Tethys provinces.

The overlying Not Formation of Aalenian to Bajocian age (Fig. 2.4) consists of mudshales that coarsen upwards into sandstones (Dalland et al., 1988). The formation is divided into two units: the muddy lower unit represents a semi-regional transgression that led to the development of lagoons or sheltered bays, whereas the sandy upper unit represents normal-regressive progradation of a deltaic or wave/tide-dominated shoreline system from the west (Dalland et al., 1988).

The Garn Formation lying above (Fig. 2.4) is of Bajocian to Bathonian age and consists mainly of medium- to coarse-grained sandstones with subordinate intercalations of coarse- to very coarse-grained sandstones (Gjelberg et al., 1987; Dalland et al., 1988; Chuhan et al., 2001). This formation is considered to represent a wave-influenced tidal environment (e.g., Quin et al., 2010; Messina et al., 2014) and its characteristics and previous studies are reviewed in more detail in the next sub-chapter 2.4.

The overlying Melke Formation of Bajocian to Oxfordian age (Fig. 2.4) consists of heterolithic sublittoral deposits and bioturbated neritic mudstones (Dalland et al., 1988). The formation is considered to represent distal shoreface and muddy offshore environments (Corfield et al., 2001). This formation is a stratigraphic time-equivalent of the Garn Fm. eastwards in the Trøndelag Platform area (Brekke et al., 2001), and is time-transgressively onlapping the Garn Fm. westwards in the Halten Terrace area (Gjelberg et al., 1987, Corfield et al., 2001; Messina et al. 2014).

The mud-dominated Melke Formation is the lowest unit of the Viking Group (Fig. 2.4) and marks the beginning of the tectonic collapse and submergence of the western hinterland in the late Middle Jurassic (Brekke et al., 2001). The rifting event that followed in the Late Jurassic combined with an eustatic sea-level rise resulted in a major palaeogeographic change that established neritic sedimentation on the Trøndelag Platform and developed an anoxic, deep neritic to bathyal environment on the Halten Terrace and farther to the west in the axial zone of the future continental break-up (Brekke et al., 2001). This phase of sedimentation was recorded by the Spekk Formation of Oxfordian to Berriasian age, which is the upper unit of the Viking Group (Fig. 2.4; Dalland et al., 1988). The Rogn Formation of Oxfordian to Kimmeridgian age (Fig. 2.4) consists of mudstones and siltstones coarsening upwards into sandstones (Dalland et al., 1988). These localized sandy bodies are coeval with the muddy Spekk Fm. (Fig. 2.4) and are probably related to deltas.

2.4 The Garn Formation

The Garn Formation (Bajocian–Bathonian) is found in most of the central parts of the Halten and Dønna terraces and in the Trøndelag Platform. The formation's thickness ranges from 31 m to 104 m in the wells used for the present study, but is known to exceed 104 m in thickness in some areas of the Halten Terrace (Dalland et al., 1988). The Garn Fm. was eroded over some structural highs, such as the Nordland Ridge that separates the Dønna Terrace and Trøndelag Platform and the Sklinna High at the western margin of the Halten Terrace (Dalland et al., 1988).

The Garn Formation (Bajocian–Bathonian) is a time-equivalent to parts of the Brent Group in the North Sea (Helland-Hansen et al., 1992) and consists of medium- to coarse-grained, moderately to well-sorted subarkosic arenites with subordinate intercalations of very coarse sandstones (Dalland et al., 1988). Gjelberg et al. (1987) had characterized the Garn Fm. (referred to as the Upper Tomma Formation at that time) in terms of four lithofacies: (1) some seemingly massive or poorly stratified, medium- to very coarse-grained sandstones; (2) stratified medium- to very coarse-grained sandstones with either trough or planar cross-stratification; (3) heterolithic deposits dominated by poorly sorted medium- to coarse-grained sandstones; and (4) bioturbated muddy to silty fine-grained sandstones and sandy to silty mudstones. The present regional study concurs with the notion of a predominance of sandstone facies, while also showing that any sand-mud heterolithic facies are lacking in the studied well cores and hence must be very local, of minor significance.

Several different palaeoenvironmental interpretations have been suggested for the Garn Formation. Gjelberg et al. (1987) suggested a shoreface environment influenced by tidal and high-energy wave processes, whereas Dalland et al. (1988) interpreted the sedimentary environment to be progradational delta lobes influenced by fluvial and wave processes. Subsequent studies have interpreted the palaeoenvironment mainly as a high-energy, wave-dominated shoreface system with more mud deposition towards the north and south (Doré, 1992; Brekke et al., 2001), while a prevalent role of tidal currents has been increasingly postulated with the recognition of tidal dunes and tidal sand ridges (Corfield et al., 2001; Elfenbein et al., 2005; Quin et al., 2010; Messina et al., 2014). A comprehensive model for the primary heterogeneity of the Garn Fm. in the Kristin Field has been developed by Messina et al. (2014).

The latest interpretations (see references above) envisaged a shoreface system prograding eastwards from an intra-rift high (Fig. 2.3) and supplying sand to the Halten Terrace narrow graben-hosted seaway dominated by tidal currents. Corfield et al. (2001) postulated a

three-stage deposition of the Garn Fm.: (1) an early Bajocian forced regression followed by lowstand sand deposition; (2) transgression with a back-stepping of littoral environment onto adjacent structural highs and with episodes of "pulsed progradation" of littoral sands; and (3) a final stage of drowning, when the littoral sands of the Garn Fm. retreated towards the highs in the early Bathonian and became covered by neritic mud of the Melke Fm.

Corfield et al. (2001) in the Smørbukk Field and Messina et al. (2014) in the Kristin Field have recognized a sharp and apparently erosional contact between the mud-dominated Not Fm. and the overlying sand-dominated Garn Fm. A similar contact is observed in wells 6506/12-3 and 6506/12-8 in the Smørbukk South Field (present study) where the Not/Garn boundary was cored. However, Corfield et al. (2001) have also reported that some other wells in the Smørbukk Field (wells 6406/2-3, 6406/3-2, 6407/4-1 and 6407/6-3) show a more gradational transition from the Not Fm. to the Garn Fm., which they attributed to a relatively conformable advance of a sandy shoreface over a muddy offshore environment.

The upper boundary of the Garn Formation shows a marked regional diachroneity, with the littoral sands of the Garn Fm. interfingering with and onlapped by the heterolithic to muddy deposits of the Melke Fm. This facies diachroneity was first recognized on a regional scale by Gjelberg et al. (1987) and has later been documented to occur on a local scale of 5–10 km by Corfield et al. (2001) and Messina et al. (2014).

3 METHODS AND TERMINOLOGY

3.1 The wells used

The present study is based on cores and geophysical logs from nine wells scattered across the Halten Terrace (Fig. 3.1). Most of the Garn Formation (>81%) was cored and recovered in wells 6407/1-3, 6506/12-3, 6506/12-5, 6506/12-8, whereas only around half of it (29–65%) was cored in wells 6406/2-6, 6406/5-1 T2, 6407/1-4, 6506/9-2 S and 6507/11-8 (Table 3.1). A total of ~500 m of cores have been logged for this study. Their detailed sedimentological logging was conducted by the author at the Weatherford Laboratories in Sandnes, Stavanger.
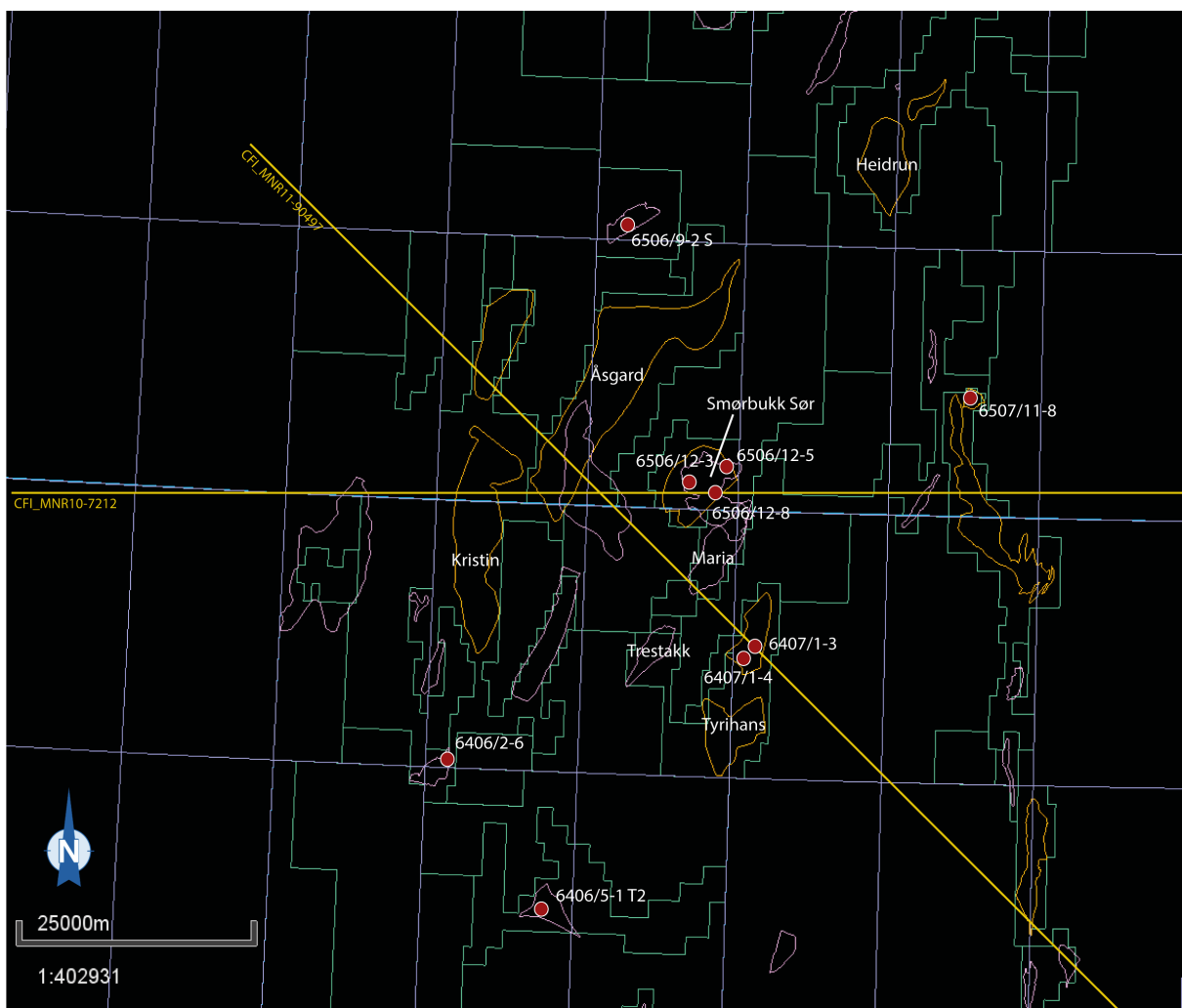

Figure 3.1: Map showing the location of wells used in present study (red points with code numbers), the two seismic lines (approximate location, in yellow) and the oil/gas fields in the Halten Terrace area (outlined in orange and purple, only some labelled). The map was generated in Petrel 2015.7.

The wells (Table 3.1) have been selected to represent both a broad area of the Garn Fm. distribution in the Halten Terrace (Fig. 3.1) and the observed range of gamma-ray log signatures of this formation (Fig. 3.2). The former criterion was to allow a regional-scale facies analysis of the Garn Fm., whereas the latter criterion was to investigate if different gamma-ray log signatures can possibly be correlated with specific sedimentary facies recognized in well cores. Both widely- and closely-spaced wells have been selected (Fig. 3.1) in order to assess the distance scale of lateral facies changes within the formation. The selection was necessarily limited by the time and budgetary constraints of present study and by the ownership of different wells in the Halten Terrace.

Table 3.1: List of cored wells used in the present study (see location in Fig. 3.1). The information given includes the name of field/prospect, the well code, the well core numbers, the cored local depth of the Garn Fm., the core thickness, the total local thickness of Garn Fm. and the thickness percentage cored in each well.

| Field/Prospect	Well	Core #	Cored depth interval in Garn Fm. (m)	Core thickness (m)	Total thickness of Garn Fm. (m)	Percentage cored (%)
Ragnfrid	6406/2-6	1	4504–4530.7	26.7	93	29
Structure south of Ragnfrid	6406/5-1 T2	1	4230–4254.4	24.4	67	36
Tyrihans/ Tyrihans North	6407/1-3	1–5	3619–3710.4	91.4	104	88
Tyrihans/ Tyrihans North	6407/1-4	2–3	3679–3739	60	101	59
Fogelberg	6506/9-2 S	1	4342–4368.7	26.7	60	45
Åsgard/ Smørbukk South	6506/12-3	1–5	3836–3906	70	86	81
Åsgard/ Smørbukk South	6506/12-5	7–11	3951–4040	89	92	97
Åsgard/ Smørbukk South	6506/12-8	2–4	3878–3955	77	81	95
Yttergryta	6507/11-8	1	2428–2448	20	31	65
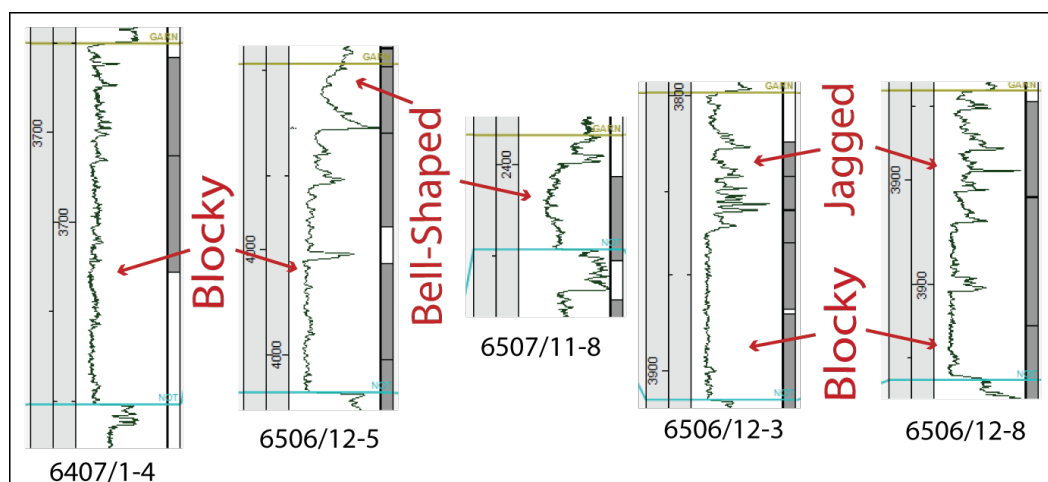
Figure 3.2: The varieties of gamma-ray log signature recognized in the Garn Fm. (examples from wells 6407/1-4, 6506/12-5, 6507/11-8, 6506/12-3 and 6506/12-8). The characteristic signatures are blocky, bell-shaped and jagged. The blue and green lines indicate the formation's base and top, respectively.

16

Several tens of wells have been drilled through the Garn Formation in Halten Terrace area over the decades of exploration, but most of them with little or no core samples and with only standard geophysical well-logs. The present project's initial hope was that the geophysical well-log signatures could possibly be translated into particular sedimentary facies on the basis of well-core samples, but this expectation appeared to be futile, apparently due to the high and greatly varied burial depths of the Garn Fm. (Table 3.1) and the variable prevalent impact of sediment diagenesis.

3.2 Well-core logging and facies analysis

Conventional detailed sedimentological logging was done, at a scale of 1:20, on the basis of B-cut core samples. The focus was on grain size, sediment colour, sedimentary structures (primary and secondary), bounding surfaces, bioturbation and organic detritus. The core logs (shown in Appendix) were first drafted by hand on standard A3 logging sheets (millimetre paper) and were subsequently digitised for display by using Adobe Illustrator CS6.

The descriptive sedimentological terminology used in this thesis is according to Harms et al. (1975, 1982) and Collinson et al. (2006), with the terms strata/laminae *set* and *co-set* as originally defined by McKee and Weir (1953). The term *sedimentary facies* refers to the basic types of sedimentary deposits that are distinguished on the basis of their bulk macroscopic characteristics, such as grain size/texture, stratification type, colour, etc., and are attributed to different modes of sediment deposition (Harms et al., 1975; Walker, 1984a). Assemblages of spatially and genetically related facies are referred to as *facies associations* and interpreted in terms of different sedimentary systems, or depositional palaeoenvironments (Collinson, 1969). The terms *parasequence* and *parasequence set* are as defined by Van Wagoner et al. (1990).

3.3 Seismic data

No seismic maps and only two seismic sections (see lines CFI_MNR10-7212 and CFI_MNR11-90497 in Fig. 3.1) were made available by Total Norge A.S. for the present study. The former seismic line is oriented W–E and transects well 6506/12-8, whereas the latter line is oriented NW–SE and transects wells 6407/1-3 and 6407/6-4 (Fig. 3.1). The purpose of this limited seismic dataset was basically to assess – on a broader regional scale – if the deposition of the Garn Fm. was truly influenced by coeval fault-block tectonic activity, as postulated earlier by local, field-scale studies (e.g., Gjelberg et al., 1987; Dalland et al., 1988; Brekke et al., 2001; Quin et al., 2010; Messina et al., 2014).

The seismic data in this study have a normal polarity, based on the strong reflector of the seabed (Fig. 3.3). This reference reflector is due to the acoustic impedance contrast between the seawater and the seabed deposits. The seismic sections were measured in time scale and are not time–depth converted. They were interpreted in this study with the use of Schlumberger's software Petrel 2015.7.
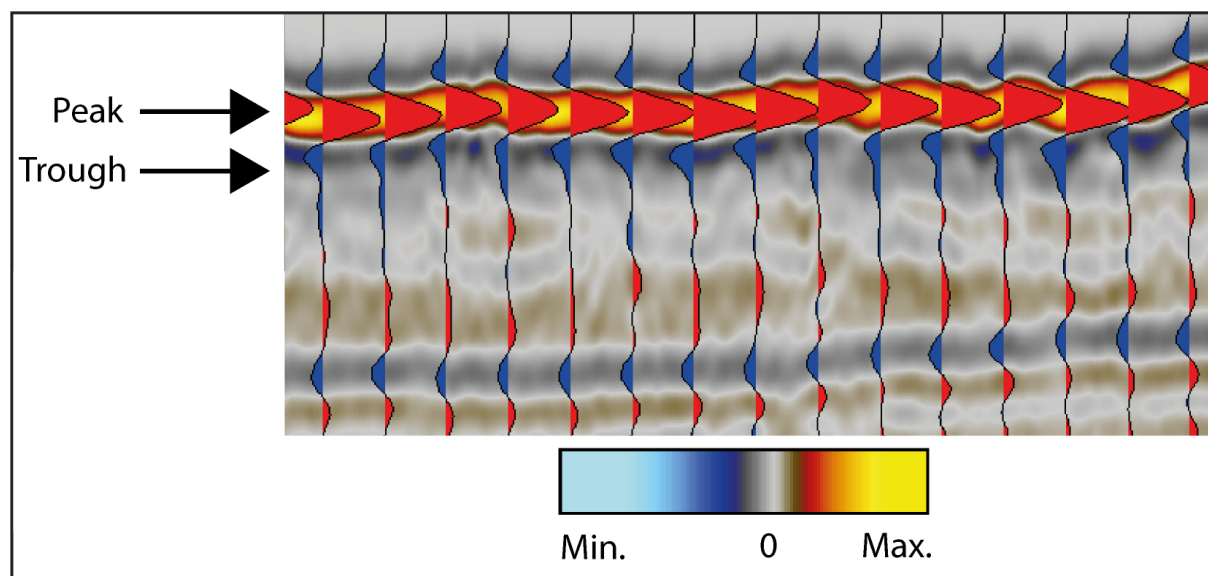

Figure 3.3: Example portion of seismic image showing normal polarity of reflectors. The uppermost red-highlighted peak represents the seabed surface. The colour scale of reflector amplitude shows the maximum amplitude in yellow and the minimum amplitude in light blue. Amplitude peaks are highlighted in red and amplitude troughs in dark blue.
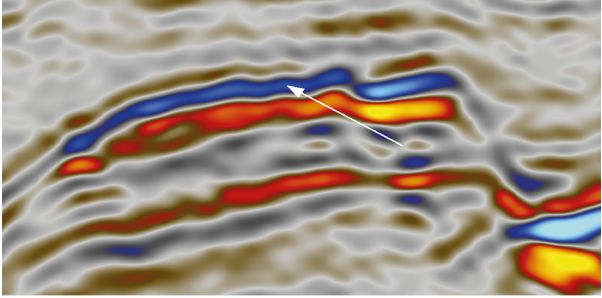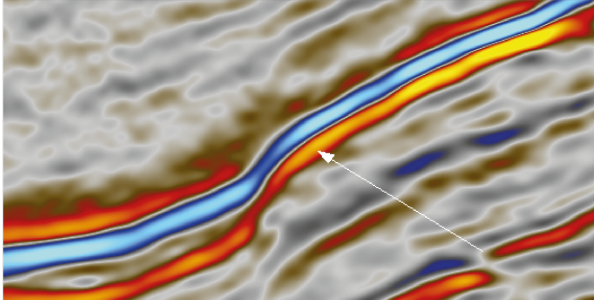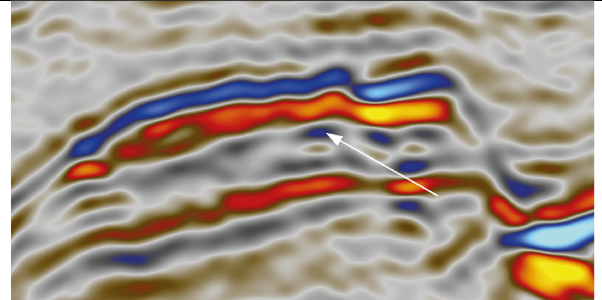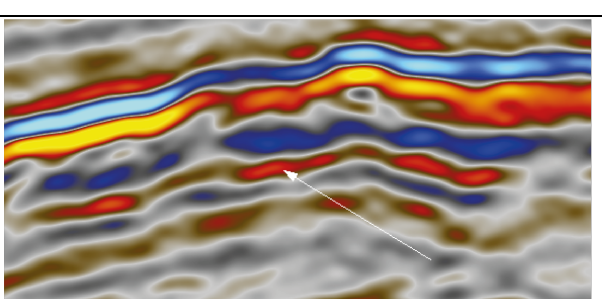
The two selected seismic sections, although optimal for regional display, are passing through or in close proximity of only three cored wells used in the present study (Table 3.2). This kind of dataset gave thus a very limited possibility for regional-scale facies analysis and palaeogeographic interpretation.

Table 3.2: Three wells that are located on or near the two seismic lines used in the present study (see Fig. 3.1). The wells were used to tie formation depths to the seismic sections. Wells 6506/12-8 and 6407/1-3 were also logged in the present study (see Appendix). The depths of the top and base of the Garn Fm. are verified according to the Norwegian Petroleum Directorate (NPD) internet data base.

Well	Depth of Garn Fm. top (m)	Depth of Garn Fm. base (m)
6506/12-8	3875	3956
6407/1-3	3600	3704
6407/6-4	2651	2752

Seismic interpretation of the Spekk Fm./base-Cretaceous unconformity (BCU) and the boundaries of the underlying Melke Fm., Garn Fm. and Not Fm. (Table 3.3) was based on synthetic seismograms with well-top depths established by NPD.

Table 3.3: Seismic expression of the key stratigraphic horizons referred to in the present study. Seismic data courtesy of TGS.

Horizon	Reflector phase	Reflector characteristics	Seismic expression
Top Spekk Fm. (BCU)	Negative amplitude (trough)	Continuous. High to medium amplitude.	
Melke Fm. top	Positive amplitude (peak)	Continuous. Medium to high amplitude	
Garn Fm. top	Negative amplitude (trough)	Discontinuous. Low to medium amplitude.	
Not Fm. top	Positive amplitude (peak)	Continuous to discontinuous. High to low amplitude.	

Seismic interpretation of the Garn Formation was limited to the recognition of local syndepositional fault activity and broad seafloor tectonic topography. The reader should understand that no realistic step-by-step structural and stratigraphic reconstruction of the Garn

Fm. deposition could possibly be derived from the limited dataset available for the present study.

4 SEDIMENTARY FACIES OF THE GARN FORMATION

4.1 Facies S$_{PPS}$: Sandstone with planar parallel-stratification

Description: This facies consists of fine- to very coarse-grained sandstone with planar parallel stratification (Fig. 4.1). The coarsest-grained strata occasionally contain scattered or concentrated granules. The units of this facies are solitary strata sets ranging in thickness from ~3 cm to ~75 cm. The boundaries are sharp, erosional or occasionally diffuse (at the contact with massive sandstone). This facies is commonly hydrocarbon-stained, pale-brown or brown in colour. Sparse to medium-grade bioturbation occurs only occasionally in this facies, represented by *Planolites* (Fig. 4.1B).

Interpretation: Based on its stratification type and highly varied grain size, facies S$_{PPS}$ is interpreted to have been deposited differently in its different occurrences. Units associated with cross-stratified sandstones (Fig. 4.1A; see facies S$_{CS}$ below) were probably deposited by unidirectional tractional currents in the lower part of the upper flow regime (Fig. 4.2A; Collinson et al., 2006), whereas those accompanied by wave-ripple cross-laminated sandstones (Fig. 4.1B) were probably deposited by waves with high orbital velocities (Fig. 4.2B; Komar and Miller, 1975). Coarse-grained units with granules (Fig. 4.1C) may represent beach-eroding storm events (Clifton and Dingler, 1984).
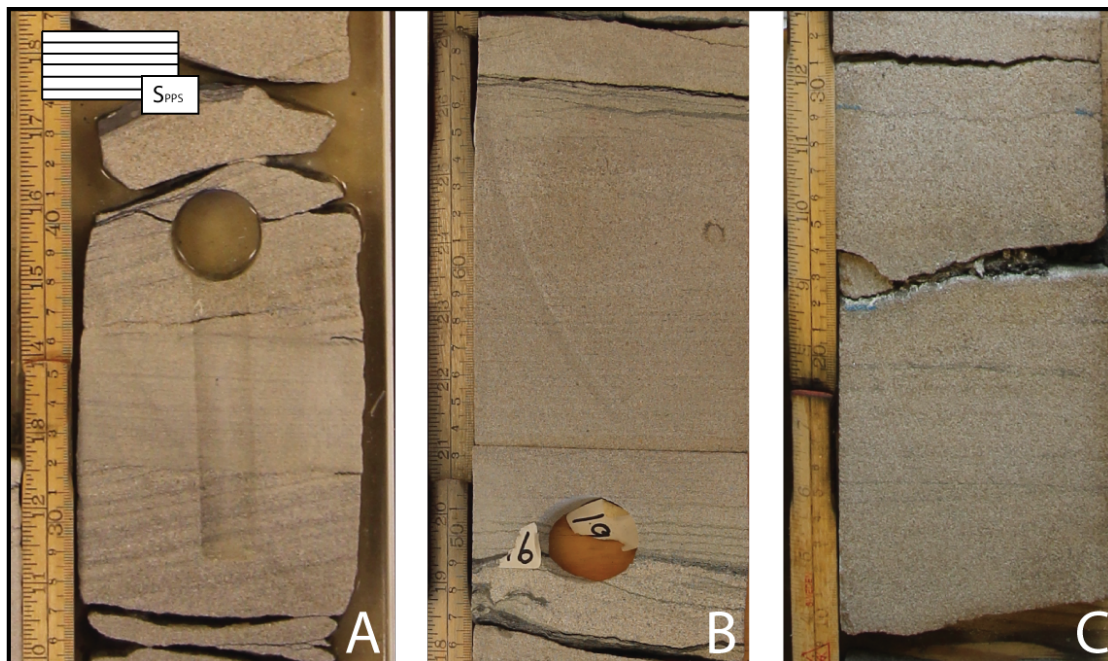

Figure 4.1: Examples of facies S$_{PPS}$ in association with (**A**) planar cross-stratified facies S$_{CS}$ and (**B**) wave-ripple cross-laminated facies S$_{RCL}$. Example **B** shows *Planolites* burrows. Example (**C**) is a coarse-grained variety of facies S$_{PPS}$. The examples are from well 6406/5-1 T2 (**A**), 6407/1-3 (**B**) and 6506/12-3 (**C**).

4.2 Facies S_{RCL}: Sandstone with ripple cross-lamination

Description: This facies (Fig. 4.3) consists mainly of fine- to medium-grained sandstones, only occasionally very fine- or coarse-grained. Their internal structure is ripple cross-lamination, commonly with mud drapes or flasers. The units of facies S_{RCL} range from solitary ripple cross-laminae sets ~1.5 cm thick to co-sets up to ~650 cm in thickness. Their upper and lower boundaries are mainly sharp, but occasionally diffuse and unclear. Sandstone colour is light grey, or pale-brown to brown where hydrocarbon-stained. The bioturbation grade varies from 0 to 4, with burrows such as *Palaeophycus*, *Skolithos*, *Rhizocorallium, Chondrites* and *Ophiomorpha*.

Ripple forms in transverse sections are mainly asymmetrical. The ripple index, *RI* (Collinson et al., 2006), is mainly in the range of 4–15. Ripple symmetry index, *RSI* (Collinson et al., 2006), varies from less than 2.5 to well above 3.
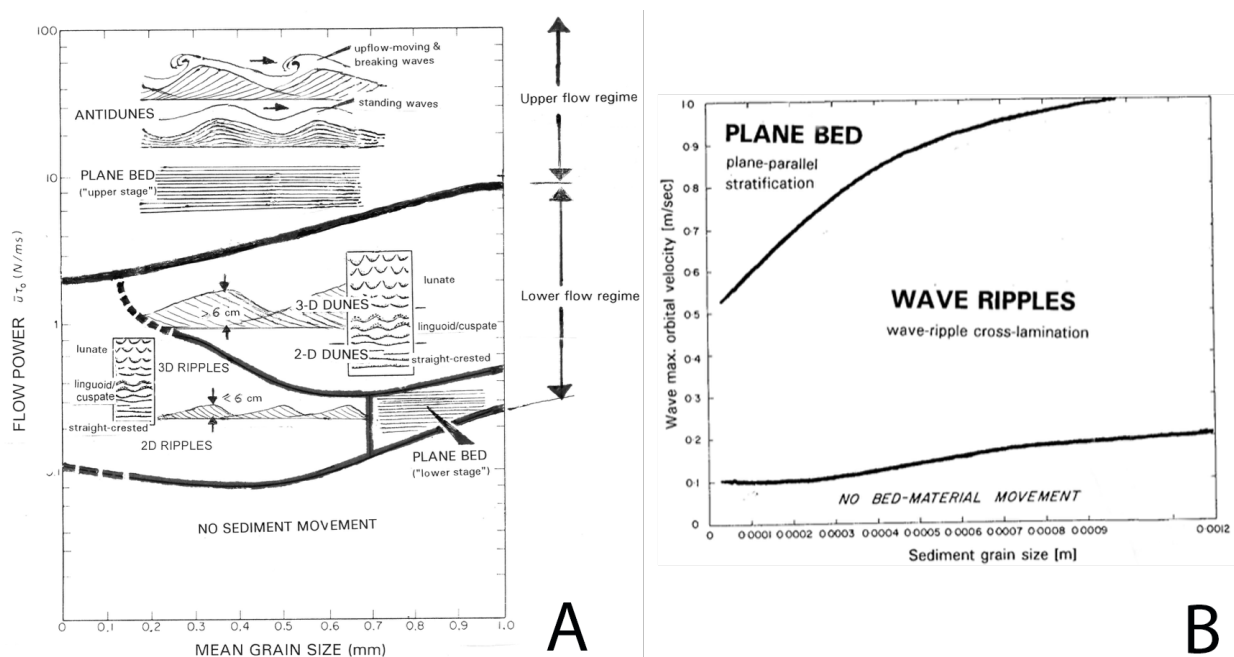

Figure 4.2: Bedforms in relation to hydraulic conditions. (**A**) Flow regimes according to bedform phase; modified with added sketches from Allen (1982). (**B**) Bedforms produced by waves; slightly modified with labels from Komar and Miller (1975).

Interpretation: Facies S_{RCL} is interpreted to be a product of sand transport in the form of migrating 2D and 3D ripples, which may indicate a weak unidirectional current in the lower part of the lower flow regime (Fig. 4.2A; Allen, 1982) or the action of waves with low near-bottom orbital velocities (Fig. 4.2B; Komar and Miller, 1975). The distinction between current and wave ripples is difficult in randomly oriented core-sample cuts. The values of RI are non-diagnostic, whereas the values of RSI indicate a mixture of current and wave ripples (see

Collinson et al., 2006). The mud drapes and flasers indicate brief episodes of hydraulic slackening, which is characteristic of tidal currents (Reineck and Singh, 1980).
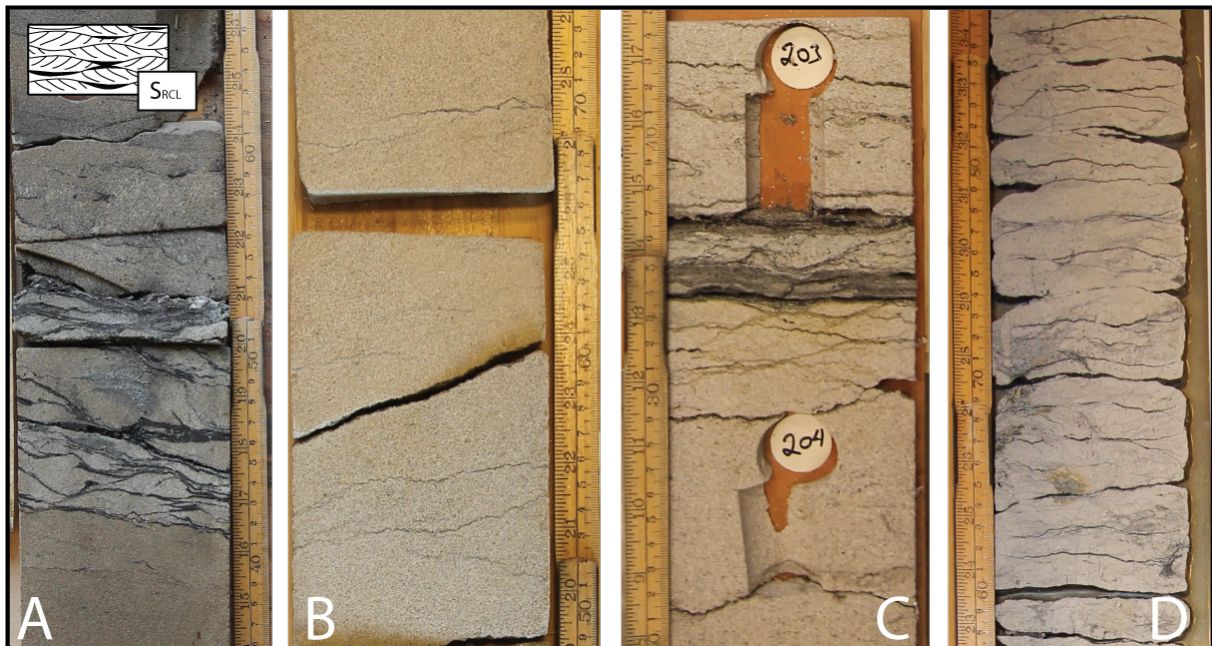

Figure 4.3: Examples of facies S_{RCL}. Note the abundant mud drapes and flasers in **A**, **C** and **D**, and the compactional microstyllolitization in **B** and **C**. The examples are from wells 6407/1-3 (**A**), 6407/1-4 (**B**), 6407/1-4 (**C**) and 6406/5-1 T2 (**D**).

4.3 Facies S_{CS}: Sandstone with planar or trough cross-stratification

Description: This facies (Fig. 4.4) consists of fine- to very coarse-grained – but predominantly medium-grained – sandstones with large-scale (i.e., dune-scale) cross-stratification. The distinction between planar and trough cross-stratification is generally difficult in core samples 8–12 cm wide, unless the boundary of cross-strata sets can be recognized as either concave-upwards or planar (e.g., Fig. 4.4B). The thickness of cross-strata sets ranges from slightly more than 7 cm to 83 cm, averaging 26 cm. The units of facies S_{CS} range from solitary cross-sets to multiple sets stacked upon one another as co-sets up to 2,64 m thick. Many co-sets in unbroken cores show evidence of bi-directional transport, but some co-sets are unidirectional and most are unspecified due to discontinuous, broken core samples. The shape of cross-strata on a core-sample scale varies from angular (constant inclination) to tangential (down-dip flattening). The former shape is most common and indicates planar cross-stratification. Sandstone colour is light grey, but pale-brown or brown where hydrocarbon-stained. The upper and lower boundaries of facies S_{CS} units are sharp (e.g., Fig. 4.4C), but are less clear where the sandstone is strongly hydrocarbon-stained. Bioturbation is relatively rare. Where present, its grade varies from sparse (1) to moderate (3) and the burrows include *Cylindrichnus*, *Skolithos, Asterosoma,*

23

Palaeophycus and *Macaronichnus*. Some cross-sets show deformation evidence of synsedimentary slumping. Cross-strata are occasionally mud-draped in the cross-set lower part, with the drapes ~0,5 cm to 4 cm thick, sporadically containing organic detritus and pinching out in up-dip direction. Backflow ripple features occur also in the lower part of some cross-strata foresets.

Interpretation: The deposits of facies S_{CS} represent tractional transport and deposition of sand in the form of migrating dunes, which indicates unidirectional currents in the upper part of the lower flow regime (Fig. 4.2A; Allen, 1982). Planar cross-stratification is attributed to straight-crested (2D) dunes, whereas trough cross-stratification represents linguoid or lunate (3D) dunes (Collinson et al., 2006). Erosional surfaces within the cross-stratified sets are attributed to fluctuations of flow velocities and thereby the generation of reactivation surfaces (Nio and Yang, 1991). Reactivation surfaces can be produced by reversing tidal currents (de Mowbray and Visser, 1984). Bidirectional cross-strata sets, mud drapes, reactivation surfaces and backflow ripples are features characteristic of tidal dunes (Reineck and Singh, 1980; Smith, 1991; Collinson et al., 2006).
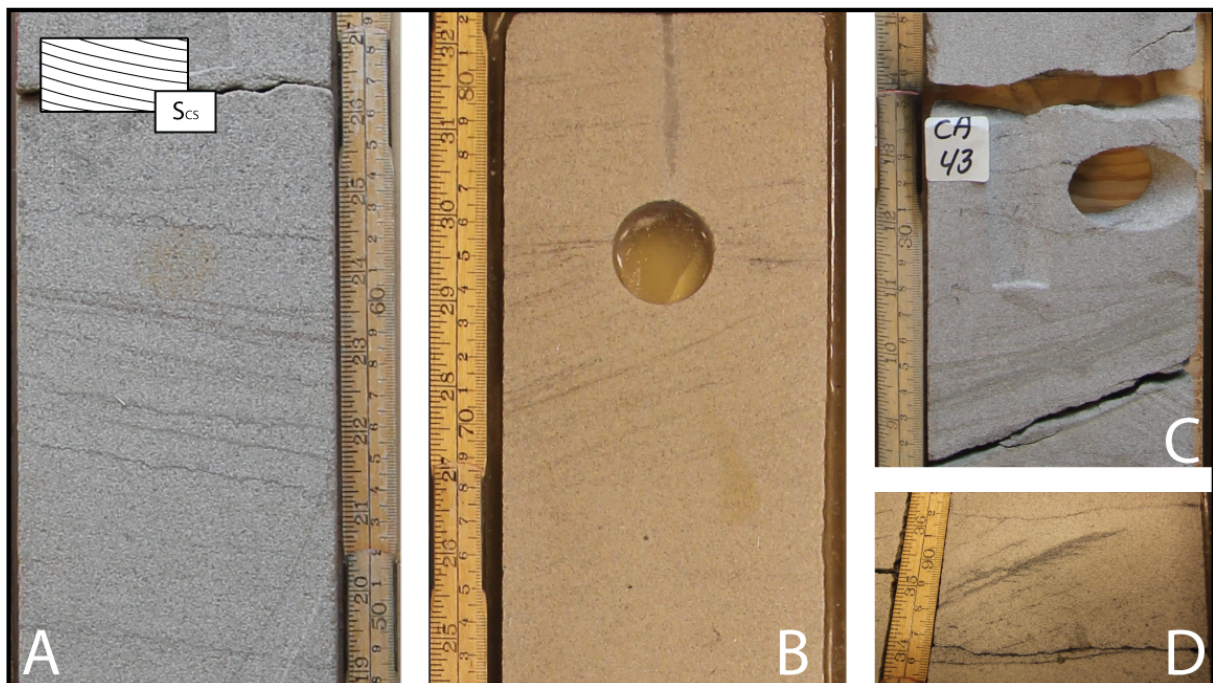

Figure 4.4: Examples of facies S_{CS}. (**A**) Set of inclined strata in a vertical well core of an otherwise horizontally-bedded succession, interpreted as planar cross-stratification. (**B**) Two vertically-stacked sets of planar cross-stratification (note their flat boundary). (**C**) Cross-strata set of facies S_{CS} overlain by facies S_{RCL}. (**D**) Backflow ripple cross-lamination and mud drapes in the lower part of cross-strata foreset. The examples are from wells 6407/1-3 (**A**), 6406/5-1 T2 (**B**), 6506/12-3 (**C**) and 6406/5-1 T2 (**D**).

4.4 Facies S$_{HCS}$: Sandstone with hummocky cross-stratification

Description: This facies consists of fine/medium- to medium/coarse-grained sandstones with a more or less distinct evidence of strata upward convexity suggesting hummocky cross-stratification (Fig. 4.5), although an unequivocal recognition of HCS in narrow core samples is obviously difficult. The units of this facies are mainly solitary sets of strata from ~10 cm to ~26 cm thick, rarely superimposed upon one another as a co-set (e.g., Fig. 4.5B). Their boundaries are sharp and often visibly erosional. Sandstone colour is mainly pale-brown or brown due to hydrocarbon staining. Bioturbation in most units of this facies is lacking, although a 5-grade bioturbation occurs at the top of one unit in well 6506/12-3, where the burrows include *Anconichnus, Planolites* and *Chondrites*.

Interpretation: The isolated beds of facies S$_{HCS}$ are interpreted to show hummocky cross-stratification and hence to represent the combined-flow conditions of marine storm events (Arnott and Southard, 1990; Dumas and Arnott, 2006). The complex interaction of storm waves with a storm-generated seaward compensational bottom current leads to the localized accretion of parallel-stratified domes known as "hummocks" (Walker, 1984b; Collinson et. al., 2006). Hummocks are relatively rare bedforms, because their formation requires an appropriate combination of the current speed, orbital wave velocity and sediment fallout rate (Dumas and Arnott, 2006).
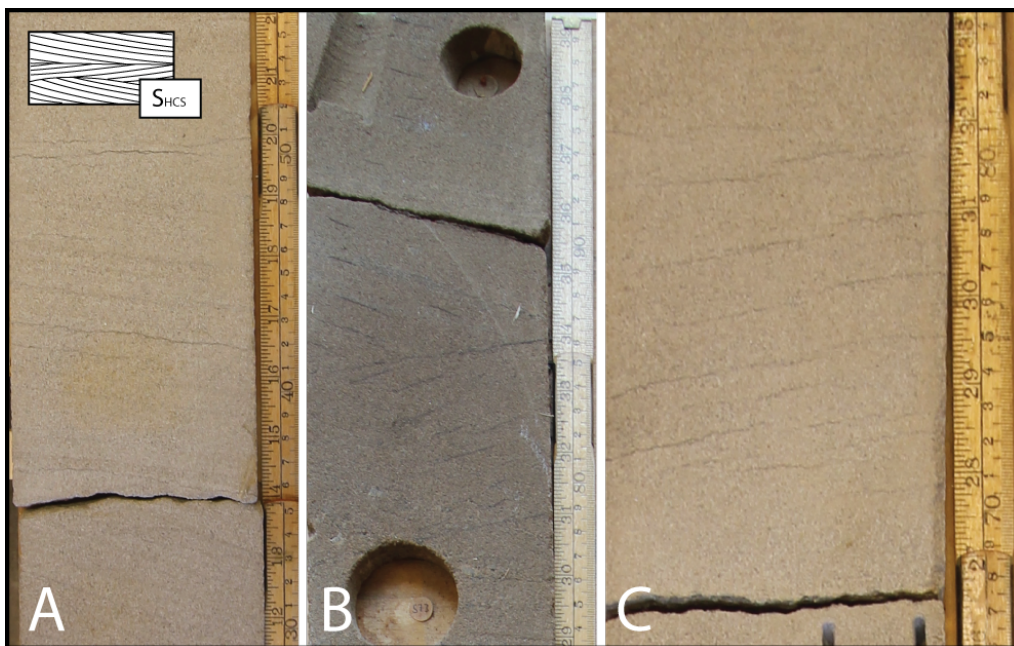

Figure 4.5: Examples of facies S$_{HCS}$ with the gently convex-upwards parallel stratification interpreted as hummocky cross-stratification. Note the two superimposed strata sets in **B**. The examples are from well 6407/1-3.

4.5 Facies S_{M1}: Massive sandstone

Description: This facies (Fig. 4.6) consists of fine- to very coarse-grained sandstones with an apparent lack of internal stratification or lamination. Although some faint 'ghosts' of planar parallel stratification or cross-stratification are locally observed, the bulk sandstone units seem to be massive. Their lower and upper boundaries are sharp in most cases, but occasionally diffuse. Sandstone colour is light grey, but pale-brown or brown where hydrocarbon staining occurred. No recognizable bioturbation is observed in this facies.

Interpretation: The origin of facies S_{M1} in association with facies S_{CS} is attributed to sporadic dune-front collapses under the impact of waves or earthquakes (Allen, 1982; Collinson et al., 2006; Hildebrandt et al., 2007). Such phenomena are well-known, for example, from the modern Messina Strait (Colella, 1990), where seafloor cables and pipelines were broken by collapses of the supporting 2D dunes (or "sandwaves"). Where associated with the wave-worked facies S_{PPS} and S_{RCL}, the isolated units of facies S_{M1} with diffuse lower boundaries are attributed to spontaneous seafloor liquefaction under the impact of storm waves (Seed and Rahman, 1978). On the other hand, the units of facies S_{M1} are often heavily stained with hydrocarbons, which obscure primary stratification; it is thus possible that some of the units of facies S_{M1} with no visible stratification were not truly massive and have been misclassified as such.
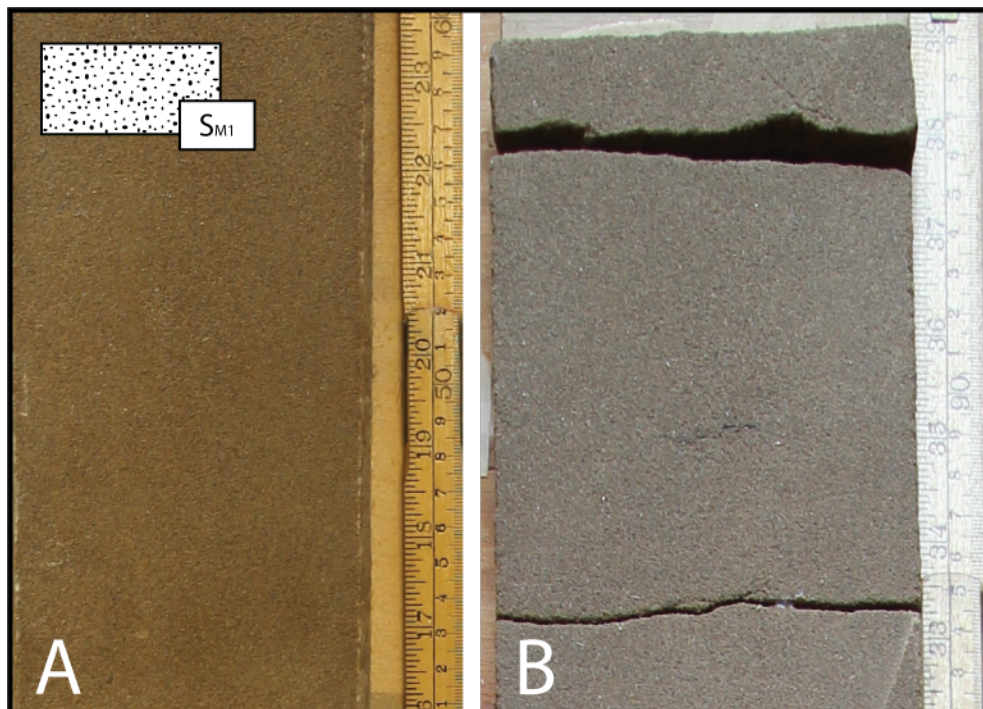

Figure 4.6: Examples of facies S_{M1} from well 6407/1-3.

4.6 Facies S$_{M2}$: Massive bioturbated sandstone

Description: This facies (Fig. 4.7) consists of very fine- to medium-grained sandstones, occasionally verging on siltstone, with an apparent lack of stratification and a high grade (5–6) of bioturbation. The units of this facies are ~17 cm to ~1640 cm thick and their lower boundaries are highly diffuse and unclear, whereas the upper boundaries are generally sharp. Sandstone colour is typically light to dark grey. Local relics of mud flasers are common and plant debris is locally found. Animal burrows include *Thalassinoides*, *Diplocraterion, Palaeophycus, Helminthoides* and *Planolites*.

Interpretation: The massive, apparently "structureless" nature of this facies is attributed to its high grade of bioturbation, which obliterated the sediment primary stratification beyond recognition (Collinson et al., 2006). Relics of mud flasers indicate that some of these bioturbated units originally represented the mud-flasered variety of facies S$_{RCL}$. The original nature of the other units of facies S$_{M2}$ is unknown. The grain size suggests possibly facies S$_{PPS}$ and/or S$_{CS}$.
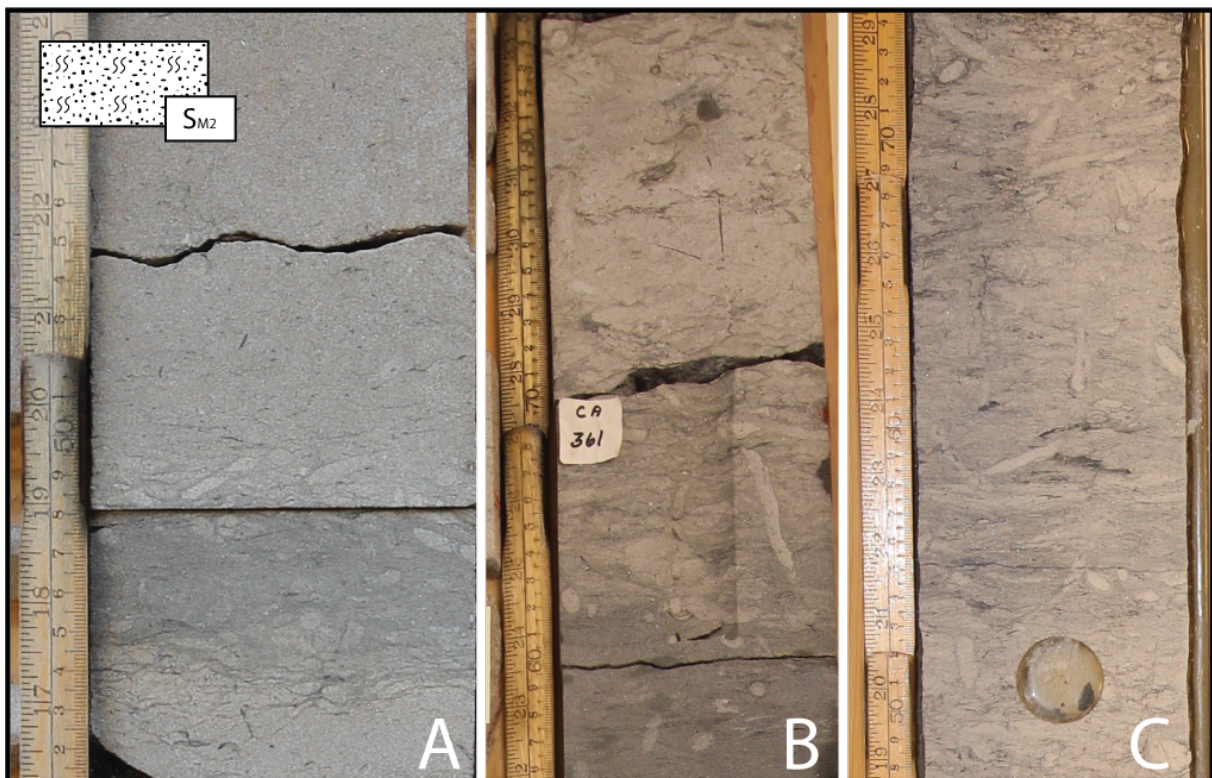

Figure 4.7: Examples of facies S$_{M2}$ with heavily bioturbated sandstone from well 6506/12-3 (**A**), 6506/12-5 (**B**) and 6406/5-1 T2 (**C**).

5 FACIES ASSOCIATIONS

Five facies associations have been recognized in the well cores and attributed to different depositional environments. The individual facies associations are described and interpreted in the present chapter, with example portions of detailed well-core logs shown for illustration and the relevant legend given in Fig. 5.1 (for complete logs and full legend, see Appendix).
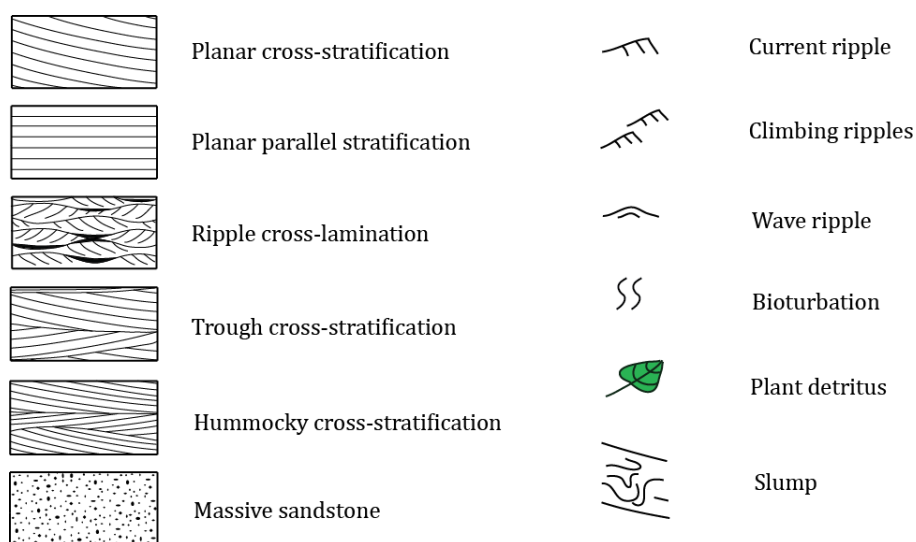
Planar cross-stratification		Current ripple	
Planar parallel stratification		Climbing ripples	
Ripple cross-lamination		Wave ripple	
Trough cross-stratification		Bioturbation	
Hummocky cross-stratification		Plant detritus	
Massive sandstone		Slump	

Figure 5.1: Legend to the core-log portions shown in Figs. 5.2 and 5.6–5.9 as illustration of facies associations.

The facies associations – with their reference code, interpretive genetic labels and facies composition – are listed in Table 5.1 as a brief guide to their spectrum.

Table 5.1: Facies associations distinguished in core material from wells 6406/2-6, 6406/5-1 T2, 6407/1-3, 6407/1-4, 6506/9-2 S, 6506/12-3, 6506/12-5, 6506/12-8 and 6507/11-8. The relative proportion of component facies is a generalized qualitative estimate based on their occurrence frequency and thickness contribution.

FACIES ASSOCIATIONS	COMPONENT FACIES
Deposits of tidal sand ridges (longitudinal bars)	Dominant: S_{CS} Subordinate: S_{RCL} Minor/sporadic: S_{PPS} & S_{M1}
Deposits of shallow subtidal sandflats	Dominant: S_{RCL} Subordinate: S_{CS} & S_{PPS} Minor/sporadic: S_{HCS} & S_{M2}
Deposits of tidal inter-ridge swales	Dominant: S_{CS}, S_{RCL} & S_{M1} Minor/sporadic: S_{PPS} & S_{HCS}
Wave-worked deposits	Dominant: S_{PPS} Subordinate: S_{RCL} Minor/sporadic: S_{CS}
Deposits of protected inter-ridge swales	Dominant: S_{M2} Subordinate/minor: S_{CS} & S_{PPS}

29

5.1 FA1: Deposits of tidal sand ridges

<u>Description:</u> This facies association (Fig. 5.2) consists of facies S_{CS} and S_{RCL} and is dominated by the former facies, with subordinate thin intercalations of facies S_{PPS} and sporadic thin interlayers of facies S_{M1}. This facies assemblage, forming units 2.80–56.36 m thick, is found as dominant in all the studied well cores.
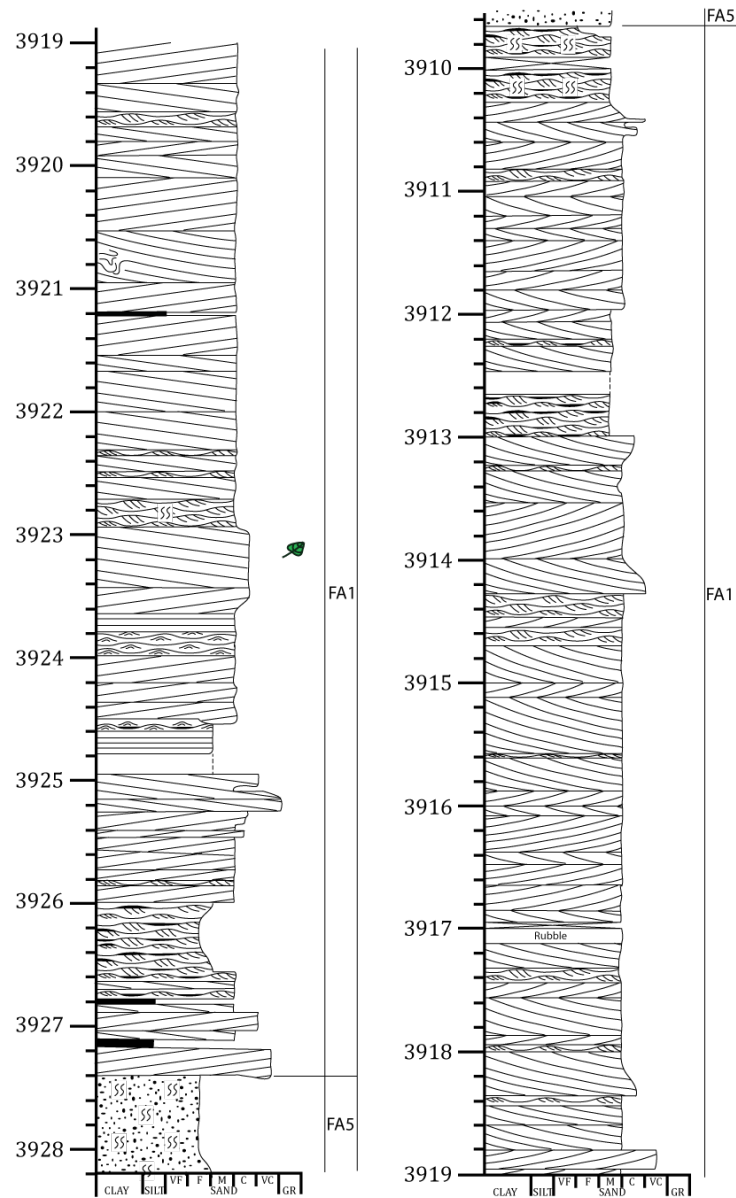

Figure 5.2: Example of facies association FA1 from well-core log 6506/12-8. For legend, see Fig. 5.1. For complete well-core log, see Appendix.

The component sandstone facies S_{RCL} represents mainly current ripple cross-lamination, commonly mud-draped and occasionally bidirectional, where associated directly with the cross-stratified sandstone facies S_{CS}, but represents mainly wave ripple cross-lamination where

associated directly with the plane parallel-stratified sandstones of facies S_{PPS}. Facies S_{CS} shows mainly planar cross-stratification, although trough cross-stratification also occurs, and the cross-strata co-sets range from unidirectional to recognizably bidirectional. The sandstones of facies S_{CS}, S_{PPS} and S_{M1} range from very fine- to very coarse-grained, but are mainly medium-grained. The sandstones of facies S_{RCL} are very fine- to fine-grained, occasionally medium-grained. Animal burrows include *Cylindrichnus*, *Skolithos*, *Asterosoma*, *Palaeophycus*, *Macaronichnus*, *Rhizocorallium, Chondrites* and *Ophiomorpha*, indicating the *Cruziana* and/or *Skolithos* ichnofacies (see Frey, 1975; McIlroy, 2004b).

Interpretation: The dominant cross-stratified sandstone facies S_{CS}, with evidence of bidirectional cross-strata sets, indicates sand deposition in the form of 2D and 3D dunes driven by tidal currents. The notion of tidal environments is supported further by mud-draped ripple cross-lamination in the associated facies S_{RCL}, which indicates alternating episodes of sand transport and slack-water conditions (Reineck and Singh, 1980; Nio and Yang, 1991). The relatively thick (up to 2.64 m) cross-strata co-sets suggest tidal sand ridges, or longitudinal bars, formed by the vertical stacking of successive dunes (Fig. 5.3; see Mutti et al., 1985; Kreisa et al., 1986; Colella and d'Alessandro, 1988; Yang and Nio, 1989; Dalrymple and Rhodes, 1995; Longhitano and Nemec, 2005; Longhitano, 2011).
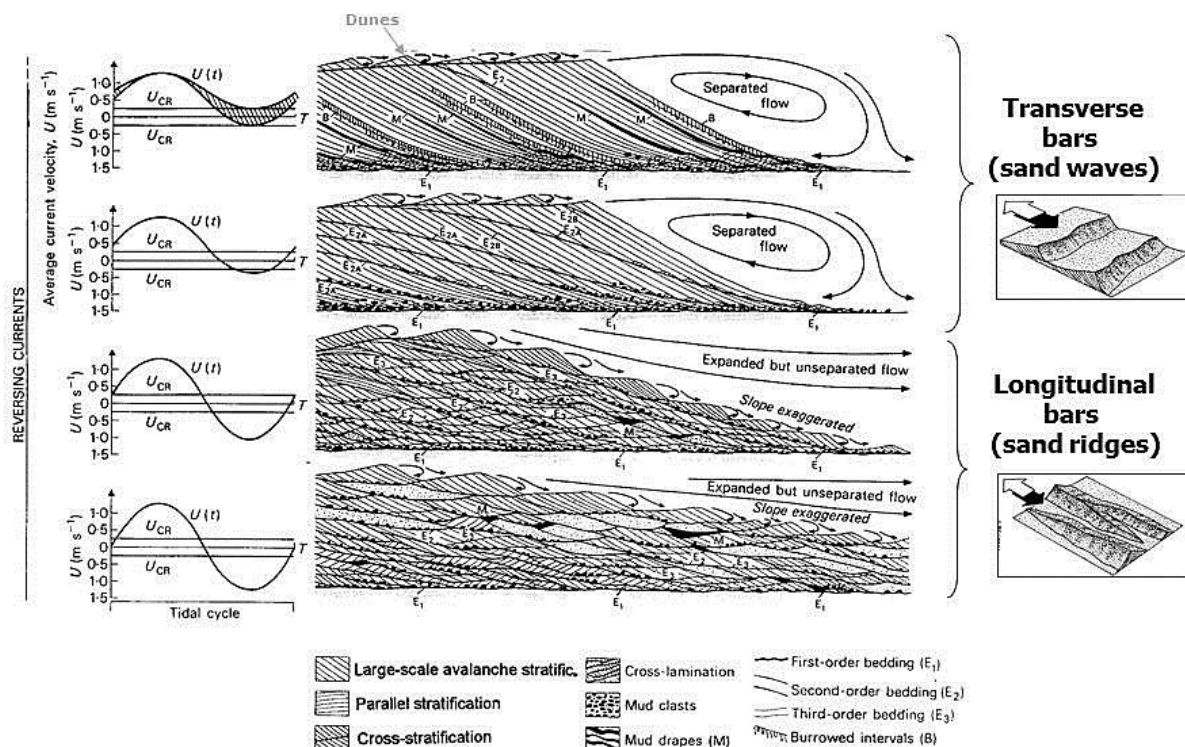

Figure 5.3: Model for the development of transverse and longitudinal tidal sand bars by a reversing tidal current (slightly elaborated from Allen, 1980). Note that the internal architecture of the tidal bar changes from a simple foreset (top) to a compound 'herringbone' dune stack (bottom) as the time-velocity pattern of the reversing current becomes symmetrical.

A similar palaeoenvironmental interpretation of the thick co-sets (up to 10–15 m) of dune cross-strata in the Garn Fm. in the Kristin Field, Halten Terrace, was suggested by Messina et al. (2014); see Fig. 5.4 below.
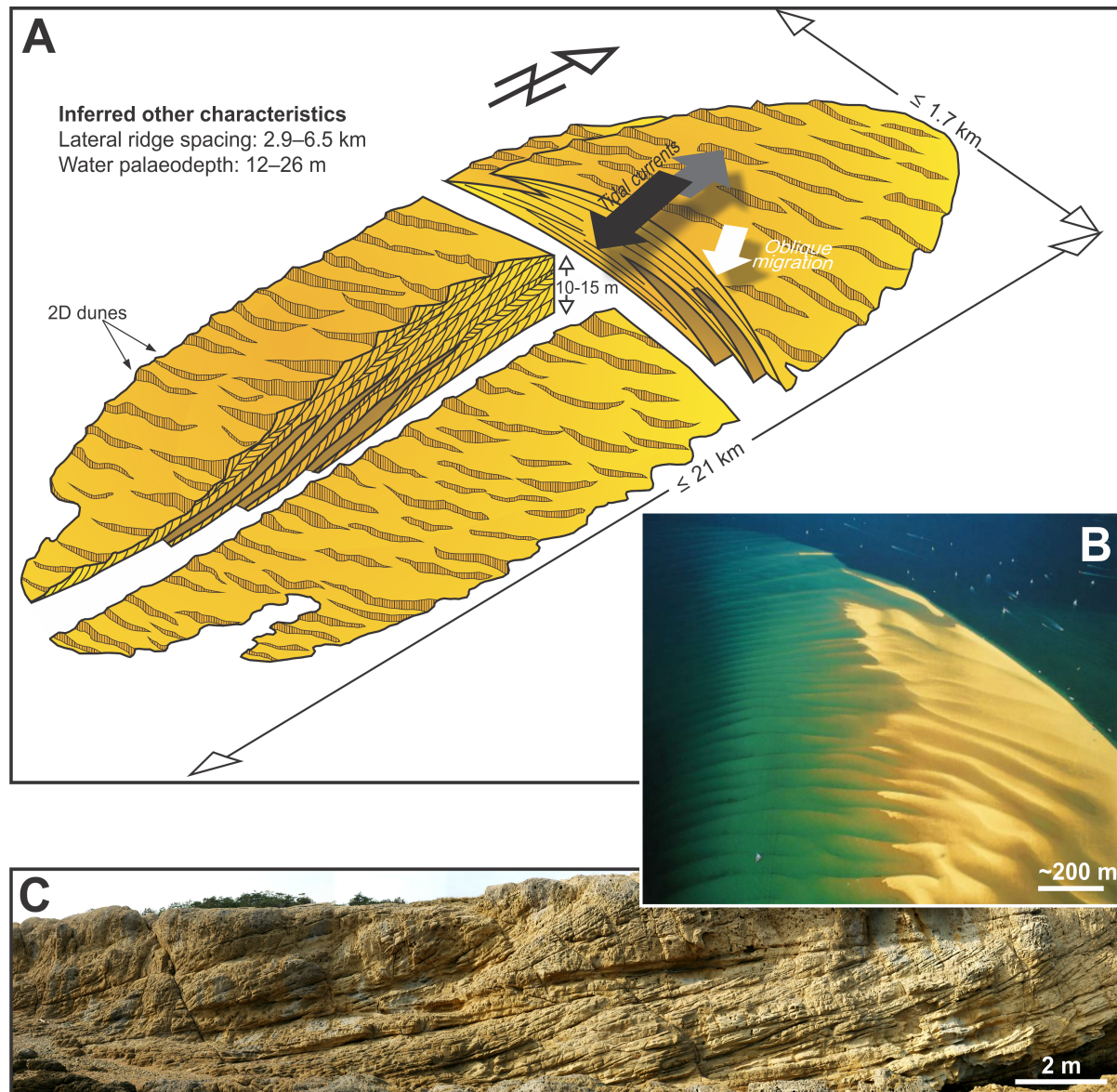

Figure 5.4: (**A**) A dimensional model for tidal sand ridges in the Garn Fm. in Kristin Field suggested by Messina et al. (2014), with (**B**) the Banc d'Arquin sand bar in the English Channel as a modern analogue and (**C**) an Eocene tidal sandstone ridge in the Rab island, Croatia, as an ancient analogue (dominant palaeocurrent direction to the left). From Messina et al. (2014).

Such vertical stacks of sand cross-strata sets are mainly composed of "compound dunes" (Dalrymple et al., 2003; Dalrymple and Choi, 2007; Desjardins et al., 2012b), which involve numerous truncation and reactivation surfaces (Fig. 5.5) formed by the reversing tidal currents. In an open-shelf setting, the compound dunes may form extensive subtidal sand sheets or be piled into flow-parallel linear ridges, as observed at present in some areas of the southern North

Sea (Van der Molen and De Swart, 2001). Modern case studies indicate that the height of tidal sand ridges may reach 40 m and their length and width are in the range of 5–120 km and 0.5–8 km, respectively (McBride, 2003). Since the direction of dune migration is mainly oblique, at 20–35°, with respect to the ridge axis (Dalrymple and Rhodes, 1995; Dalrymple, 2010), the sand ridge tends to migrate laterally during its progradation (Fig. 5.4A). A single tidal ridge may fill in an entire narrow marine strait (see Longhitano and Nemec, 2005).
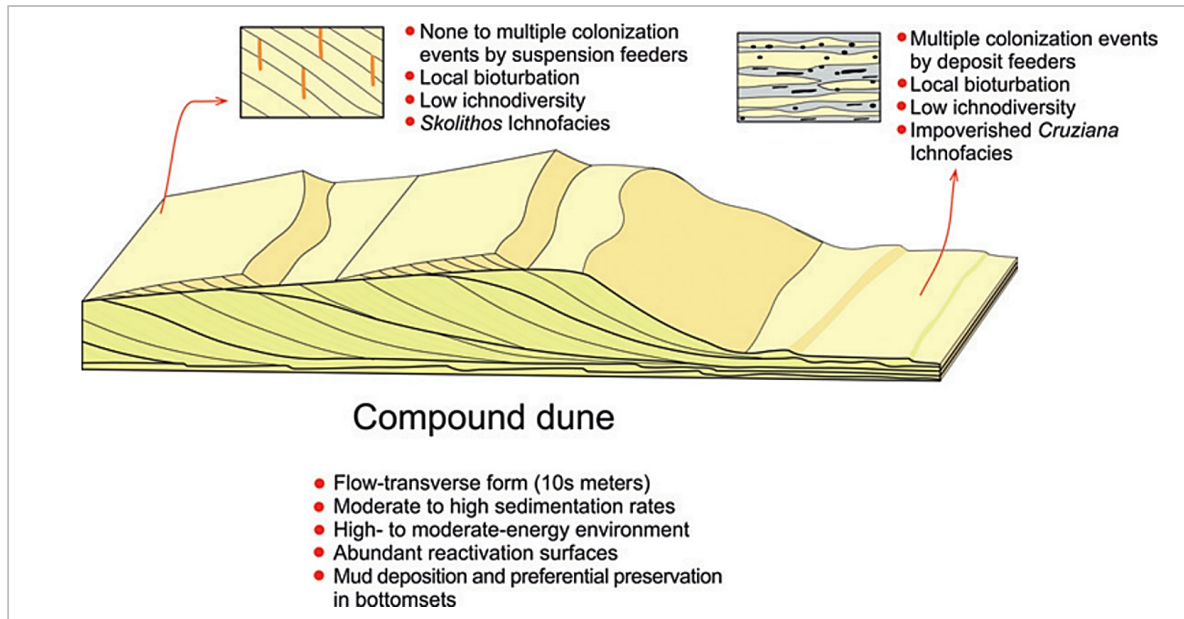

Figure 5.5: An integrated sedimentological and ichnological model for subtidal compound dunes (from Desjardins et al., 2012a).

Apart from the mud drapes in facies S$_{RCL}$, the general lack of muddy facies interbeds indicates that the mud in this sedimentary system was almost perennially in suspension, probably due to an intense wave action accompanying the reversing tidal currents (see Longhitano and Nemec, 2005; Davis and Dalrymple, 2012; Olariu et al., 2012a). This interpretation is consistent with the general notion that sand ridges form along the high-energy thalweg of tidal currents in the deepest zone of a marine strait, where also the wave action would be at its local maximum (Reineck, 1963; Klein, 1970; Langhorne, 1973; Reineck and Singh, 1980; Dalrymple, 1992; Longhitano and Nemec, 2005; Dalrymple, 2010; Davis and Dalrymple, 2012).

The transport of sand in the form of current ripples (facies S$_{RCL}$) occurred probably over the dunes, with a low preservation potential of ripples, and in the hydraulic "shadow" of dunes at their toes, where also the episodic fallout of mud would occur (Fig. 5.5). Bioturbation is generally limited, which suggests a mobile substrate, but facies S$_{RCL}$ tends to be significantly

more burrowed than facies S_{CS}, which indicates preferential animal colonization of the dune toe zones (Fig. 5.5; see Davis and Dalrymple, 2012; Desjardins et al., 2012a).

The apparent overall diversity of trace fossils in FA1 may be due to an intricate environmental combination of the deposit-feeding organisms active in tidal facies S_{RCL} (such as *Asterosoma*, *Macaronichnus*, *Rhizocorallium* and *Chondrites*, characteristic of the archetypal *Cruziana* ichnofacies; see Desjardins et al., 2012b; Olariu et al., 2012a) and the suspension-feeder organisms of the *Skolithos* ichnofacies in the wave-worked facies S_{RCL} and facies S_{PPS} (see Frey, 1975; McIlroy, 2004b). Facies S_{CS} only rarely show burrows, which indicates a relatively high mobility of tidal dunes.

The interbeds of facies S_{PPS} in FA1 most probably represent transient influences of storm wave base with high orbital wave velocities (Komar and Miller, 1975), whereas the sporadic interlayers of facies S_{M1} are attributed to occasional dune-front collapses, perhaps under the impact of storm waves or earthquake-related liquefaction (Seed and Rahman, 1978; Okusa and Uchida, 1980; Nishi and Kraus, 1997). The wave-worked facies S_{PPS} and S_{RCL} would also form where the build-up of the subtidal sand ridge had reached the fairweather wave base.

5.2 FA2: Deposits of shallow subtidal sandflats

Description: This facies association (Fig. 5.6) consists of sandstone facies S_{RCL} and S_{CS}, and is dominated by the former facies. Facies S_{RCL} in this association represents almost exclusively current ripples, occasionally recognizable as bidirectional, and generally abounds in mud drapes or flasers. Subordinate are thin intercalations of facies S_{PPS} and S_{HCS} and rare thin interlayers of facies S_{M2}. This facies assemblage is found in nearly all of the studied well cores, forming units 2.50–25.20 m thick, and – next to FA1 – is the second dominant facies association. Its component facies S_{CS} occurs mainly as isolated cross-strata sets or as relatively thin co-sets, occasionally with a bidirectional dip of cross-strata. The sandstones are dominantly medium-grained, but sporadically very fine-grained (facies S_{RCL}) or very coarse-grained (facies S_{CS} and S_{PPS}). Burrows include *Palaeophycus*, *Skolithos*, *Rhizocorallium, Chondrites* and *Ophiomorpha*, indicating the *Cruziana* or *Skolithos* ichnofacies.

Interpretation: The volumetrically dominant facies S_{RCL}, with its mud drapes and flasers, is a typical product of tidal sandflat environment (Nio and Yang, 1991; Dalrymple, 1992, 2010). Facies S_{RCL} implies an action of relatively weak, reversing tidal currents, while the lack of evidence of episodic subaerial exposure suggests shallow-water subtidal conditions.
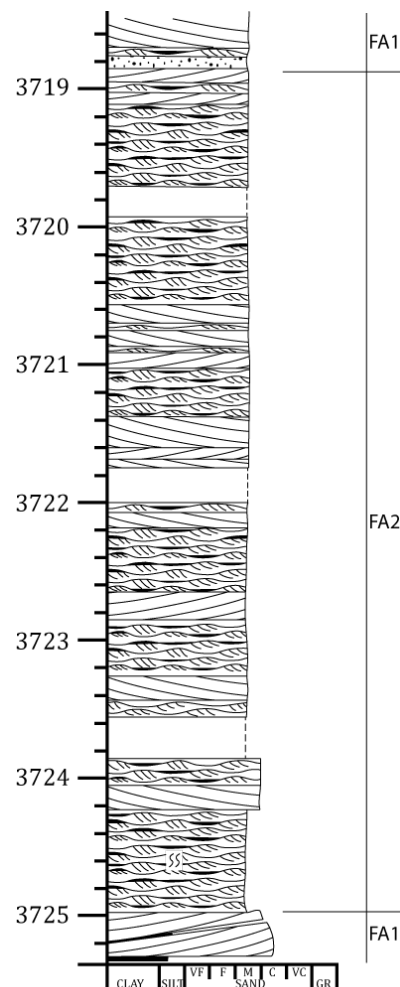
Figure 5.6: Example of facies association FA2 from well-core log 6407/1-4. For legend, see Fig. 5.1. For complete well-core log, see Appendix.

The associated isolated sets and thin co-sets of cross-strata (facies S_{CS}) may represent spring-tide phases of increased tidal range and flow power or may be the infill deposits of poorly-defined, shallow ebb-tide creeks draining the sandflat area (see Reineck and Singh, 1980; Dalrymple, 1992, 2010; Davis and Dalrymple, 2012). The lack of significant, continuous mudstone interlayers indicates that the energy of the tidal currents and accompanying waves was sufficiently high to keep most of the delivered sediment mud fraction in suspension or persistent resuspension.

Interbeds of facies S_{PPS} and S_{HCS} indicate brief influences of storm-wave base with high orbital wave velocities and episodic conditions of storm-generated combined flow, although some occurrences of this former facies may alternatively represent tidal currents with a flow power too high for the formation of ripples, but with a flow depth too shallow for the formation of dunes (Dalrymple et al., 1990). Sporadic interbeds of facies S_{M2} indicate short episodes of

intense seafloor bioturbation and suggest either an abrupt local deepening of water, perhaps due to fault-related subsidence, or a temporal abandonment of particular area by the laterally shifting of tidal currents.

The evidence, taken together, indicates storm-influenced subtidal sandflats with a moderate but episodically high hydraulic energy and a persistent action of tidal currents, as is typical of open marine tidal coasts and perhaps some horst-hosted intra-shelf shoals (see Dalrymple, 2010). The notion of fluctuating hydraulic energy is supported further by the ichnofauna assemblages. Zones of high energy in tidal flats are generally characterized by low-diversity assemblages of suspension feeders or passive predators, such as *Skolithos* (Simpson, 1991; Mángano and Buatois, 2004). In zones of moderate to low energy, the ichnodiversity increases and burrows tend to be more dominated by horizontal traces of deposit-feeders and grazers, such as *Chondrites* and *Rhizocorallium* (Mángano, 2002). The occurrence of both types of ichnofauna in FA2 thus indicates some markedly fluctuating local energy conditions.

5.3 FA3: Deposits of tidal inter-ridge swales

Description: This facies association (Fig. 5.7) consists of the sandstone facies S_{CS}, S_{RCL} and S_{M1}, accompanied by minor occurrences of facies S_{HCS} and S_{PPS}. The sandstones are almost uniformly fine/medium-grained. This facies assemblage has been found in only two well cores (6407/1-3 and 6507/11-8), where it forms packages 15.28 m and 2.08 m thick, respectively. Units of facies S_{CS} are mainly co-sets and show evidence of bidirectional, reversing flow. As in the two previous facies associations, facies S_{RCL} represents chiefly current ripples (with sporadic delicate mud flasers) where associated directly with the cross-stratified facies S_{CS}, but represents mainly wave ripples where associated with the sporadic planar parallel-stratified facies S_{PPS}. No bioturbation has been recognized in this facies association.

Interpretation: The deposits of FA3, dominated by facies S_{CS}, S_{RCL} and S_{M1}, resemble those of FA1, except for the greater proportion of the massive sandstones of facies M_1 in FA3 and the highly localized occurrences of this facies association (as it seems to have been found just by chance in only two wells). Notably, FA3 is also directly associated with FA1, splitting the latter (well 6407/1-3) or underlying it (well 6507/11-8), which may indicate their genetic morphodynamic link.
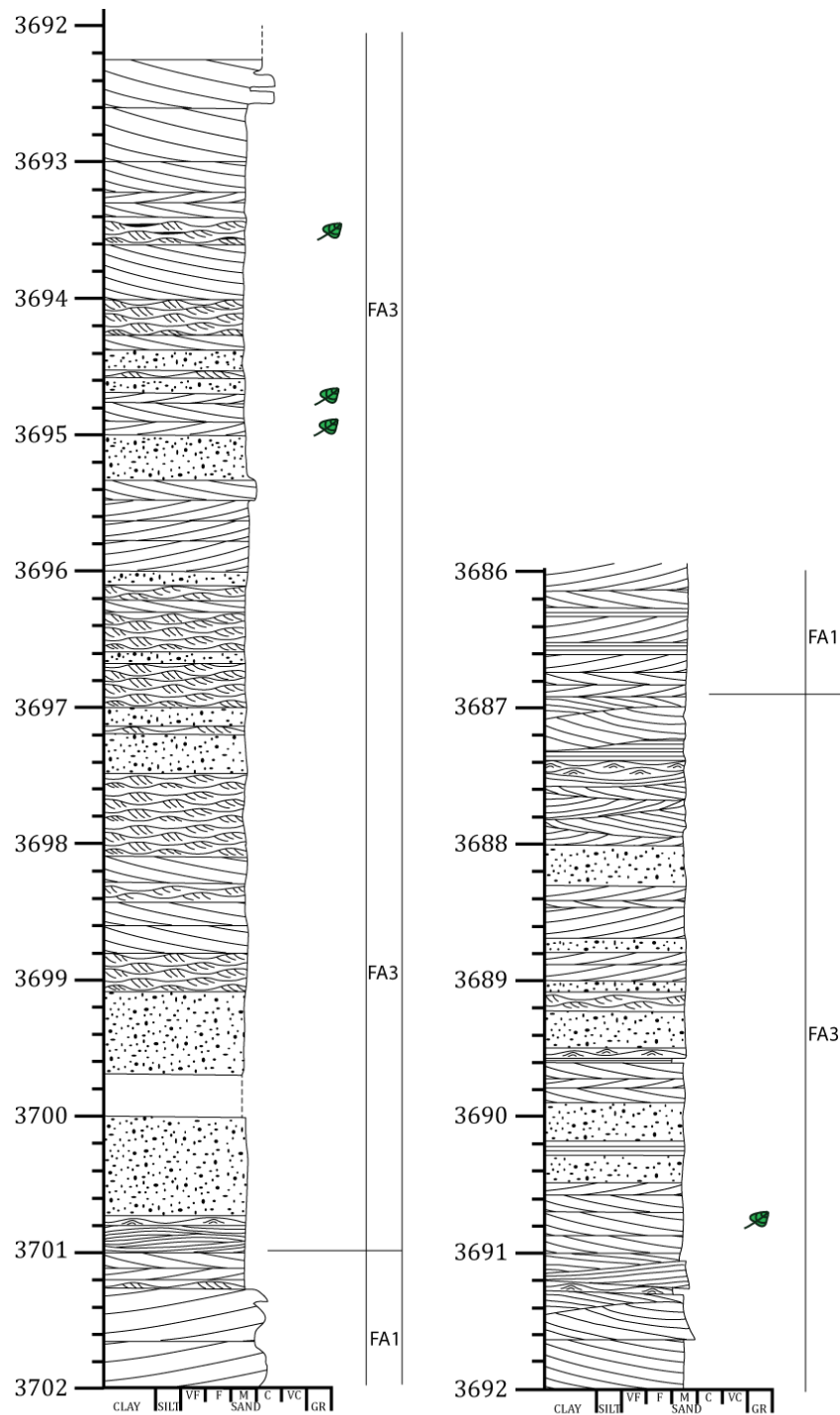
Figure 5.7: Example of facies association FA3 from well-core logs 6407/1-3. For legend, see Fig. 5.1. For complete well-core logs, see Appendix.

FA3 was clearly formed by perennial tidal currents allowing very little or virtually no mud fallout, although it shows also minor signatures of storm-wave influence (facies S_{PPS} with wave-worked S_{RCL}) and combined-flow conditions (facies S_{HCS}). On the basis of its direct association with FA1 and limited spatial extent, FA3 is interpreted to be deposits of the narrow swales

separating the tidal sand ridges of FA1 and buried by a lateral migration of the latter (cf. Fig. 5.4A). The transient swales tend to funnel the near-bottom current and boost local sand transport, while causing ridge-flank collapses (facies S_{M1}) and rendering the local environment unsuitable for animal colonization (Swift and Field, 1981; Dyer and Huntley, 1999; Liu et al., 2007). Little or no mud will be deposited in such swales, especially if the wave-generated ambient turbulence persists (Swift, 1975; Montenat et al., 1987; Longhitano and Nemec, 2005), although fine-grained sediment may be deposited in some other swales, morphologically sheltered in the hydraulic "shadow" of prevalent tidal currents (Hein, 1987; see further FA5 below).

5.4 FA4: Wave-worked deposits

Description: This sandy facies association (Fig. 5.8) consists of facies S_{PPS} intercalated with thin interbeds of facies S_{RCL} (mainly wave ripples) and S_{CS} (planar cross-stratification). The sandstone grain size is mainly medium/coarse, with occasional minor interlayers of finer or coarser sand fractions. This facies assemblage has been encountered in only one well-core (6507/11-8), where it forms two units 1 m and >2.79 m thick – each overlying FA1. No bioturbation has been recognized in this facies association.
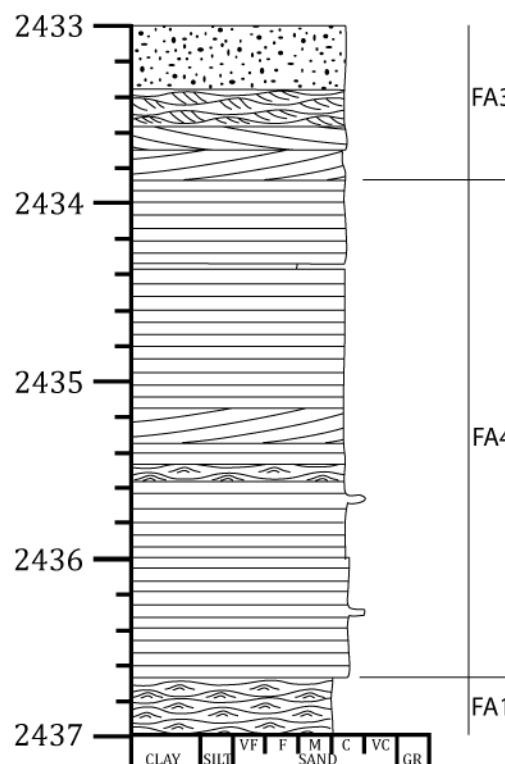

Figure 5.8: Example of facies association FA4 from well-core log 6507/11-8. For legend, see Fig. 5.1. For complete well-core log, see Appendix.

38

Interpretation: The planar parallel-stratification accompanied by wave ripple cross-lamination indicates deposition by waves with high (facies S_{PPS}) to low (facies S_{RCL}) orbital velocities (see Komar and Miller, 1975; Clifton and Dingler, 1984). The occurrence of FA4 as a capping of FA1 suggests deposition in littoral shoals where the aggrading progradational tidal sand ridges (Fig. 5.4) had reached the fairweather wave base as the limit of their accommodation space – before the local seafloor was taken down by a new pulse of tectonic subsidence (see Boersma, 1969; Hubbard et al., 1979; Roep et al., 1979; Swift et al., 1979; Short, 1991; Cacchione et al., 1994). Cross-strata sets (facies S_{CS}) with reversing palaeocurrent direction are non-reworked relics of primary tidal transport.

5.5 FA5: Deposits of protected inter-ridge swales

Description: This facies association is dominated by the heavily bioturbated facies S_{M2} with thin intercalations of facies S_{CS} and S_{PPS} (Fig. 5.9). FA5 was found in only four well-core logs (6406/5-1T2, 6506/12-3, 6506/12-5 and 6506/12-8), where it forms units from 1.20 m to >16.48 m thick. The sandstones are medium- to very fine-grained, in some units verging on siltstone. Animal trace fossils include *Thalassinoides, Diplocraterion, Palaeophycus, Helminthoides* and *Planolites*, which seem to represent the *Cruziana* ichnofacies.

Interpretation: FA5 shows evidence of both tidal transport (facies S_{CS}) and minor influence of high-energy waves (facies S_{PPS}), but is generally the finest-grained and heavily bioturbated (grade 5–6) sandstone of facies S_{M2}. Its deposition is thought to have occurred in some relatively protected swales between bifurcating tidal sand ridges (Fig. 5.10; Hein, 1987), where the *Cruziana* ichnofauna could thrive due to the limited and mainly episodic sediment transport pulses. The trace-fossil assemblages in FA5 indicate, indeed, a deep littoral to sublittoral sedimentary environment. Although *Palaeophycus* is known to be common in both high- and low-energy littoral environments and *Diplocraterion* may suggest middle shoreface (Stanistreet, 1989), whereas the occurrence of *Thalassinoides* suggests a lower shoreface to offshore bathymetry (Cotter, 1975; Howard and Frey, 1985) and *Helminthoides* is generally associated with sheltered low-energy environments (Bockelie, 1991; Young and Rosenthal, 1991).

FA5 is thus inferred to be genetically a sister of FA3, but deposited in different morphodynamic environmental conditions – within inter-ridge swales sheltered from the perennial tidal and wave action and only episodically subject to these processes.
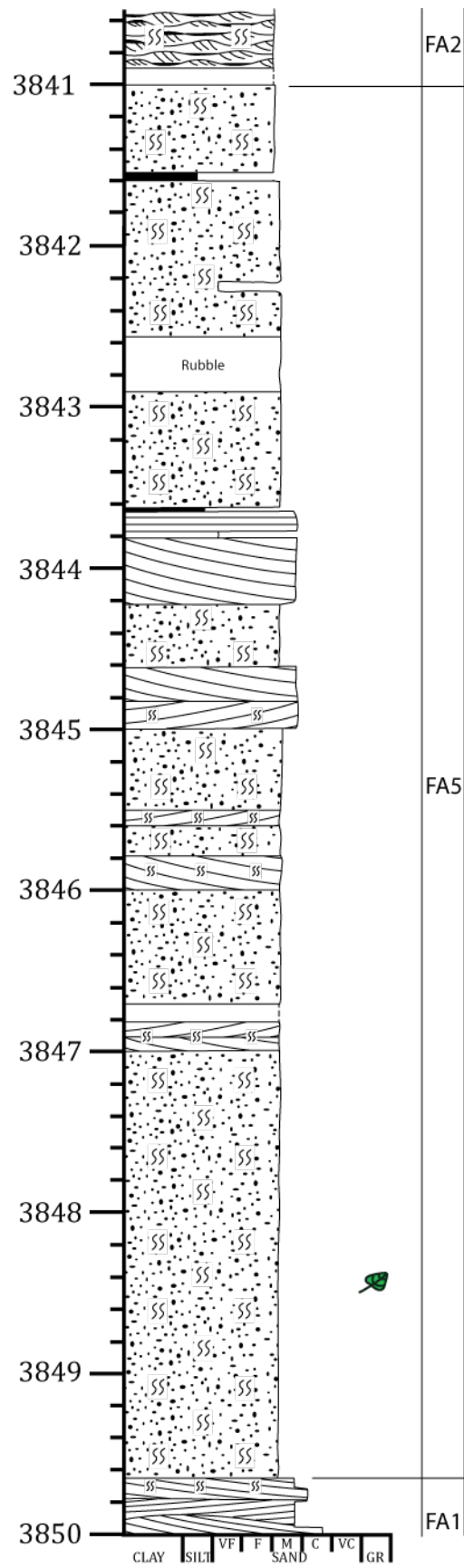
Figure 5.9: Example of facies association FA5 from well-core log 6506/12-3. For legend, see Fig. 5.1. For complete well-core log, see Appendix.
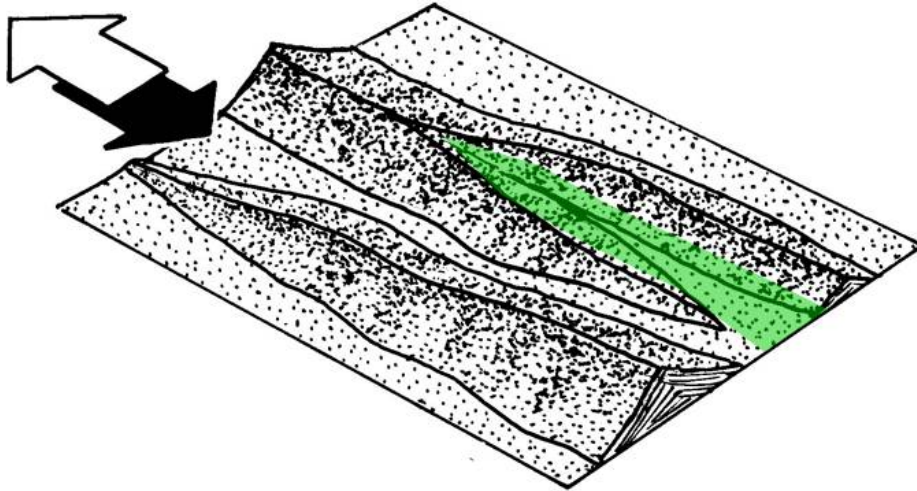
Figure 5.10: Bifurcation of tidal sand ridges provides sheltered zones (area marked in green) where both Cruziana ichnofauna may thrive and relatively fine-grained sediment can be deposited (see Hein, 1987). The black arrow indicates the prevalent direction of reversing tidal currents.

6 ANALYSIS OF SEISMIC SECTIONS AND GEOPHYSICAL WELL-LOGS

6.1 Seismic interpretation

Only two seismic sections, trending W–E and NW–SE across the Halten Terrace (Fig. 3.1), have been available for the present study. Since the Halten Terrace in Jurassic time was a shelf area subject to tectonic extension, with its marginal outer parts (such as the Sklinna Ridge, Fig. 2.1) nearing an ultimate collapse, the seismic sections have been interpreted here in terms of the criteria generally used in such settings for extensional tectonics and fault-block rotation (Figs. 6.1 and 6.2).
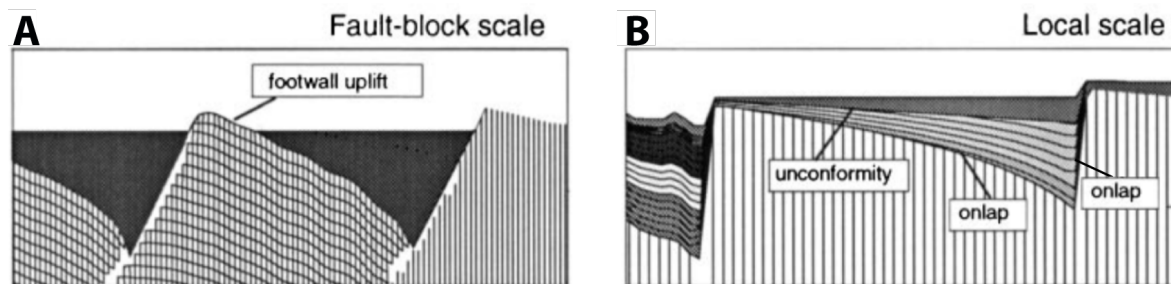

Figure 6.1: Development of a sedimentary basin or sub-basin depocentre in a fault-block tectonic setting. (**A**) Simple case of a hanging-wall subsidence and footwall uplift, resulting in (**B**) wedge-shape bed sets onlapping the pre-rift bedrock. Slightly modified from Ter Voorde et al. (1997).
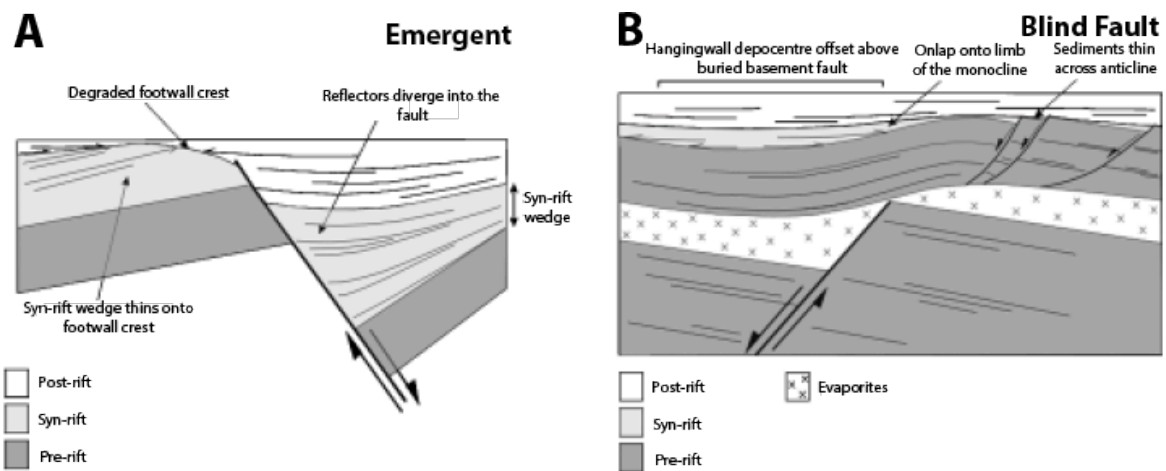

Figure 6.2: (**A**) Wedge-shape bed sets onlapping the pre-rift bedrock with fault drag. (**B**) A synclinal growth flexure associated with the propagation of a buried blind-fault tip. Slightly modified from Marsh et al. (2014).

The application of these general interpretation criteria in the present study is shown as a series of three examples in Fig. 6.3. The key features considered were the base and top of the Garn Formation, the lateral continuity of the Garn Fm. across a particular fault, its cross-fault thickness jump and the context possibility of its syn- or post-depositional removal by erosion.
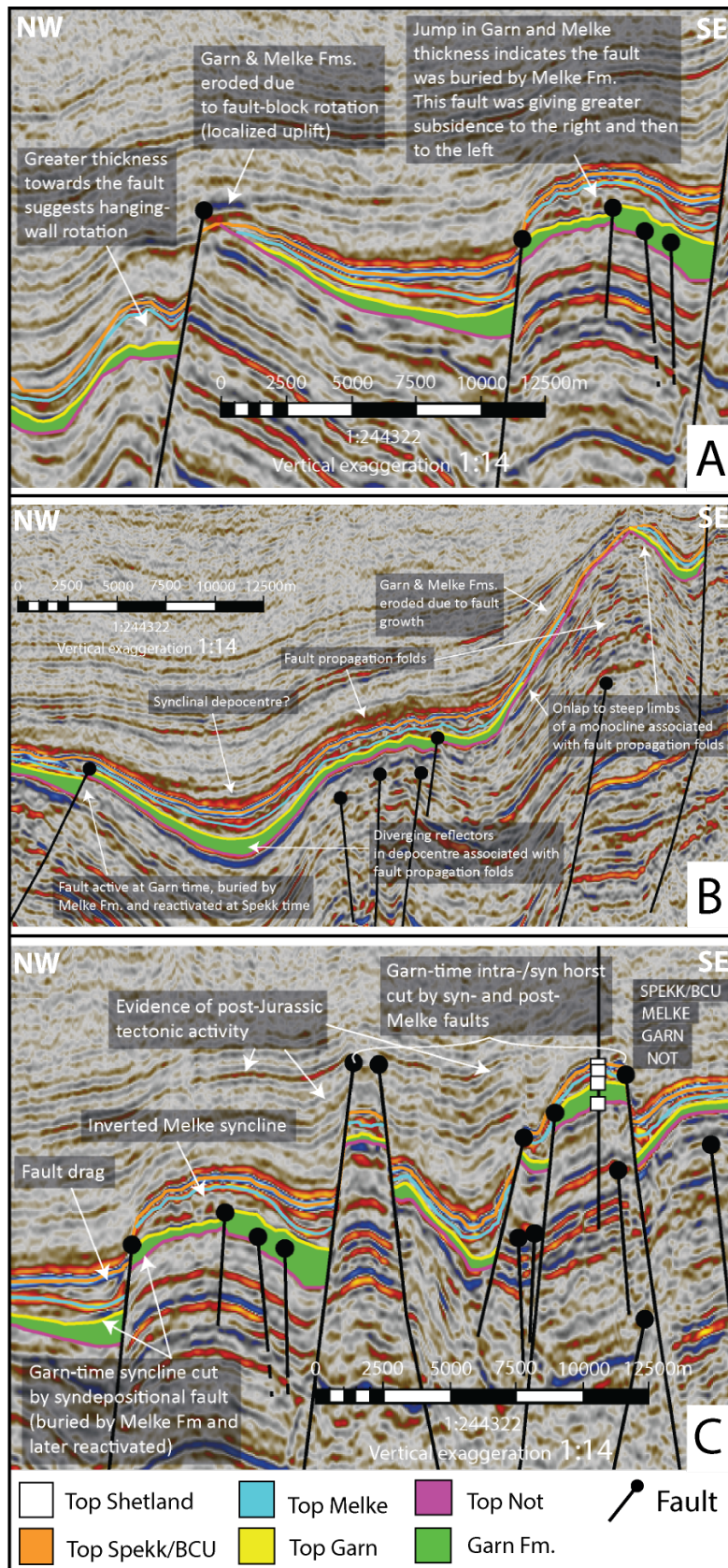
Figure 6.3: Example details of the interpretation of seismic section NW–SE (Fig. 3.1). (**A**) Evidence of syn-rift deposition with sediment erosion at footwall crests and deposition in hanging-wall depocentres. (**B**) Evidence of pulses of tectonic activity by fault reactivation and syn- to post-rift deformation of the Garn Fm. Note the geometries suggesting development of fault-propagation folds. (**C**) Evidence of post-Jurassic tectonic activity shown by the upward curving of seismic reflectors. Seismic data courtesy of TGS.

The interpretive evidence derived here from the seismic sections substantiates the notion of a lateral variation in facies associations and varied, fault-controlled seafloor topography inferred from the sedimentological study of well cores. From each seismic section (Figs. 6.4B and 6.5B), a hypothetical model of the seafloor tectonic topography at the sedimentation time of the Garn Formation has been derived (Figs. 6.4A and 6.5A). Although the models are schematic, based on OWT in seconds and are not quite realistic in terms of thickness distribution, they indicate that the deposition of the Garn Fm. was apparently controlled by the varied seafloor topography of incipient grabens and half-grabens. A more realistic reconstruction could be done by a depth-conversion of seismic data before using reverse basin-modelling techniques and comparing basin reconstructions with information on palaeo-water depths derived from well and seismic data (e.g., see Bell et al., 2014). However, such a reconstruction is not attempted in the present sedimentological study, and the reader is referred to Corfield and Sharp (2000), Marsh et al. (2010) and Bell et al. (2014) for a structural synthesis of the Halten Terrace. The aim of the simple analysis in the present case was merely to verify the notion that the area of Garn Fm. sedimentation in Halten Terrace was bathymetrically compartmentalized into an array of NE-trending grabens and half-grabens, which might have enhanced the action of tidal currents (as postulated for the Kristin Field by Messina et al., 2014).

The displacement of an initially horizontal surface that intersects a fault will be greatest at the fault itself, and decrease with increasing distance away from the fault. This generates footwall uplift and hanging-wall subsidence, the latter of which creates a sedimentary basin (e.g., Gupta et al., 1998; Fig. 6.1A). This geometry will however be affected by fault propagation and forced folding (e.g., Gawthorpe et al., 1997; Withjack et al., 1990). Greater accommodation space in the sedimentary basin is created as the displacement accumulates on the boundary fault through time. Although the deepening factor is only seen in cross-section, the basin will also widen through time because of the width of the hanging-wall deflection increases with increasing fault displacement (Barnett et al., 1987). The length of the basin also increases through time due to increase of the fault length as the displacement accumulates (e.g., Cowie, 1998). The growth of the basin in depth, width and length through time will produce progressive onlap of syn-rift deposits on pre-rift rocks (Figs. 6.1B and 6.2A). This phenomenon is recognizable from the wedge-shaped geometry of rock packages in which syn-rift strata show thickening towards the boundary fault and onlap pre-rift rocks (Figs. 6.1B and 6.2A).

These wedges generally thin out onto the footwall crests, where truncation and onlap is observed (Figs. 6.1B and 6.2A). In some cases, the footwall crest might also become exposed as small islands (Fig. 6.1A) which are likely to be affected by erosion, resulting in a source of

local sediment supply for the subsiding basins in the hanging-wall. Downdip from the footwall crest, the seismic reflectors diverge towards the boundary fault where they onlap the hanging-wall dipslope (Fig. 6.1B). This geometry of reflectors defines the characteristic syn-rift wedge commonly observed in seismic data (cf. Prosser, 1993). Geometries associated with the evolution of fault propagation folds will in contrast exhibit reflectors diverging into hanging-wall depocentres from a point located above a buried fault tip and may also onlap the steep limbs of monoclines (Fig. 6.2B; Corfield and Sharp, 2000, Marsh et al., 2014). Such features are recognizable in the NW–SE seismic section (Fig. 6.5B), as highlighted in Figure 6.3B. The fault propagation folds are probably related to blind faults that were active beneath a layer of Triassic salt (Fig. 6.2B; see Corfield and Sharp, 2000; Marsh et al., 2014).

Evidence of fault-block rotation during sedimentation includes erosion of the Garn and Melke formations in areas of localized uplift (Fig. 6.3A) and greater thickness towards the bounding faults (Fig. 6.3A–C), resulting in the wedge-shape geometry of the formations (Fig. 6.3A–C, cf. Figs. 6.1B and 6.2A). Some faults active during the Garn time seem to have been buried during sedimentation of the Melke Formation and later reactivated (Fig. 6.3B–C).

The complex structural evolution of horst and graben structures with displaced Garn Formation, as observed in several places across the Halten Terrace (Figs. 6.3A–C, 6.4B and 6.5B), reveals post-Jurassic tectonic activity – as postulated by Brekke et al. (2001) for the Middle Jurassic to Early Cretaceous regional rifting phase. Most of these structures were probably formed during the Late Jurassic when rifting was most prominent in the Halten and Dønna terraces, before transferring out into the Møre and Vøring basins to the west during Early Cretaceous (Nøttvedt et al., 2008). Post-Jurassic tectonic activity is evident by the "curving" of seismic reflectors, which represents post-Jurassic deposits being dragged along the fault planes of some horst structures (Fig. 6.3C).
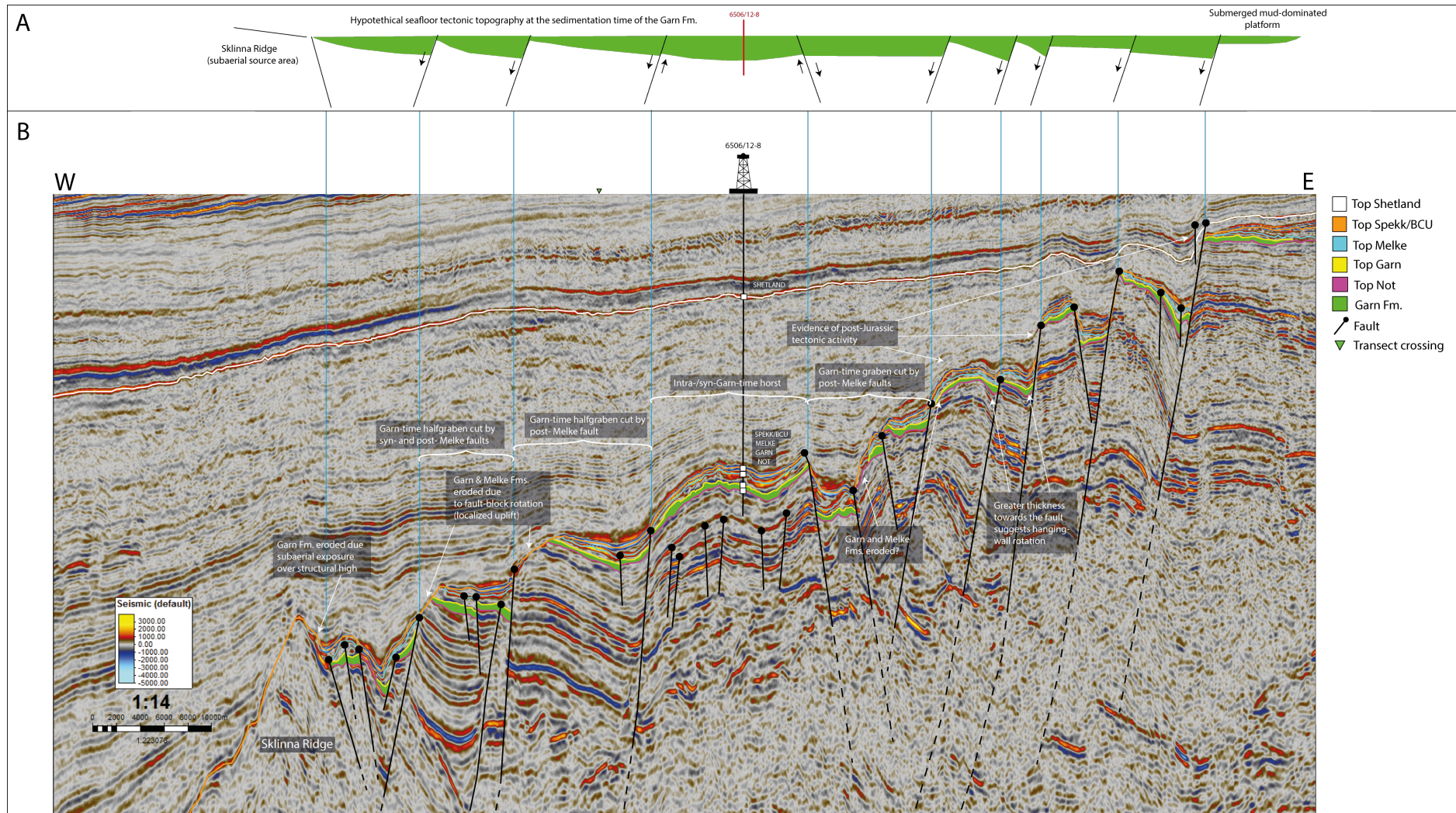
Figure 6.4: W–E seismic section across the Halten Terrace (see Fig. 3.1 for approximate location). (**A**) Model of interpreted seafloor tectonic topography at the sedimentation time of the Garn Fm. (**B**) Interpretation of faults and seismic horizons for the Shetland Gp., Spekk Fm./base-Cretaceous unconformity (BCU), Melke Fm., Garn Fm. and Not Fm. Note the indicated cases of erosion due to localized uplift with possible subaerial exposure, the thickening of the Garn Fm. towards boundary faults (wedge-shaped geometry) and areas of post-Jurassic tectonic activity. Seismic data vertically exaggerated (1:14) prior to generating the display image in Petrel. Seismic data courtesy of TGS.
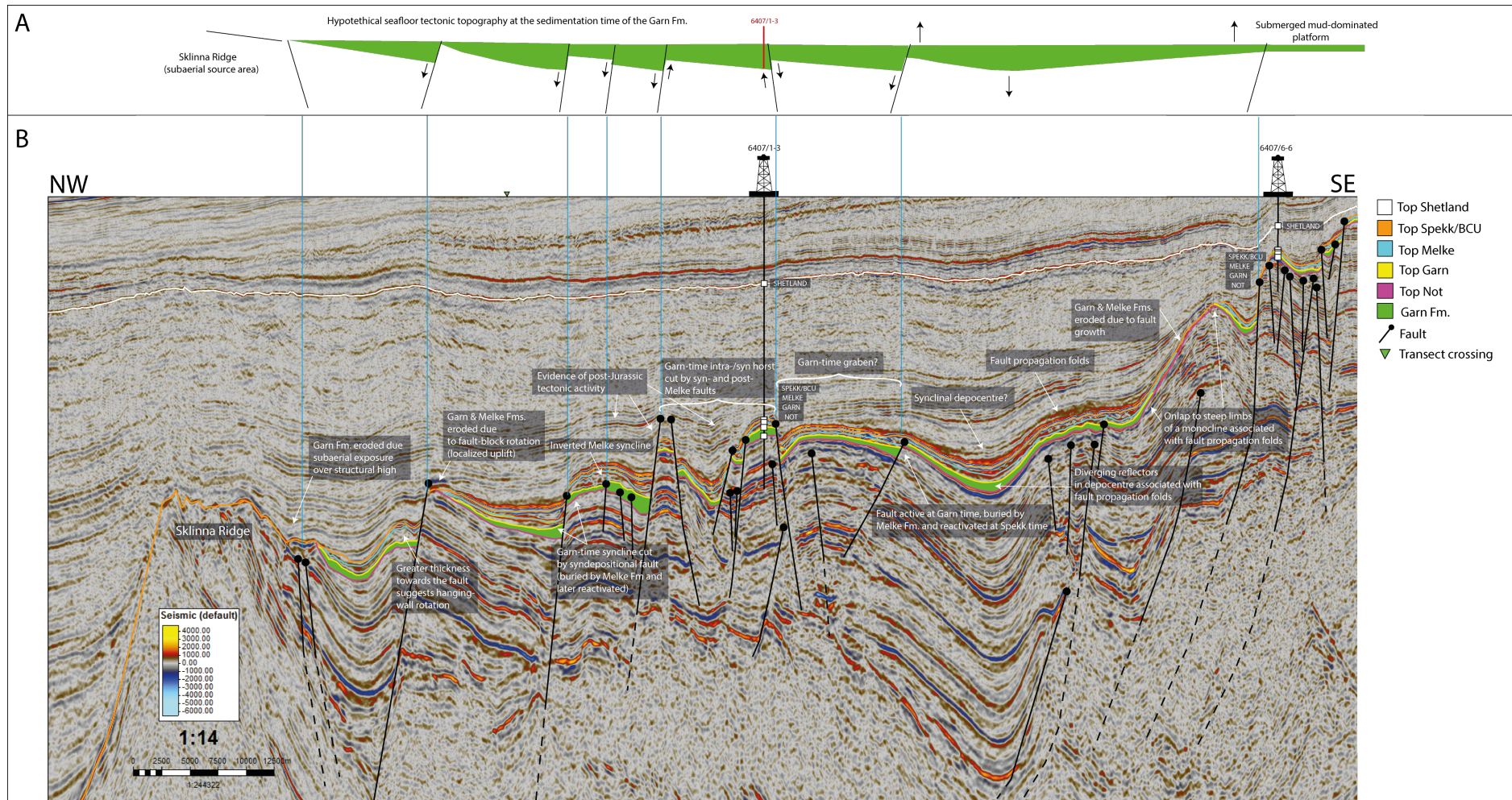
Figure 6.5: NW–SE seismic section across the Halten Terrace (see Fig. 3.1 for approximate location). (**A**) Model of interpreted seafloor tectonic topography at the sedimentation time of the Garn Fm. Well 6407/1-4 has been projected onto the section line. (**B**) Interpretation of faults and seismic horizons for the Shetland Gp., Spekk Fm./base-Cretaceous unconformity (BCU), Melke Fm., Garn Fm. and Not Fm. Note the indicated cases of erosion due to localized uplift with possible subaerial exposure, the thickening of the Garn Fm. towards boundary faults (wedge-shaped geometry) and areas of post-Jurassic tectonic activity. Seismic data vertically exaggerated (1:14) prior to generating the display image in Petrel. Seismic data courtesy of TGS.

6.2 Well-log interpretation

The distinction of sedimentary facies and their genetic assemblages (associations) is crucial in both petroleum exploration and reservoir geo-modelling, because facies are the primary control of petrophysical characteristics and fluid flow. Facies provide also crucial information on depositional processes and sedimentary environments (e.g., Walker, 1984a).

Sedimentary facies, similarly as ichnofacies and carbonate microfacies, are distinguished on the basis of well-core samples. However, for technical and economic reasons, wells are only sporadically cored over the entire stratigraphic interval of interest, whereas deviated and horizontal wells are problematic to retrieve core samples from. Geophysical wireline well-logs are incomparably wider available, and hence it is always worth trying to extrapolate the facies information from well cores onto wireline logs and use the latter as interpretive proxies. Such efforts have been made on quantitative basis by using statistical methods, such as discriminant analysis (e.g., Avseth et al., 2001; Tang et al., 2004) and Naïve-Bayes classifier (e.g., Li and Anderson-Sprecher, 2006), or methods focusing on the application of Artificial Neural Network (ANN) (e.g., Wong et al., 1995; Bhatt and Helle, 2002) and fuzzy logic (e.g., Cuddy, 2000; Saggaf and Nebrija, 2003). Common to all these approaches is that facies identification relies on the probability that the wireline log values for particular sedimentary facies in a cored well are the same for the facies of a non-cored well.

An attempt to link facies or their associations recognized in well cores with specific signatures of wireline logs has also been made – on a semi-quantitative visual basis – in the present study. The individual facies distinguished in well cores were assigned different colours (see well-core logs in Appendix) and these colour layers were then laid over the corresponding gamma-ray wireline logs (Fig. 6.6). The gamma-ray log is widely used to distinguish sandstones from shales (e.g., Serra, 1984) and might then help to distinguish sandstone facies from mudstone facies and mudstone-bearing heterolithic facies. The results helped to distinguish hypothetical parasequences composed of shallowing-upward facies associations (Fig. 6.6), but showed no obvious general link between the wireline log signature and specific sedimentary facies or even facies association. As discussed further in the next chapter, the local burial depth of the Garn Formation is highly varied – from less than 2.5 km to more than 4.5 km (Table 3.1) – and the related differential impact of diagenetic processes had apparently obscured the primary signature of sedimentary facies. The use of wireline logs from numerous non-cored wells in the study area as facies proxies thus appeared to be infeasible.
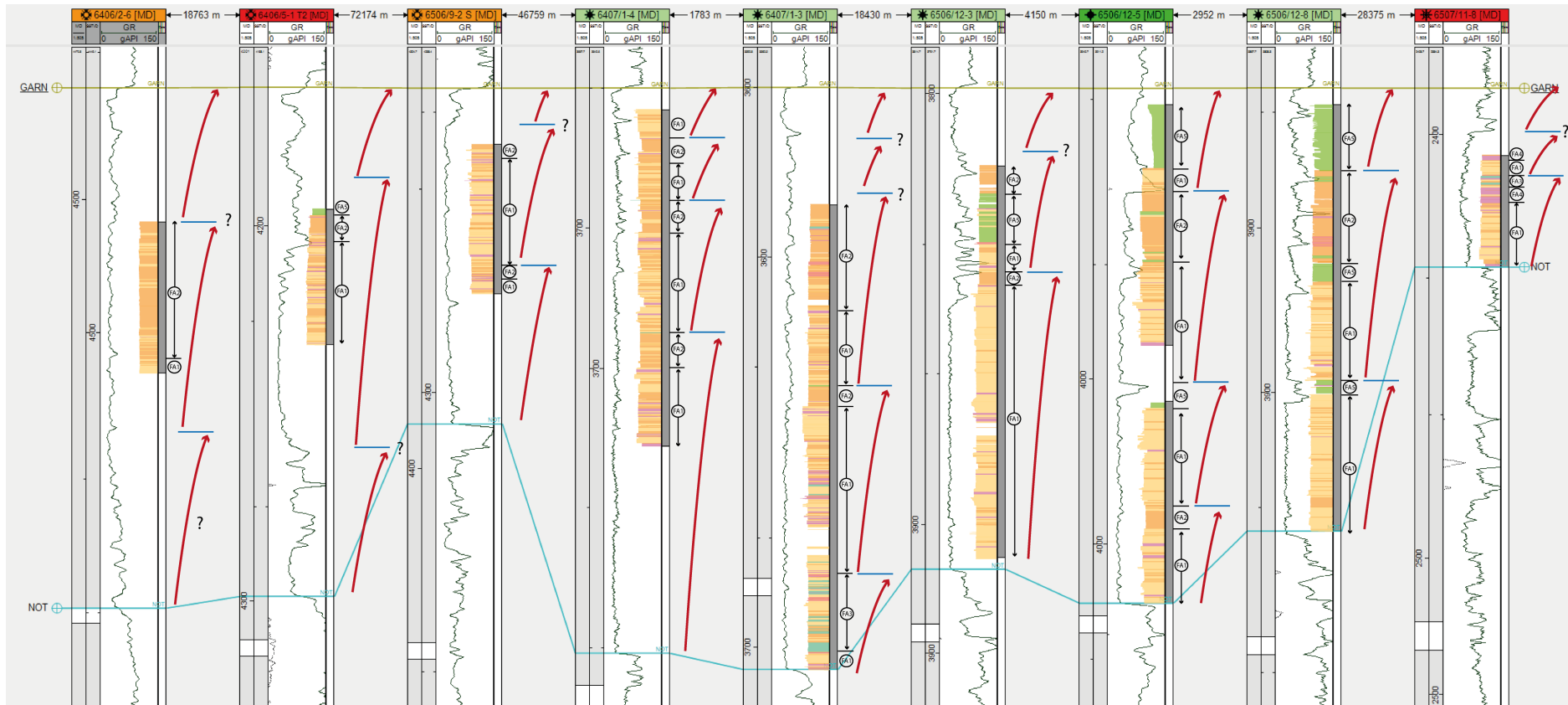
Figure 6.6: Interpretive extrapolation of sedimentary facies and their associations to gamma-ray logs (with standard API units of 0–150). The well logs are flattened to the top of Garn Fm. Facies colours are as in the Appendix, with five facies associations (FA1–5) distinguished. Note the shallowing-upwards facies successions bounded by marine-flooding surfaces and interpreted as parasequences. The laterally varied thickness and number of parasequences is attributed to syndepositional fault tectonics (differential seafloor subsidence).

7 DISCUSSION

7.1 East Greenland as regional analogue

It is widely accepted that the exposed geology of East Greenland serves as a comparative 'story book' for the Mid-Norway Continental Shelf. Although the East Greenland area in Jurassic was separated from the Norwegian Sea by an array of elongate islands (Fig. 7.1), many of the evolutionary trends in the structural and stratigraphic development are similar as a mirror image of the two margins of the proto-North Atlantic seaway (Ramberg et al. 2013).
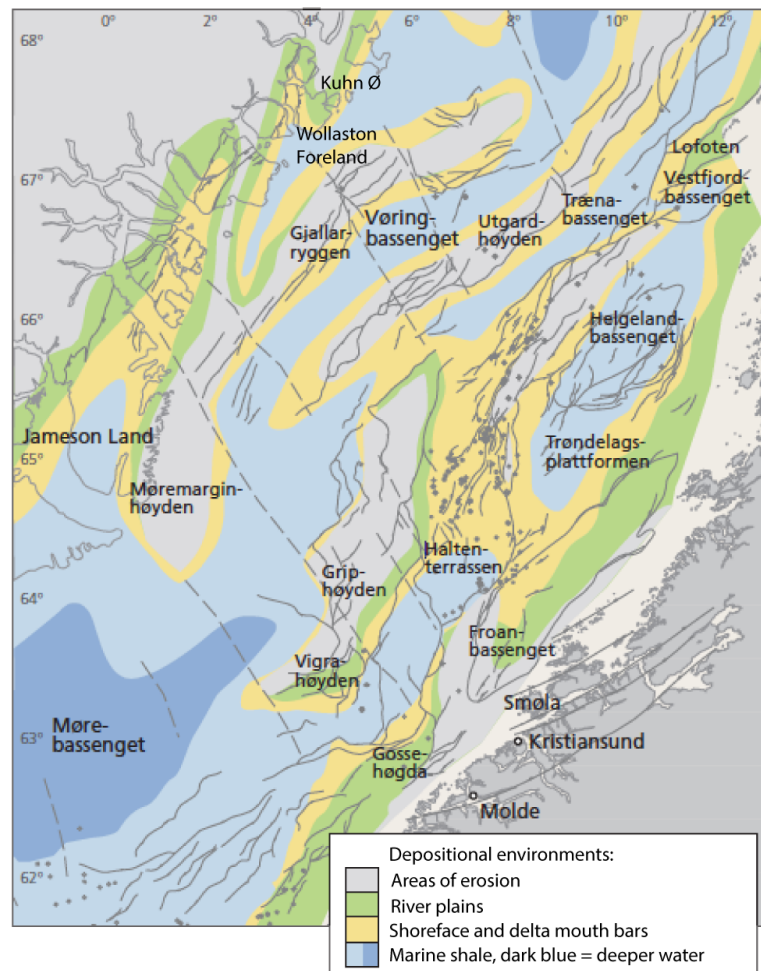
Figure 7.1: The proto-North Atlantic area between East Greenland and Mid-Norway comprised many narrow, NE-trending basins separated by elongate islands that became local sediment sources for the seaway's sub-basins in Mid-Jurassic. The Halten Terrace was one of these sub-basins. Slightly modified from Ramberg et al. (2013); note that their interpretation of depositional environments, based on earlier studies, still does not invoke any tidal deposits.

The Pelion Formation in East Greenland is time-equivalent of the Norwegian Sea Garn Formation. In the southern part of East Greenland, a deep-water basin known as the Jameson Land Basin formed in the Late Devonian to Early Permian time and continued to evolve

throughout the Mesozoic (Surlyk, 2003). The basin shows an overall layer-cake stratigraphy without major lateral changes in thickness, which is strongly in contrast to the Wollaston Foreland Basin to the north (Fig. 7.2; Surlyk, 2003). The structural development of this basin in Jurassic, in terms of its rotational fault-block tectonics (Fig. 7.2) and sedimentary environments (Surlyk, 2003) resembles closely – as a mirror image – that of the Halten Terrace (see earlier Figs. 2.2, 6.4 and 6.5).
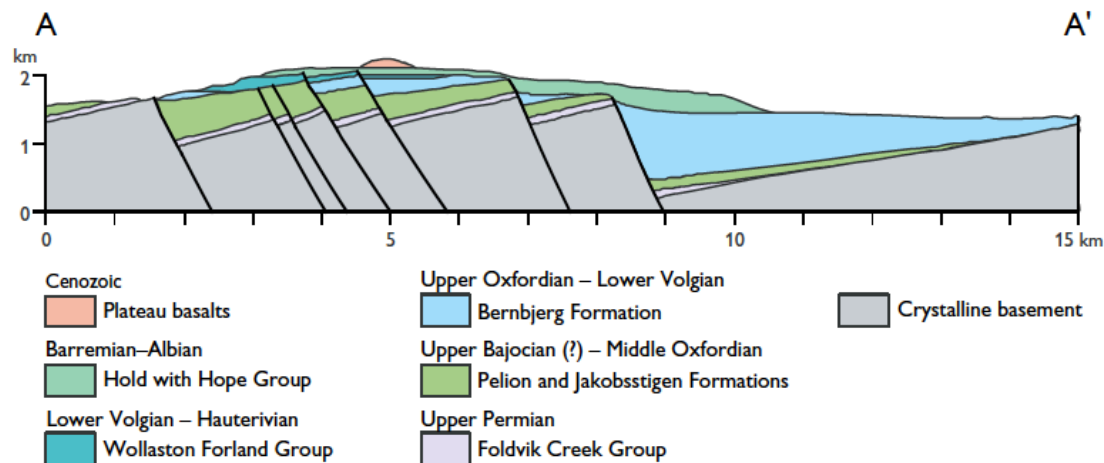

Figure 7.2: Cross-section through the Wollaston Foreland Basin, trending from the NW (A) to SE (A') (after Surlyk, 2003). Note the rotated fault blocks and half-grabens, similar as in the Halten Terrace (Figs. 2.2, 6.4 and 6.5). The bright-green deposits of the Pelion Fm. are time-equivalent of the Garn Fm. in the present study.

The Middle to Late Jurassic succession in Wollaston Foreland Basin is, like the Mid-Jurassic Garn Fm. in the Halten Terrace area, confined to fault-bounded sub-basins and shows similarities in both sedimentary facies and stratigraphic evolution in terms of a complex interplay of fault-controlled subsidence and impact of major eustatic sea-level changes (Surlyk et al., 1981). Surlyk and Clemmensen (1983) described the Pelion Fm. (up to 500 m thick) of the Wollaston Forland Basin in terms of five facies: (1) bidirectional large- and giant-scale cross-stratified sandstones; (2) structureless sandstones; (3) small-scale cross-laminated sandstones; (4) heterolithic deposits with occasional coal seams; and (5) wave-worked sandstones rich in oyster shells. The deposition was interpreted to have occurred in a tidally-dominated south-facing marine embayment with bayhead river deltas supplying sand from the north (Surlyk and Clemmensen, 1983).

By comparison, the Halten Terrace is thought to have been split into an array of incipient grabens and half-grabens that acted as narrow straits, rather than embayments. The main sand supply came from the adjacent islandic landmass to the northwest, and although some small

deltas might be involved – the main transport and dispersal of sand was by tidal currents accompanied by perennially wave action. Little or no deltaic deposits have thus far been documented within the Garn Fm. in the Halten Terrace (see Messina et al., 2014).

7.2 Sedimentary environment of the Garn Formation

The Middle Jurassic (Bajocian–Bathonian) Garn Formation (Fig. 2.4) in the Halten Terrace area has a sharp and apparently erosional contact with the underlying mud-dominated Not Formation, interpreted to be a regionally significant erosional surface of an intra-early Bajocian regression and possibly structural tilting (Corfield et al. 2001). The Garn Fm. is considered to be a transgressive succession that culminated in, and in the upper part also interfingered with, the heterolithic or muddy neritic deposits of the overlying Melke Fm. (Corfield et al., 2001; Messina et al., 2014).

In the present study, the Garn Formation in the Halten Terrace is interpreted in terms of a tidally-driven environment dominated by tidal sand-ridge deposits (FA1) intercalated with the deposits of sheltered (FA5) or non-sheltered (FA3) inter-ridge swales, commonly shallowing upwards into subtidal sandflat deposits (FA2) and occasionally into wave-worked deposits (FA4) (Table 5.1). The sedimentation was controlled by the Halten Terrace's active extensional fault-block tectonics (Figs. 6.4 and 6.5), whereby the differential seafloor topography of the NE-trending grabens, half-grabens and horst blocks both enhanced the NE–SW tidal currents and provided the accommodation space for sand accumulation.

The early studies of the Garn Formation envisioned a shoreface depositional environment with variable wave, fluvial and tidal influences. Gjelberg et al. (1987) initially envisioned the sedimentary environment of the Garn Formation as a sandy shoreface environment comprising SE-prograding delta lobes influenced by wave and tidal processes. This early interpretation was maintained by Dalland et al. (1988) and was brought to an extreme vision of fluvial influence by a more recent study – based on a single well core (6506/12-1) in the Smørbukk Field – by Fylling (2010), who envisaged the Garn Fm. as a vertical stack of amalgamated braid-delta fluvial bars and marine-flooded braid-delta deposits. The main argument for fluvial origin was that the succession showed internal evidence of episodic erosion and abrupt grain-size changes, a dominance of large-scale (i.e., dune scale) cross-stratification and an absence of marine trace fossils. However, the lack of marine trace fossils in the Garn Fm. is not true in the light of the present regional study (see evidence in Chapter 4) and also both the abundance of large-scale cross-stratification and the episodic erosion and abrupt increases in sediment grain size can be easily explained in terms of a wave-influenced tidal

environment (Chapter 5; see also Clifton and Dingler, 1984; Kreisa et al., 1986; Colella and d'Alessandro, 1988; Arnott, 1993; Longhitano and Nemec, 2005; Desjardins et al., 2012a; Messina et al., 2014). Notably, the evidence of sedimentary facies from the well 6506/12-1 studied by Fylling (2010) – as shown by NPD's well-core photographs – reveals a close resemblance to the facies identified in the present study and explained in terms of a tide-dominated environment (see Chapter 4). The present study concurs with the notion of a main sediment delivery via shoreface and deltaic systems from the NW (Gjelberg et al., 1987; Dalland et al., 1988; Messina et al., 2014), while also supporting the notion of Messina et al. (2014) that the sedimentary environment of the Garn Fm. in Halten Terrace was topographically differentiated by syndepositional fault-block tectonics and strongly influenced by the action NE–SW tidal currents.

Regional palaeogeographic reconstructions suggest that the Early to Middle Jurassic sedimentation most likely occurred within a narrow seaway extending from the open Boreal Sea in the north, bounded by a sand-supplying landmass to the west and the Trøndelag Platform to the east (Fig. 2.3), and reaching out to the open Tethys Ocean in the south (Gjelberg et al., 1987; Doré, 1992; Brekke et al., 2001; Nøttvedt et al., 2008). The sand-supplying landmass probably consisted of an island or islands (Fig. 7.1), which would have had small water catchments (Messina et al., 2014) and thereby unlikely to form large river deltas stretching out onto the Halten Terrace area, as postulated by Dalland et al. (1988).

Narrow seaways and straits that link large open-sea water bodies are a unique depositional setting where geomorphic constriction and possibly a slight difference in water elevation at the two ends of the strait can lead to amplification of tidal and/or oceanographic currents (Montenat et al., 1987; Colella and d'Alessandro, 1988; Pratt, 1990; Sztanó and Boer, 1995). As a result, their sedimentary dynamics, facies organization and response to relative sea-level changes are unlike any other shallow-marine environments (Anastas et al., 2006).

The deposition of the Garn Formation occurred in a syn-rift regional setting (Figs. 6.3, 6.4 and 6.5), where sediment accumulated in a series of incipient shallow grabens (Fig. 7.3) and half-grabens (Fig. 7.4) that formed due to extensional faulting or fault-propagated flexuring (Blystad et al., 1995; Corfield and Sharp, 2000; Corfield et al., 2001; Marsh et al., 2010). In the axial parts of the tectonic grabens and half-grabens within the Halten seaway (Figs. 6.4 and 6.5), tidal sand-ridges were formed by amplified tidal currents (Corfield et al., 2001; Messina et al., 2014), whose southwards flows might have dominated due to enhancement by boreal storms (see McBride, 2003). The fault-controlled development of accommodation space was spatially differential (Figs. 6.4 and 6.5) and driven by pulses of tectonic extension, which

resulted in deposition of upwards-shallowing parasequences punctuated by marine flooding surfaces (Fig. 6.6).
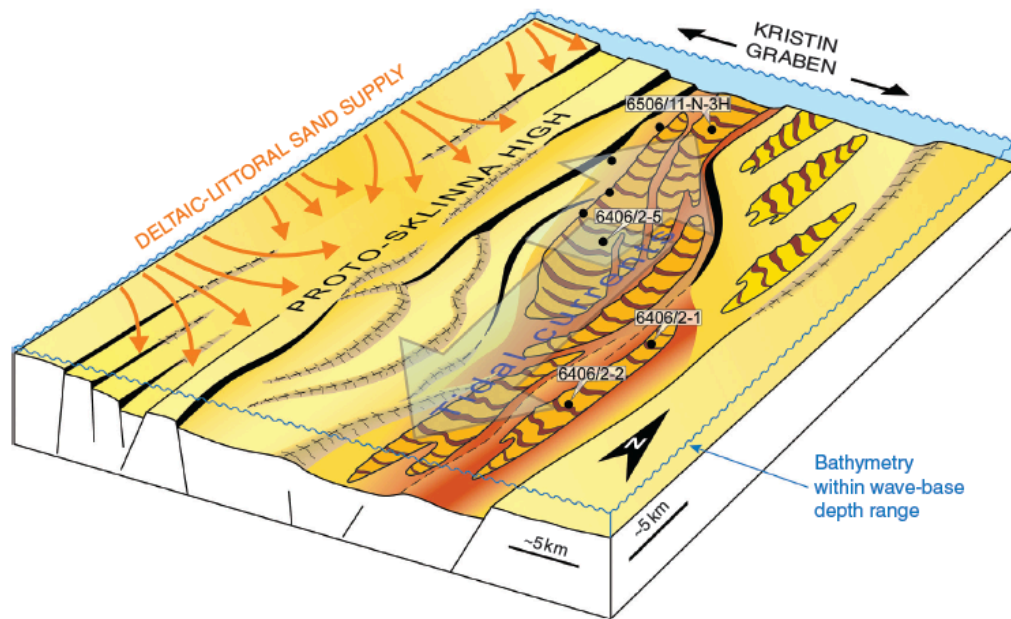

Figure 7.3: Hypothetical reconstruction of the sedimentary environment of Garn Fm. in the Kristin Field by Messina et al. (2014). Note the incipient Kristin graben, conveying enhanced tidal currents, and the development of tidal sand ridges. The reconstructed Kristin graben is at the outer margin of the Halten Terrace, bounded to the NW by the Sklinna High. A similar pattern of sedimentation may have characterized at least some of the other incipient grabens within the Halten Terrace area (see Figs. 6.4 and 6.5).
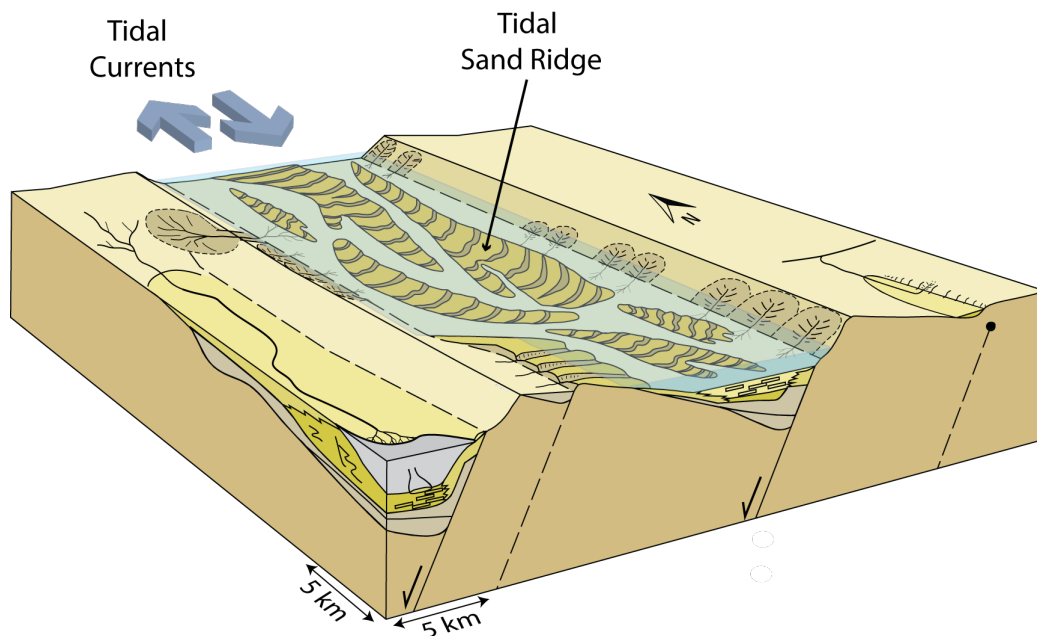
Figure 7.4: Hypothetical model for the formation of tidal sand ridges in a half-graben. Redrawn and slightly modified from Gawthorpe and Leeder (2000). A similar pattern of sedimentation may have characterized some of the other incipient half-grabens in the Halten Terrace area (see Figs. 6.4 and 6.5).

The dominant role of tidal currents for the Garn Formation was not recognized in the early studies (see Fig. 7.1), but has been increasingly postulated with the recognition of tidal dunes and tidal sand ridges (Corfield et al., 2001; Elfenbein et al., 2005; Quin et al., 2010; Messina et al., 2014). The present study concurs with this interpretation by recognizing the dominance of tidal sand-ridge deposits (FA1) in all studied wells, and thereby demonstrating a regional significance of the sedimentation model postulated by Messina et al. (2014) for the Kristin Field. Shelf sand ridges are thought to develop during marine transgression under the following four conditions (Snedden and Dalrymple, 1999): (1) a seafloor topography with pre-existing irregularities; (2) an adequate supply of sand; (3) sand-transporting tidal and/or storm-driven currents; and (4) sufficient time for the sand to be moulded into a ridge or a field of ridges. All these conditions would appear to have been fulfilled in the area of the Mid-Jurassic Halten Terrace.

Tidal longitudinal bars (sand ridges) and transverse bars (sand waves) (Fig. 5.3) abound on modern transgressive shelves (e.g., Houbolt, 1968; Swift and Field, 1981; Thomas and Anderson, 1994; Berné et al., 1998, 2002; Reynaud et al., 1999; Snedden and Dalrymple, 1999; Trentesaux et al., 1999; Snedden et al., 2011), but their common occurrence in ancient transgressive shelf settings has only recently begun to be recognized (Corfield et al., 2001; Longhitano and Nemec, 2005; Michaud, 2011; Olariu et al., 2012b; Schwarz, 2012; Messina et al., 2014; Leva López et al., 2016). This evidence runs counter to the earlier notions that tidal sand bars in a transgressive shelf setting cannot form because of the declining sand supply and that, even if formed, they have a poor preservation potential (Berné et al., 2002; Coe and Church, 2003). Another reason hindering recognition of tidal sand bars in ancient shelf settings was the lack of a facies model for their development. Leva López et al. (2016) proposed an architectural facies model for tidal bars formed in open-marine shelf settings and encased in mud. However, this model differs from the models proposed for shelf-hosted, tide-dominated and persistently wave-influenced narrow seaways, where mud tends to be kept in perennial suspension by waves, chiefly sand is deposited and where tidal sand bars are the seaway's main morphodynamic element (Colella and d'Alessandro, 1988; Longhitano and Nemec, 2005; Longhitano et al., 2012; Messina et al., 2014). It is these models that are particularly relevant to the sedimentary infill of the incipient grabens and half-grabens of the rifting pre-collapse Halten Terrace seaway (Figs. 6.4 and 6.5).

In such strait-like settings, the main transport of sand was by the confinement-boosted tidal currents, while the upper accommodation limit for tidal sand-bar growth was defined by the water depth and fairweather wave base. Messina et al. (2014) suggested a fairweather wave

base at a water depth of 5 m as a reasonable estimate for such marine settings. Therefore, the build-up of sand-bar deposits (FA1) would generally culminate in the shoal-water deposits of subtidal sandflat (FA2) or wave-worked shoal-water deposits (FA4) (Fig. 6.6). The sand deposition on the inter-graben horsts and half-graben elevated margins was limited to these shoal-water deposits of FA2 and FA4 (Table 5.1). Sand was probably swept from the horsts and footwall crests into the hangingwall depozones during phases of decreased accommodation (see Yielding, 1990; Ter Voorde et al., 1997). The diverging and converging topographic configuration of the tidal ridges (Figs. 7.3 and 7.4) resulted in both sheltered and non-sheltered inter-ridge swales, where the deposits of FA5 and FA3 (Table 5.1) were accumulated, respectively.

The present study thus concurs with the study by Messina et al. (2014) from the Kristin Field, where the following three facies associations in the Garn Formation were recognized: tidal sand-ridge deposits, inter-ridge swale-fill deposits and wave-worked littoral deposits. Although wave-worked deposits in the present case have been recognized in only one well (6507/11-8, Fig. 6.6), it should be kept in mind that the hypothetical Kristin graben was at the land-bound outer margin of the Halten Terrace seaway (Fig. 7.3), where sand supply was highest, bathymetry was shallower and where accommodation could have been more frequently exhausted. The wells used for the present study are from the seaway's axial part and from the thickest zones of the Garn Fm., which means local grabens and half-grabens. The inter-graben horst blocks and half-graben margin zones, where the deposits of FA4 (Table 5.1) would expectedly dominate, are hardly represented by well cores in the present study. The tidal currents in the seaway's axial part were likely strongest, whereby the shallowing of water there promoted formation of subtidal sandflats, rather than allowing wave action to prevail on the seafloor, before another pulse of tectonic subsidence increased the accommodation again and permitted a new generation of sand ridges to develop.

The deposition of the Garn Formation in the Halten Terrace seaway was incremental, controlled by pulses of tectonic subsidence, and was mainly aggradational (Elfenbein et al., 2005), although involving both progradation and lateral migration of successive tidal sand ridges (Messina et al., 2014). The latter authors have hypothetically suggested that the prevalent tidal-current direction was towards the south (SW), on the account of a stormy Boreal Sea wave climate to the north.

Corfield et al. (2001) recognized several episodes of minor transgressions and normal regressions within the Garn Fm. in the Smørbukk and Smørbukk South fields, yet without specifying their exact number. Messina et al. (2014) in the Kristin Field at the outer (NW)

margin of the Halten Terrace recognized sixteen transgressive–regressive parasequences. However, this outer marginal zone of the seaway was probably the most sensitive to the interplay of bathymetric changes and pulses of sediment supply. The present study from the seaway's main axial zone has recognized on a local well-core basis between 3 and 5 transgressive–regressive parasequences which are ~7–58 m thick (Fig. 6.6). This comparative evidence suggests that the Halten Terrace in Mid-Jurassic time acted as a synclinal seaway compartmentalized by fault-block tectonics into grabens and half-grabens, with spatially varied bathymetric responses and parasequence thicknesses, and with the seaway's outer marginal zone being much more sensitive to relative sea-level changes than its axial zone. The seaway's sequence stratigraphy, driven by local tectonics, thus cannot be used as a simple record of lower-order eustatic sea-level changes, even though such may in reality have been involved (see Eriksson and Simpson, 1990).

The variable thickness, apparent diachroneity and highly differential burial depth of the Garn Formation has been recognized on both a regional scale (Gjelberg et al. (1987) and a local scale of 5–10 km (Corfield et al., 2001; Messina et al., 2014). Interpretation of seismic data by Corfield et al. (2001) indicated an occurrence of "older" Garn sandstones of early to earliest-late Bajocian age in the northern part of a synclinal depocentre between the Smørbukk and Smørbukk South fields, and "younger" Garn sandstones (late Bajocian to early Bathonian in age) on the structural highs of the Smørbukk South Field and in the crestal areas of the Smørbukk Field (Fig. 7.5). A similar relationship – with the wave-worked sandstones of uppermost Garn Fm. retreating onto the basin-margin high while interfingering basinwards with the expanding muddy heterolithic deposits of the lower Melke Fm. – was recognized by Messina et al. (2014) along the eastern margin of the hypothetical graben in the Kristin Field (Fig. 7.3). A similar high diachroneity characterizes the upper boundary of the time-equivalent Pelion Fm. in East Greenland, where the shallow-marine littoral sandstones pass southwards into silty, micaceous neritic mudstones of the Fossilbjerget Fm. (Surlyk, 2003).
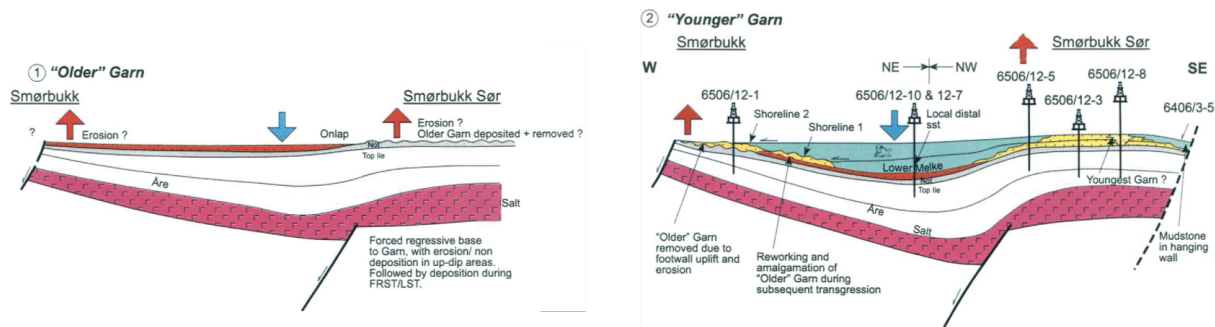
Figure 7.5*: A simplified model proposed by Corfield et al. (2001) for the tectono-stratigraphic development of the Garn Fm. sandstones and Melke Fm. mudstones in relation to the growth of the Smørbukk and Smørbukk South structures. Note that the "older" Garn sandstones are restricted to a synclinal depocentre, whereas the "younger" Garn sandstones are onlapping structural highs/crestal areas and are coeval with the Melke mudstones deposited along the syncline axis.

Corfield et al. (2001) thus concluded, on the basis of seismic, wireline well-log and biostratigraphic data, that there is a clear time-correspondence between the up-dip Garn sands on structural highs and the down-dip Melke mudstones in the basin lows (Fig. 7.5). This may have occurred because the sea-level rise forced the shoreline to back-step onto structural highs, where the "older" Garn sands were absent or removed and replaced by "younger" Garn sands concurrently with the deposition and expansion of muddy Melke facies in the synclinal axial zones of the basin grabens and half-grabens (Corfield et al., 2001; Messina et al., 2014).

    The limited dataset available in the present study does not allow confirming these interpretations from the Smørbukk, Smørbukk South and Kristin fields, but the evidence from the NW–SE seismic section (see Figs. 6.3B and 6.5B) seems to be consistent with the notion of a topographically controlled, marked short-distance diachroneity of the Garn/Not lithostratigraphic boundary. Anyway, the interpretive stratigraphic model of a diachronous expansion of the Garn Fm. sands onto the flanks of the basin grabens and half-grabens – with a concurrent replacement of sand by the Melke Fm. neritic mud along the local depoaxes – is an important addition to the general pattern of Mid-Jurassic sedimention in the Halten Terrace area and also bears important implications both for the spatial sand predictions in subsurface exploration and for the development of actual reservoir geo-models.

7.3 Problems with an extrapolation of well-core facies to wireline logs

Extrapolation of well-core sedimentary facies to non-cored wireline logs has long been a universally attractive and widely attempted search for a 'holy-grail', as it might allow turning the wireline logs directly into facies logs. Various quantitative (statistical or stochastic) and semi-quantitative attempts have been made in the literature to establish a possible correspondence of wireline logs with well-core facies (see earlier review in Chapter 6.2), but

few successes have thus far been reported. A semi-quantitative 'wild-shot' attempt has also been duly made in the present study by trying to correlate well-core sedimentary facies with specific and potentially diagnostic gamma-ray wireline signatures (Fig. 6.6). The geophysical gamma-ray well log is known to be the most sensitive wireline log when it comes to the recognition of lithofacies, such as 'clean' sandstones, mud-rich sandstones (wackes), heterolithic interlayered mudstone-sandstone deposits and pure mudstones (e.g., Serra, 1984).

This attempt has proven to be unsuccessful, showing no obvious general link between the wireline log signature and specific sedimentary facies or even facies association (see Fig. 6.6). The individual well-cores are from very different burial depths (from less than 2.5 km to more than 4.5 km; see Table 3.1), and the effect of their depth-related differential diagenesis (cementation) has apparently overwhelmed the signal of the primary heterogeneity of their sedimentary facies. The Garn Fm. sandstones in some well cores are moderately cemented, while being heavily cemented with silica and showing micro-styllotization in deeper cores. The Garn Fm. in its different parts was invaded by hydrocarbons at its different burial stages, which suppressed cementation at different stages of advance. In its other parts, the formation was not invaded by hydrocarbons at all and the diagenesis there proceeded even to a micro-styllotization stage (see Figs. 4.3B–C). Quin et al. (2010) reported on the formation of micro-styllolites in thin muddy drapes and micaceous sandstone laminae in the Kristin Field. Corfield et al. (2001) in the Smørbukk South Field reported on the development of early diagenetic cements from well cores in both up-dip (structurally high) and down-dip (original depozone) parts of the Garn Fm., which indicates a profound restructuring of the Mid-Norway Shelf by its eventual Palaeocene collapse and the opening of the North Atlantic oceanic branch. In short, the differential diagenetic history and highly differential burial depth appear to have obscured the primary signature of facies heterogeneity in the Garn Fm. on a regional scale in terms of the resulting wireline signature.

8 CONCLUSIONS

The sedimentary succession of the mid-Jurassic Garn Formation in Halten Terrace area, Mid-Norway Continental Shelf, has been studied on the basis of selected well cores, wireline logs and seismic sections with an aim to improve the general understanding of its sedimentary environment and to assess the role of contemporaneous fault tectonics in its deposition. This sedimentological study leads to the following main conclusions:

- The evidence from widely spread wells, including core samples from 9 wells and wireline logs from nearly 30 wells, indicates that the Garn Fm. is virtually dominated by sandstones on regional scale. The thickness of Garn Fm. commonly exceeds 100 m, but is highly varied on a local scale, within the lateral distances of 5–10 km.

- The sandstone succession is interpreted to represent tidal sand ridges (longitudinal bars) accompanied by deposits of sheltered or non-sheltered inter-ridge swales and commonly shallowing upwards into subtidal sandflat deposits. Sandflat deposits are common as sedimentation episodes, but are rarely prominent, whereas subordinate wave-worked littoral deposits are only locally prominent. This palaeoenvironmental interpretation supports the notion that the mid-Jurassic Halten Terrace seaway was virtually dominated by tidal currents, but was also differentiated bathymetrically by syndepositional fault-block tectonics.

- The evidence from seismic sections indicates that the sedimentation of the Garn Fm. was widely controlled by contemporaneous extensional-fault activity, with the main sand deposition confined to incipient (shelf pre-collapse) grabens and half-grabens.

- Facies analysis confirms the notion that the Garn Fm. is a transgressive succession composed of transgressive to normal-regressive parasequences and is therefore interpreted as a transgressive parasequences set. However, the sedimentation was tectonically-controlled and the number of parasequences depended on the local fault activity. The present study from the axial part of the Halten Terrace seaway indicates 3–5 such parasequences on a local basis, but the number of parasequences apparently increases towards the seaway's more sensitive western (NW) margin – where up to 16 parasequences were recognized by Messina et al. (2014).

- The translation of wireline well-log signatures into well-core sedimentary facies appears to be an impossible task in the present case, where the Garn Fm. – due to the post-Cretaceous collapse of the Mid-Norway Shelf margin – reached a burial depth ranging from <2.5 km

to >4.5 km. The differential diagenetic effect of the spatially differential sediment burial has virtually obscured the primary properties of sedimentary facies.

As a recommendation for future research, the present study suggests the following main lines of further detailed investigation:

- A full-scale 3-D seismic-image analysis of the Garn Fm., which could verify the notion of syndepositional fault activity, with incipient grabens and half-grabens, in the mid-Jurassic Halten Terrace area.

- A detailed analysis of core and wireline well-logs to check if the deposits at similar burial depth may still bear some wireline-log signatures recognizably correlative with core-log facies.

- A challenging source-to-sink budgeting study of the system of sand supply and dispersal in tidally-dominated seaways supplied with sand delivered laterally and distributed longitudinally along the seaway axis by reversing tidal currents.

REFERENCES

Allen, J. R. L., 1980, Sand waves: a model of origin and internal structure: Sedimentary Geology, v. 26, p. 281–328.

Allen, J. R. L., 1982, Sedimentary Structures: Their Character and Physical Basis: Developments in Sedimentology, 30A. Elsevier, Amsterdam, 593 p.

Anastas, A. S., Dalrymple, R. W., James, N. P., and Nelson, C. S., 2006, Lithofacies and dynamics of a cool-water carbonate seaway: mid-Tertiary, Te Kuiti Group, New Zealand: Geological Society, London, Special Publication, v. 255, p. 245–268.

Arnott, R. W. C., 1993, Quasi-planar laminated sandstone beds of the Lower Cretaceous Bootlegger Member, north-central Montana: evidence of combined-flow sedimentation: Journal of Sedimentary Petrology, v. 63, 488–494.

Avseth, P., Mukerji, T., Jørstad, A., Mavko, G., and Veggeland, T., 2001, Seismic reservoir mapping from 3-D AVO in a North Sea turbidite system: Geophysics, v. 66, p. 1157–1176.

Bann, K. L., Fielding, C. R., MacEachern, J. A., and Tye, S. C., 2004, Differentation of estuarine and offshore marine deposits using integrated ichnology and sedimentology: Permian Pebbley Beach Formation, Sydney Basin, Australia. In: McIlroy, D. (ed.), The Application of Ichnology to Palaeoenvironmental and Stratigraphic Analysis: Geological Society, London, Special Publication, v. 228, p. 179–211

Barnett, J. A., Mortimer, J., Rippon, J. H., Walsh, J. J., and Watterson, J., 1987, Displacement geometry in the volume containing a single normal fault: AAPG Bulletin, v. 71, p. 925–937.

Bell, R., Jackson, C., Elliott, G., Gawthorpe, R., Sharp, I. R., and Michelsen, L., 2014, Insights into the development of major rift-related unconformities from geologically constrained subsidence modelling: Halten Terrace, offshore mid Norway: Basin Research, v. 26, p. 203–224.

Berné, S., Lericolais, G., Marsset, T., Bourillet, J. F., and De Batist, M., 1998, Erosional offshore sand ridges and lowstand shorefaces: examples from tide-and wave-dominated environments of France: Journal of Sedimentary Research, v. 68, p. 540–555.

Berné, S., Vagner, P., Guichard, F., Lericolais, G., Liu, Z., Trentesaux, A., Yin, P., and Yi, H. I., 2002, Pleistocene forced regressions and tidal sand ridges in the East China Sea: Marine Geology, v. 188, p. 293–315.

Bhatt, A., and Helle, H. B., 2002, Determination of facies from well logs using modular neural networks: Petroleum Geoscience, v. 8, p. 217–228.

Blystad, P., Brekke, H., Færseth, R., B., Larsen, B. T., Skogseid, J., and Tørudbakken, B., 1995, Structural Elements of the Norwegian Continental Shelf, Part II: The Norwegian Sea Region: Norwegian Petroleum Directorate Bulletin 8, Stavanger, 45 p.

Bockelie, J. F., 1991, Ichnofabric Mapping and Interpretation of Jurassic Reservoir Rocks of the Norwegian North Sea: PALAIOS, v. 6, p. 206–215.

Boersma, J., 1969, Internal structure of some tidal mega-ripples on a shoal in the Westerschelde estuary, the Netherlands: report of a preliminary investigation: Netherlands Journal of Geosciences/Geologie en Mijnbouw, v. 48, p. 409–414.

Braathen, A., Osmundsen, P. T., Nordgulen, O., Roberts, D., and Meyer, G. B., 2002, Orogen-parallel extension of the Caledonides in northern Central Norway: an overview: Norwegian Journal of Geology, v. 82, p. 225–242.

Brekke, H., 2000, The tectonic evolution of the Norwegian Sea continental margin, with emphasis on the Voring and More basins: Geological Society, London, Special Publication, v. 167, p. 327–378.

Brekke, H., Dahlgren, S., Nyland, B., and Magnus, C. 1999. The prospectivity of the Vøring and Møre basins on the Norwegian Sea continental margin. In: Fleet, A. J., and Boldy, S. A. R. (eds.), Petroleum Geology of Northwest Europe: Proceedings of the 5th Conference, Geological Society, London, p. 261–274.

Brekke, H., Sjulstad, H. I., Magnus, C. & Williams, R. W., 2001, Sedimentary environments offshore Norway—an overview. In: Martinsen, O. J., and Dreyer, T. (eds.), Sedimentary Environments Offshore Norway – Palaeozoic to Recent: Norwegian Petroleum Society, Special Publication, v. 10, p. 7–37.

Bukovics, C., Cartier, E. G., Shaw, N. D., and Ziegler, P. A., 1984, Structure and development of the mid-Norway Continental Margin. In: Spencer, A. M., Johnsen, Mørk, A., Nysæther, E., Songstad, P., and Spinnangr, Å. (eds.), Petroleum Geology of the North European Margin: Graham and Trotman, London, p. 407–423.

Bukovics, C., and Ziegler, P. A., 1985, Tectonic development of the Mid-Norway continental margin: Marine and Petroleum Geology, v. 2, p. 2–22.

Cacchione, D. A., Drake, D. E., Ferreira, J. T., and Tate, G. B., 1994, Bottom stress estimates and sand transport on northern California inner continental shelf: Continental Shelf Research, v. 14, p. 1273–1289.

Chuhan, F. A., Bjørlykke, K., and Lowrey, C. J., 2001, Closed-system burial diagenesis in reservoir sandstones: Examples from the Garn Formation at Haltenbanken area, offshore mid-Norway: Journal of Sedimentary Research, v. 71, p. 15–26.

Clifton, H. E., and Dingler, J. R., 1984, Wave-formed structures and paleoenvironmental reconstruction: Marine Geology, v. 60, p. 165–198.

Coe, A. L, and Church, K. D., 2003, Sequence Stratigraphy and sea-level change. In: Coe, A. L. (ed.), The Sedimentary Record of Sea-Level Change: The Open University, Cambridge, p. 57–98.

Colella, A., 1990, Active tidal sand waves at bathyal depths observed from submersible and bathysphere (Messina Strait, southern Italy). In: Abstracts, IAS 13th International Sedimentological Congress (Nottingham, 26–31 August 1990), p. 98–99.

Colella, A., and d'Alessandro, A., 1988, Sand waves, Echinocardium traces and their bathyal depositional setting (Monte Torre Palaeostrait, Plio-Pleistocene, southern Italy): Sedimentology, v. 35, p. 219–237.

Collinson, J. D., 1969, The sedimentology of the Grindslow Shales and the Kinderscout Grit; a deltaic complex in the Namurian of northern England: Journal of Sedimentary Petrology, v. 39, p. 194–221.

Collinson, J. D., Thompson, D. B., and Mountney, N., 2006, Sedimentary Structures, 3rd edn.: Hertfordshire, England, Terra Publishing, 292 p.

Corfield, S., and Sharp, I., 2000, Structural style and stratigraphic architecture of fault propagation folding in extensional settings: a seismic example from the Smørbukk area, Halten Terrace, Mid-Norway: Basin Research, v. 12, p. 329–341.

Corfield, S., Sharp, I., Häger, K.-O., Dreyer, T., and Underhill, J., 2001, An integrated study of the Garn and Melke formations (Middle to Upper Jurassic) of the Smørbukk area, Halten Terrace, mid-Norway. In: Martinsen, O. J., and Dreyer, T. (eds.), Sedimentary Environments Offshore Norway – Palaeozoic to Recent: Norwegian Petroleum Society, Special Publication, v. 10, p. 199–210.

Cotter, E., 1975, Late Cretaceous sedimentation in a low-energy coastal zone: the Ferron Sandstone of Utah: Journal of Sedimentary Research, v. 45, p. 669–685.

Cowie, P. A., 1998, Normal fault growth in three-dimensions in continental and oceanic crust. In: Buck, W. R., Delaney, P. T., Karson, J. A., and Lagabrielle, Y. (eds.), Faulting and Magmatism at Mid-Ocean Ridges, Geophysical Monograph 106, p. 325–348.

Cuddy, S., 2000, Litho-facies and permeability prediction from electrical logs using fuzzy logic: SPE Reservoir Evaluation & Engineering, v. 3, p. 319–324.

Dalland, A., Worsley, D., and Ofstad, K., 1988, A lithostratigraphic scheme for the Mesozoic and Cenozoic succession offshore mid- and northern Norway: Norwegian Petroleum Directorate Bulletin 4, Stavanger, 65 p.

Dalrymple, R. W., 1984, Morphology and internal structure of sandwaves in the Bay of Fundy: Sedimentology, v. 31, p. 365–382.

Dalrymple, R. W., 1992, Tidal depositional systems. In: Walker R. G., James N. P. (eds.), Facies Models – Response to Sea Level Change: Geological Association of Canada, St. John's, Newfoundland, p. 195–218.

Dalrymple, R. W., 2010, Tidal Depositional systems. In: Dalrymple, R. W., James, N. P. (eds.), Facies Models 4. GEOText6: Geological Association of Canada, St. John's, Newfoundland, p. 199–208.

Dalrymple, R. W., Baker, E. K., Harris, P. T., and Hughes, M. G., 2003, Sedimentology and stratigraphy of a tide-dominated, foreland-basin delta (Fly River, Papua New Guinea). In: Sidi, F. H., Nummedal, D., Imbert, P., Darman, H., and Posamentier, H. W. (eds.), Tropical Deltas of Southeast Asia–Sedimentology, Stratigraphy, and Petroleum Geology: SEPM Special Publication, v. 76, p. 147–173.

Dalrymple, R. W., and Choi, K., 2007, Morphologic and facies trends through the fluvial–marine transition in tide-dominated depositional systems: a schematic framework for environmental and sequence-stratigraphic interpretation: Earth-Science Reviews, v. 81, p. 135–174.

Dalrymple, R. W., Knight, R., Zaitlin, B. A. and Middleton, G. V., 1990, Dynamics and facies model of a macrotidal sand-bar complex, Cobequid Bay – Salmon River Estuary (Bay of Fundy): Sedimentology, v. 37, p. 577–612.

Dalrymple, R. W., and Rhodes, R. N., 1995, Estuarine dunes and bars. In: Perillo, G. M. E. (ed.), Geomorphology and Sedimentology of Estuaries. Developments in Sedimentology, v. 53, p. 359–422. Elsevier, Amsterdam.

Davis, R. A., and Dalrymple, R. W. (eds.), 2012, Principles of Tidal Sedimentology, Springer, New York, 621 p.

De Mowbray, T., and Visser, M. J., 1984, Reactivation surfaces in subtidal channel deposits, Oosterschelde, southwest Netherlands: Journal of Sedimentary Research, v. 54, p. 811–824.

Desjardins, P. R., Buatois, L. A., and Mángano, M. G., 2012a, Tidal flats and subtidal sand bodies. In: Dirk, K., and Richard, G. B. (eds.), Trace Fossils as Indicators of Sedimentary Environments: Developments in Sedimentology, v. 64, p. 529–561. Elsevier, Amsterdam.

Desjardins, P. R., Buatois, L. A., Pratt, B. R., and Mángano, M. G., 2012b, Sedimentological–ichnological model for tide-dominated shelf sandbodies: Lower Cambrian Gog Group of western Canada: Sedimentology, v. 59, p. 1452–1477.

Doré, A. G., 1991, The structural foundation and evolution of Mesozoic seaways between Europe and the Arctic: Palaeogeography, Palaeoclimatology, Palaeoecology, v. 87, p. 441–492.

Doré, A. G., 1992, Synoptic palaeogeography of the Northeast Atlantic Seaway: late Permian to Cretaceous: Geological Society, London, Special Publication, v. 62, p. 421–446.

Doré, A. G., Lundin, E., Jensen, L., Birkeland, Ø., Eliassen, P., and Fichler, C., 1999, Principal tectonic events in the evolution of the northwest European Atlantic margin. In: Fleet, A. J., and Boldy, S. A. R. (eds.), Petroleum Geology of Northwest Europe: Proceedings of the 5th Conference, Geological Society, London, p. 41–61.

Dumas, S. and Arnott, R. W. C., 2006, Origin of hummocky and swaley cross-stratification – the controlling influence of unidirectional current strength and aggradation rate: Geology, v. 34, p. 1073–1076.

Dyer, K. R., and Huntley, D. A., 1999, The origin, classification and modeling of sand banks and ridges: Continental Shelf Research, v. 19, p. 1285–1330.

Ehrenberg, S., Dalland, A., Nadeau, P., Mearns, E., and Amundsen, E., 1998, Origin of chlorite enrichment and neodymium isotopic anomalies in Haltenbanken sandstones: Marine and Petroleum Geology, v. 15, p. 403–425.

Ehrenberg, S., Gjerstad, H., and Hadler-Jacobsen, F., 1992, Smørbukk Field: A Gas Condensate Fault Trap in the Haltenbanken Province, Offshore Mid-Norway. In: Halbouty, M. T. (ed.), Giant Oil and Gas Fields of the Decade 1978–1988: American Association of Petroleum Geologists, Memoir 54, p. 323–348.

Elfenbein, C., Husby, Ø., and Ringrose, P., 2005, Geologically-based estimation of kv/kh ratios: an example from the Garn Formation, Tyrihans field, mid-Norway. In: Doré, A. G. (ed.), North-West Europe and Global Perspectives: Proceedings of the 6th Petroleum Geology Converence, Geological Society, London, p. 537–543.

Elliott, G. M., Wilson, P., Jackson, C. A. L., Gawthorpe, R. L., Michelsen, L., and Sharp, I. R., 2012, The linkage between fault throw and footwall scarp erosion patterns: an example from the Bremstein Fault Complex, offshore Mid-Norway: Basin Research, v. 24, p. 180–197.

Eriksson, K. A., and Simpson, E. L., 1990, Recognition of high-frequency sea-level fluctuations in Proterozoic siliciclastic tidal deposits, Mount Isa, Australia: Geology, v. 18, p. 474–477.

Frey, R. W. (ed.), 1975, The Study of Trace Fossils. Springer-Verlag, Berlin, 562 pp.

Fylling, B., 2010, Sedimentological Development of the Fangst Group, Halten Terrace, Mid-Norway [Master thesis]: University of Bergen, 91 p.

Gabrielsen, R. H., and Robinson, C., 1984, Tectonic inhomogeneities of the Kristiansund—Bodø Fault Complex, offshore mid-Norway. In: Spencer, A. M., Johnsen, Mørk, A., Nysæther, E., Songstad, P., and Spinnangr, Å. (eds.), Petroleum Geology of the North European Margin: Norwegian Petroleum Society, Graham and Trotman, London p. 397–496.

Galloway, W. E., and Hobday, E., 1983, Terrigenous Clastic Depositional Systems: Applications to Petroleum, Coal, and Uranium Exploration, Springer-Verlag, New York, 411 p.

Gawthorpe, R. L., and Leeder, M., 2000, Tectono-sedimentary evolution of active extensional basins: Basin Research, v. 12, p. 195–218.

Gawthorpe, R. L., Sharp, I., Underhill, J. R., and Gupta, S., 1997, Linked sequence stratigraphic and structural evolution of propagating normal faults: Geology, v. 25, p. 795–798.

Gjelberg, J., Dreyer, T., Høie, A., Tjelland, T., and Lilleng, T., 1987, Late Triassic to Mid-Jurassic sandbody development on the Barents and Mid-Norwegian shelf. In: Brooks, J., and Glennie, K. (eds.), Petroleum Geology of North West Europe: Graham and Trotman, London, p. 1105–1129.

Gupta, S., Cowie, P. A., Dawers, N. H., and Underhill, J. R., 1998, A mechanism to explain rift-basin subsidence and stratigraphic patterns through fault-array evolution: Geology, v. 26, p. 595–598.

Harms, J. C., Southard, J. B., and Walker, R. G., 1982, Structures and Sequences in Clastic Rocks: Society of Economic Paleontologists and Mineralogists, Short Course, v. 9, 250 pp.

Harms, J. C., Southard, J. B., Spearing, D. R., and Walker, R. G., 1975, Depositional environments as interpreted from primary sedimentary structures and stratification

sequences: Society of Economic Paleontologists and Mineralogists, Short Course, v. 2, 161 pp.

Hein, F. J., 1987, Tidal/littoral offshore shelf deposits – Lower Cambrian Gog Group, Southern Rocky Mountains, Canada: Sedimentary Geology, v. 52, p. 155–182.

Helland-Hansen, W., Ashton, M., Lømo, L., and Steel, R., 1992, Advance and retreat of the Brent delta: recent contributions to the depositional model. In: Morton, A. C., Haszeldine, R. S., Giles, M. R., and Brown S. (eds.), Geology of the Brent Group: Geological Society, London, Special Publication, v. 61, p. 109–127.

Hildebrandt, C. and Egenhoff, S., 2007, Shallow-marine massive sandstone sheets as indicators of palaeoseismic liquefaction – An example from the Ordovician shelf of Central Bolivia: Sedimentary Geology, v. 202, p. 581–595.

Houbolt, J., 1968, Recent sediments in the southern bight of the North Sea: Geologie en mijnbouw, v. 47, p. 245–273.

Howard, J. D., and Frey, R. W., 1985, Physical and biogenic aspects of backbarrier sedimentary sequences, Georgia Coast, U.S.A: Marine Geology, v. 63, p. 77–127.

Hubbard, D. K., Oertel, G., and Nummedal, D., 1979, The role of waves and tidal currents in the development of tidal-inlet sedimentary structures and sand body geometry: examples from North Carolina, South Carolina, and Georgia: Journal of Sedimentary Research, v. 49, p. 1073–1092.

Kjærefjord, J., 1999, Bayfill successions in the Lower Jurassic Åre Formation, Offshore Norway: Sedimentology and heterogeneity based on subsurface data from the Heidrun Field and analog data from the Upper Cretaceous Neslen Formation, eastern Book Cliffs, Utah. In: Hentz, T. F. (ed.), Advanced Reservoir Characterization for the Twenty-First Century: SEPM, Gulf Coast Section, Special Publication, 19th Annual Research Converence, p. 149–157.

Klein, G. D., 1970, Tidal origin of a Precambrian quartzite—the lower fine-grained quartzite (middle Dalradian) of Islay, Scotland: Journal of Sedimentary Petrology, v. 40, p. 973–985.

Koch, J. O., and Heum, O. R., 1995, Exploration trends of the Halten Terrace. In: Hanslien, S. (ed.), Petroleum Exploration and Exploitation in Norway: Norwegian Petroleum Society, Special Publication, v. 4, p. 235–251.

Komar, P. D. and Miller, M. C., 1975, The initiation of oscillatory ripple marks and the development of plane-bed at high shear stresses under waves: Journal of Sedimentary Petrology, v. 45, p. 697–703.

Kreisa, R. D., Moiola, R. J. and Nøttvedt, A., 1986, Tidal sand wave facies, Rancho Rojo Sandstone (Permian), Arizona. In: Knight, R. J., and McLean, J. R. (eds.), Shelf Sands and Sandstones: Canadian Society of Petroleum Geologists, Memoir 11, p. 277–291.

Langhorne, D., 1973, A sandwave field in the outer Thames estuary, Great Britain: Marine Geology, v. 14, p. 129–143.

Leva López, J., Rossi, V. M., Olariu, C., and Steel, R. J., 2016, Architecture and recognition criteria of ancient shelf ridges; an example from Campanian Almond Formation in Hanna Basin, USA: Sedimentology, v. 63, p. 1651–1676.

Li, Y., and Anderson-Sprecher, R., 2006, Facies identification from well logs: A comparison of discriminant analysis and naïve Bayes classifier: Journal of Petroleum Science and Engineering, v. 53, p. 149–157.

Liu, Z., Berné, S., Saito, Y., Yu, H., Trentesaux, A., Uehara, K., Yin, P., Liu, J. P., Li, C., Hu, G., and Wang, X., 2007, Internal architecture and mobility of tidal sand ridges in the East China Sea: Continental Shelf Research, v. 27, p. 1820–1834.

Longhitano, S. G., 2011, The record of tidal cycles in mixed silici–bioclastic deposits: examples from small Plio–Pleistocene peripheral basins of the microtidal Central Mediterranean Sea: Sedimentology, v. 58, p. 691–719.

Longhitano, S. G., Mellere, D., Steel, R. J., and Ainsworth, R. B., 2012, Tidal depositional systems in the rock record: a review and new insights. Sedimentary Geology, v. 279, p. 2–22.

Longhitano, S. G. and Nemec, W., 2005, Statistical analysis of bed thickness variation in a Tortonian succession of biocalcarenitic tidal dunes, Amantea Basin, Calabria, southern Italy: Sedimentary Geology, v. 179, p. 195–224.

Mángano, M. G., Buatois, L. A., West, R. R., and Maples, C. G., 2002, Ichnology of a Pennsylvanian equatorial tidal flat: the Stull Shale Member at Waverly, eastern Kansas: Kansas Geological Survey Bulletin, v. 245, 133 p.

Mángano, M. G., and Buatois, L. A., 2004, Reconstructing early Phanerozoic intertidal ecosystems: Ichnology of the Cambrian Campanario Formation in northwest Argentina: Fossils and Strata, v. 51, p. 17–38.

Marsh, N., Imber, J., Holdsworth, R., Brockbank, P., and Ringrose, P., 2010, The structural evolution of the Halten Terrace, offshore Mid-Norway: extensional fault growth and strain localisation in a multi-layer brittle–ductile system: Basin Research, v. 22, p. 195–214.

Martinius, A. W., Kaas, I., Næss, A., Helgesen, G., Kjærefjord, J. M., and Leith, D. A., 2001, Sedimentology of the heterolithic and tide-dominated Tilje Formation (Early Jurassic, Halten Terrace, offshore mid-Norway). In: Martinsen, O. J., and Dreyer, T. (eds.), Sedimentary Environments Offshore Norway – Palaeozoic to Recent: Norwegian Petroleum Society, Special Publication, v. 10, p. 103–144.

McBride, R. A., 2003, Offshore sand banks and linear sand ridges. In: Middleton, G. V. (ed.), Encyclopedia of Sediments and Sedimentary Rocks: Kluiver Academic Publishers, Dordrecht, p. 737–739.

McIlroy, D. 2004a. Ichnofabrics and sedimentary facies of a tide-dominated delta: Jurassic Ile Formation of Kristin Field, Haltenbanken, offshore Mid-Norway. In: McIlroy, D. (ed.), 2004, The Application of Ichnology to Palaeoenvironmental and Stratigraphic Analysis: Geological Society, London, Special Publication, v. 228, p. 237–272.

McIlroy, D. (ed.), 2004b, The Application of Ichnology to Palaeoenvironmental and Stratigraphic Analysis: Geological Society, London, Special Publication, v. 228, 490 p.

McKee, E. D., and Weir, G. W., 1953, Terminology for stratification and cross-stratification in sedimentary rocks: Geological Society of America Bulletin, v. 64, p. 381–390.

Messina, C., Nemec, W., Martinius, A. W., and Elfenbein, C., 2014, The Garn Formation (Bajocian-Bathonian) in the Kristin Field, Halten Terrace: its origin, facies architecture and primary heterogeneity model. In: Martinius, A. W., Ravnås, R., Howell, J. A., Steel, R. J., and Wonham, J. P. (eds.), From Depositional Systems to Sedimentary Successions on the Norwegian Continental Margin: International Association of Sedimentologists, Special Publication, v. 46, p. 513–550.

Michaud, K. J., 2011, Facies Architecture and Stratigraphy of Tidal Ridges in the Eocene Roda Formation, Northern Spain [Master thesis]: Queen's University, Kingston, Ontario, 137 p.

Middleton, G. V., and Southard, J. B., 1984, Mechanics of Sediment Movement. Lecture Notes, SEPM Short Course 3: Society of Economic Paleontologists and Mineralogists, Tulsa, 246 p.

Montenat, C., Barrier, P., and Di Geronimo, I., 1987, The Strait of Messina, past and present: a review. Doc. Trav. IGAL (Paris), p. 7–13.

Mutti, E., Rosell, J., Allen, G., Fonnesu, F., and Sgavetti, M., 1985, The Eocene Baronia tide dominated delta-shelf system in the Ager Basin. In: Excursion Guidebook: Proceedings 6th International Association of Sedimentologists European Regional Meeting, p. 577–600.

Nio, S.-D., and Yang, C.-S., 1991, Diagnostic attributes of clastic tidal deposits: a review. In: Smith, D. G., Reinson, G. E., Zaitlin B. A., and Rahmani, R. A. (eds.), Clastic Tidal Sedimentology: Canadian Society of Petroleum Geologists, v. 16, p. 3–28.

Nishi, R., and Kraus, N. C., 1997, Mechanism and calculation of sand dune erosion by storms. In: Proceedings of the 25th Coastal Engineering Conference, ASCE, p. 3034–3047.

NPD, 2014, CO_2 Storage Atlas – Norwegian Continental Shelf. http://www.npd.no/en/Publications/Reports/Compiled-CO2-atlas/; available also at: http://www.npd.no/Global/Norsk/3-Publikasjoner/Rapporter/CO2-samleatlas/Chapter-5.pdf [Accessed 15.03.17].

NPD, 2017, Factpages, Norwegian Petroleum Directorate, http://www.npd.no, Norwegian Petroleum Directorate.

Nøttvedt, A., Johannessen, E. P., and Surlyk, F., 2008, The mesozoic of western Scandinavia and East Greenland: Episodes, v. 31, p. 59–65.

Okusa, S., and Uchida, A., 1980, Pore-water pressure change in submarine sediments due to waves: Marine Georesources & Geotechnology, v. 4, p. 145–161.

Olariu, C., Steel, R. J., Dalrymple, R. W., and Gingras, M. K., 2012a, Tidal dunes versus tidal bars: the sedimentological and architectural characteristics of compound dunes in a tidal seaway, the lower Baronia Sandstone (Lower Eocene), Ager Basin, Spain: Sedimentary Geology, v. 279, p. 134–155.

Olariu, M. I., Olariu, C., Steel, R. J., Dalrymple, R. W., and Martinius, A. W., 2012b, Anatomy of a laterally migrating tidal bar in front of a delta system: Esdolomada Member, Roda Formation, Tremp-Graus Basin, Spain: Sedimentology, v. 59, p. 356–378.

Pascoe, R., Hooper, R., Storhaug, K., and Harper, H., 1999, Evolution of extensional styles at the southern termination of the Nordland Ridge, Mid-Norway: a response to variations in coupling above Triassic salt. In: Fleet, A. J., and Boldy, S. A. R. (eds.), Petroleum Geology of Northwest Europe: Proceedings of the 5th Conference, Geological Society, London, p. 83–90.

Pedersen, T., Harms, J., Harris, N., Mitchell, R., and Tooby, K., 1989, The role of correlation in generating the Heidrun Field geological model. In: Collinson, J. D. (ed.), Correlation in Hydrocarbon Exploration: Norwegian Petroleum Society, Graham and Trotman, London, p. 327-338.

Pratt, L. J., 1990, The Physical Oceanography of Sea Straits: NATO ASI Series, Kluwer Academic, Dordrecht, v. 318, 587 p.

Price, S. P., and Whitham, A. G., 1997, Exhumed hydrocarbon traps in East Greenland: analogs for the Lower-Middle Jurassic play of Northwest Europe: AAPG Bulletin, v. 81, p. 196–221.

Prosser, S., 1993, Rift-related linked depositional systems and their seismic expression: Geological Society, London, Special Publication, v. 71, p. 35–66.

Quin, J. G., Zweigel, P., Eldholm, E., Hansen, O. R., Christoffersen, K. R., and Zaostrovski, A., 2010, Sedimentology and unexpected pressure decline: the HP/HT Kristin Field. In: Vining, S. C., and Pickering, S. C. (eds.), From Mature Basins to New Frontiers: Petroleum Geology Conference Series, Geological Society, London, v. 7, p. 419–429.

Ramberg, I. B., Bryhni, I., Nøttvedt, A., and Rangnes, K. (eds.), 2013. Landet blir til: Norges geologi: Norsk Geologisk Forening, Trondheim, 654 p.

Reineck, H. E., 1963, Sedimentgefüge im Bereich der südlichen Nordsee: Abhandlungen der Senckenbergischen Naturforschen Gesellschaft, v. 505, 138 p.

Reineck, H. E., and Singh, I. B., 1980, Depositional Sedimentary Environments, with Reference to Terrigenous Clastics. Springer-Verlag, Berlin, 549 p.

Reynaud, J. Y., Tessier, B., Proust, J. N., Dalrymple, R., Marsset, T., De Batist, M., Bourillet, J. F., and Lericolais, G., 1999, Eustatic and hydrodynamic controls on the architecture of a deep shelf sand bank (Celtic Sea): Sedimentology, v. 46, p. 703–721.

Roep, T. B., Beets, D., Dronkert, H., and Pagnier, H., 1979, A prograding coastal sequence of wave-built structures of Messinian age, Sorbas, Almeria, Spain: Sedimentary Geology, v. 22, p. 135–163.

Saggaf, M., and Nebrija, L., 2003, A fuzzy logic approach for the estimation of facies from wire-line logs: AAPG bulletin, v. 87, p. 1223–1240.

Schwarz, E., 2012, Sharp-based marine sandstone bodies in the Mulichinco Formation (Lower Cretaceous), Neuquén Basin, Argentina: remnants of transgressive offshore sand ridges: Sedimentology, v. 59, p. 1478–1508.

Seed, H. B., and Rahman, M., 1978, Wave-induced pore pressure in relation to ocean floor stability of cohesionless soils: Marine Georesources & Geotechnology, v. 3, p. 123–150.

Seidler, L., Steel, R., Stemmerik, L., and Surlyk, F., 2004, North Atlantic marine rifting in the Early Triassic: new evidence from East Greenland: Journal of the Geological Society of London, v. 161, p. 583–592.

Serra, O., 1984, Fundamentals of well-log interpretation: 1. The acquisition of logging data: Developments of Petroleum Science, 15A, 354 pp.

Short, A., 1991, Macro-meso tidal beach morphodynamics: an overview: Journal of Coastal Research, v. 7, p. 417–436.

Simpson, E. L., 1991, An exhumed, Lower Cambrian tidal flat: the Antietam Formation, central Virginia, USA. In: Smith, D. G., Reinson, G. E., Zaitlin, B. A., and Rahmani, R. A. (eds.), Clastic Tidal Sedimentology: Canadian Society of Petroleum Geologists, Memoir 16, p. 123–134.

Skilbrei, J. R., Olesen, O., Osmundsen, P. T., Kihle, O., Aaro, S., and Fjellanger, E., 2002, A study of basement structures and onshore-offshore correlations in Central Norway: Norwegian Journal of Geology, v. 82, p. 263–280.

Skogseid, J., Planke, S., Faleide, J. I., Pedersen, T., Eldholm, O., and Neverdal, F., 2000, NE Atlantic continental rifting and volcanic margin formation. In: Nøttvedt, A. (ed.), Dynamics of the Norwegian Margin: Geological Society, London, Special Publication, v. 167, p. 295–326.

Smith, D. G., Reinson, G. E., Zaitlin B. A., and Rahmani, R. A. (eds.), 1991, Clastic Tidal Sedimentology: Canadian Society of Petroleum Geologists, Memoir 16, 387 p.

Snedden, J. W., and Dalrymple, R. W., 1999, Modern shelf sand ridges: from historical perspective to a unified hydrodynamic and evolutionary model. In: Bergman, K. M., and Snedden, J. W. (eds.), Isolated Shallow Marine Sand Bodies: Sequence Stratigraphic Analysis and Sedimentological Perspectives: SEPM Special Publication, v. 64, p. 13–28.

Snedden, J. W., Tillman, R. W., and Culver, S. J., 2011, Genesis and evolution of a mid-shelf, storm-built sand ridge, New Jersey continental shelf, USA: Journal of Sedimentary Research, v. 81, p. 534–552.

Spencer, A., Birkeland, Ø., and Koch, J.-O., 1993, Petroleum geology of the proven hydrocarbon basins, offshore Norway: First Break, v. 11, 161–176.

Stanistreet, I. G., 1989, Trace fossil associations related to facies of an upper Ordovician low wave energy shoreface and shelf, Oslo, Asker district, Norway: Lethaia, v. 22, p. 345–357.

Surlyk, F., 1990, Timing, style and sedimentary evolution of Late Palaeozoic–Mesozoic extensional basins of East Greenland. In: Hardman, R. P. F., and Brooks, J. (eds.), Tectonic events responsible for Britain's oil and gas reserves: Geological Society, London, Special Publication, v. 55, p. 107–125.

Surlyk, F., 2003, The Jurassic of East Greenland: a sedimentary record of thermal subsidence, onset and culmination of rifting. In: Ineson, J. R., and Surlyk, F. (eds.), The Jurassic of Denmark and Greenland: Geological Survey of Denmark and Greenland Bulletin, v. 1, p. 659–722.

Surlyk, F., Clemmensen, L. B., and Larsen, H. C., 1981, Post-Paleozoic evolution of the East Greenland continental margin. In: Kerr, J. W., and Ferguson, A. J. (eds.), Geology of the North Atlantic Borderlands: Canadian Society of Petroleum Geologists, Memoir 7, p. 611–645.

Surlyk, F., and Clemmensen, L. B., 1983, Rift propagation and eustacy as controlling factors during Jurassic inshore and shelf sedimentation in northern East Greenland: Sedimentary Geology, v. 34, p. 119–43.

Svela, K. E., 2001, Sedimentary facies in the fluvial-dominated Åre Formation as seen in the Åre 1 Member in the Heidrun Field. In: Martinsen, O. J., and Dreyer, T. (eds.), Sedimentary Environments Offshore Norway – Palaeozoic to Recent: Norwegian Petroleum Society, Special Publication, v. 10, p. 87–102.

Swiecicki, T., Gibbs, P. B., Farrow, G. E., and Coward, M. P., 1998, A tectonostratigraphic framework for the Mid-Norway region: Marine and Petroleum Geology, v. 15, p. 245–276.

Swift, D. J. P., 1975, Tidal sand ridges and shoal-retreat massifs: Marine Geology, v. 18, p. 105–134.

Swift, D. J. P., and Field, M. E., 1981, Evolution of a classic sand ridge field: Maryland sector, North American inner shelf: Sedimentology, v. 28, p. 461–482.

Swift, D. J. P., Freeland, G. and Young, R., 1979, Time and space distribution of megaripples and associated bedforms, Middle Atlantic Bight, North American Atlantic Shelf: Sedimentology, v. 26, p. 389–406.

Sztanó, O., and Boer, P. L., 1995, Basin dimensions and morphology as controls on amplification of tidal motions (the Early Miocene North Hungarian Bay): Sedimentology, v. 42, p. 665–682.

Tang, H., White, C., Zeng, X., Gani, M., and Bhattacharya, J., 2004, Comparison of multivariate statistical algorithms for wireline log facies classification: AAPG Annual Meeting Abstract, v. 88, 13 pp.

Taylor, A. M., and Goldring, R., 1992, Description and analysis of bioturbation and ichnofabric: Journal of the Geological Society of London, v. 150, p. 141–148.

Ter Voorde, M., Ravnås, R., Færseth, R., and Cloetingh, S., 1997, Tectonic modelling of the Middle Jurassic syn-rift stratigraphy in the Oseberg–Brage area, northern Viking Graben: Basin Research, v. 9, p. 133–150.

Thomas, M. A., and Anderson, J. B., 1994, Sea-level controls on the facies architecture of the Trinity/Sabine incised-valley system, Texas continental shelf. In: Dalrymple, R. W., Boyd, R., and Zaitlin, B. A. (eds.), Incised-Valley Systems: Origin and Sedimentary Sequences: SEPM Special Publication, v. 51, p. 63–82.

Torsvik, T. H., Carlos, D., Mosar, J., Cocks, L. R. M., and Malme, T. N., 2002, Global Reconstructions and North Atlantic Paleogeography 440 Ma to Recent. In: Eide, E. A. (coord.), BATLAS – Mid-Norway plate reconstruction atlas with global and Atlantic perspectives: Geological Survey of Norway, pp. 18–39.

Trentesaux, A., Stolk, A., and Berné, S., 1999, Sedimentology and stratigraphy of a tidal sand bank in the southern North Sea: Marine Geology, v. 159, p. 253–272.

Van der Molen, J., and De Swart, H. E., 2001, Holocene tidal conditions and tide-induced sand transport in the southern North Sea: Journal of Geophysical Research, v. 106, p. 9339–9362

Van Wagoner, J. C., Mitchum, R. M., Campion, K. M., and Rahmanian, V. D., 1990, Siliciclastic sequence stratigraphy in well logs, cores, and outcrops: concepts for high-resolution correlation of time and facies: American Association of Petroleum Geologists, Methods in Exploration Series, v. 7, 55 pp.

Walker, R. G., 1984a, General introduction: facies, facies sequences and facies models. In: Walker, R., G. (ed.), Facies Models, 2nd edn.: Geological Association of Canada, Geoscience Canada Reprint Series, v. 1, p. 1–9.

Walker, R.G., 1984b, Shelf and shallow marine sands. In: Walker, R., G. (ed.), Facies Models, 2nd edn.: Geological Association of Canada, Geoscience Canada Reprint Series, v. 1, p. 141–170.

Whitham, A. G., Price, S. P., Koraini, A. M., and Kelly, S. R. A., 1999, Cretaceous (post-Valanginian) sedimentation and rift events in NE Greenland (71–77 degrees N). In: Fleet, A. J., and Boldy, S. A. R. (eds.), Petroleum Geology of Northwest Europe: Proceedings of the 5th Conference, Geological Society, London, pp. 325–336.

Withjack, M. O., Olson, J., and Peterson, E., 1990, Experimental models of extensional forced folds: AAPG Bulletin, v. 74, p. 1038–1054.

Wong, P., Jian, F., and Taggart, I., 1995, A critical comparison of neural networks and discriminant analysis in lithofacies, porosity and permeability predictions: Journal of Petroleum Geology, v. 18, p. 191–206.

Yang, C.-S., and Nio, S.-D., 1989, An ebb-tide delta depositional model—a comparison between the modern Eastern Scheldt tidal basin (southwest Netherlands) and the Lower Eocene Roda Sandstone in the southern Pyrenees (Spain): Sedimentary Geology, v. 64, p. 175–196.

Yielding, G., 1990, Footwall uplift associated with Late Jurassic normal faulting in the northern North Sea: Journal of the Geological Society of London, v. 147, p. 219–222.

Young, H. R., and Rosenthal, L. R. P., 1991, Stratigraphic framework of the Mississippian Lodgepole Formation in the Virden and Daly oilfields of Southwestern Manitoba. In: Christopher, J. E. and Haidl, F. M. (eds.), Sixth International Williston Basin Symposium: Saskatchewan Geological Society Special Publication, p. 113–122.

Ziegler, P. A., 1988, Evolution of the Arctic–North Atlantic and the Western Tethys: Tulsa, Oklahoma, American Association of Petroleum Geologists, Memoir 43, 198 p.

APPENDIX:

Sedimentological well-core logs

LEGEND CORE DESCRIPTION
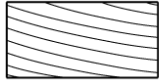
Planar cross-stratification
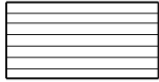
Planar parallel stratification

Ripple cross-lamination
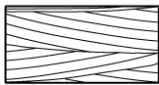
Trough cross-stratification

Hummocky cross-stratification
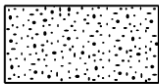
Massive sandstone

Current ripple

Climbing ripples

Wave ripple

Bioturbation

Bioturbation grade

Plant detritus

Slump
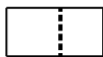
Seal peal

No core

Mud-draped foreset

FACIES COLOUR CODE

S_{CS}: Sandstone with planar or trough cross-stratification

S_{RCL}: Sandstone with ripple cross-lamination

S_{HCS}: Sandstone with hummocky cross-stratification

S_{PPS}: Sandstone with planar parallel stratification

S_{M1}: Massive sandstone

S_{M2}: Massive, highly bioturbated sandstone

BIOTURBATION GRADE

Grade	Classification	Visual Representation
0	Bioturbation absent	
1	Sparse bioturbation, bedding distinct, few discrete traces	
2	Uncommon bioturbation, bedding distinct, low trace density	
3	Moderate bioturbation, bedding boundaries sharp, traces discrete, overlap rare	
4	Common bioturbation, bedding boundaries indistinct, high trace density with overlap common	
5	Abundant bioturbation, bedding completely disturbed (just visible)	
6	Complete bioturbation, total biogenic homogenization of sediment	

From Bann (2004), based on original concepts
by Reineck (1963) and Taylor and Goldring (1993)

Well 6406/2-6

Logging scale 1:20
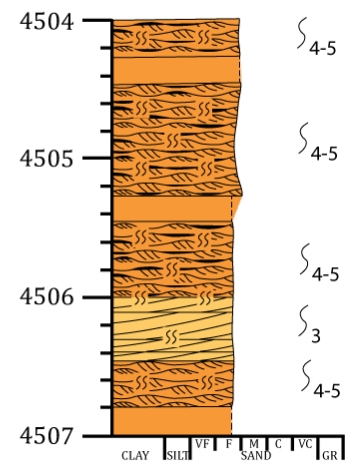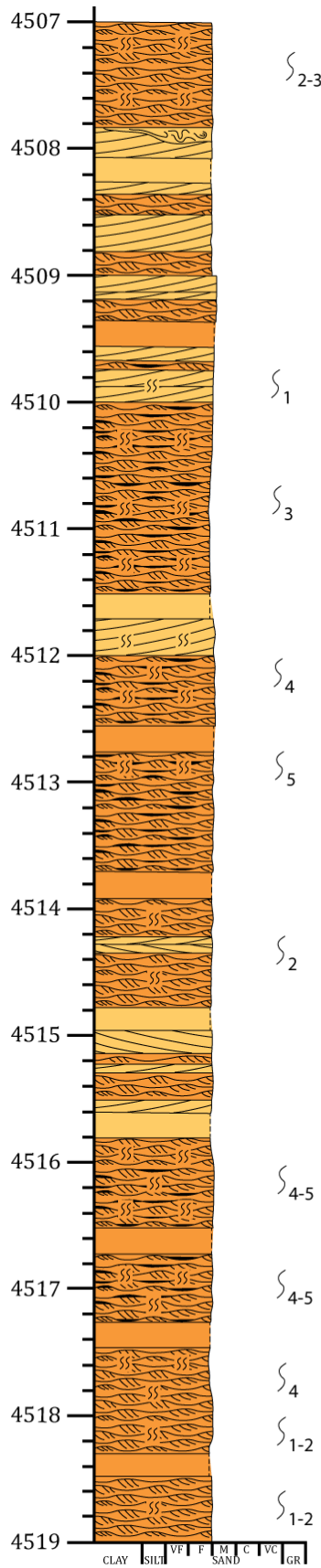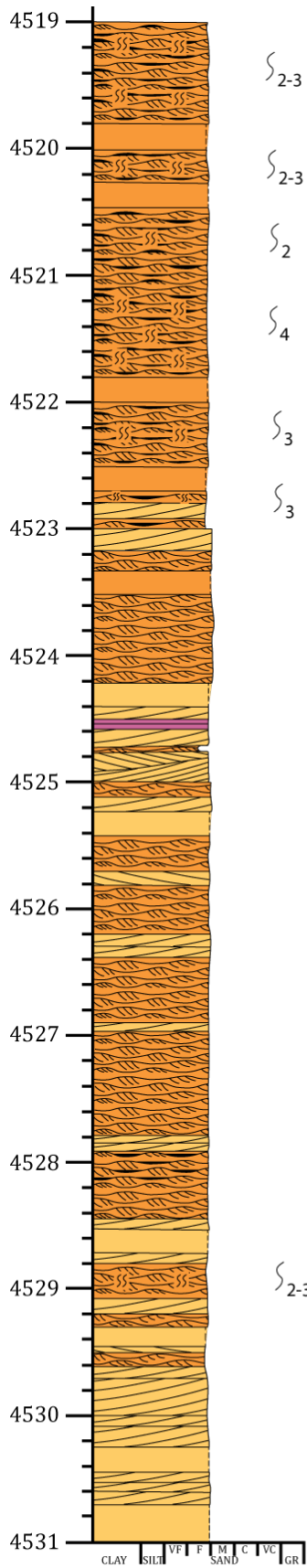
Well 6406/5-1 T2

Logging scale 1:20
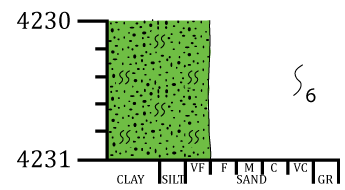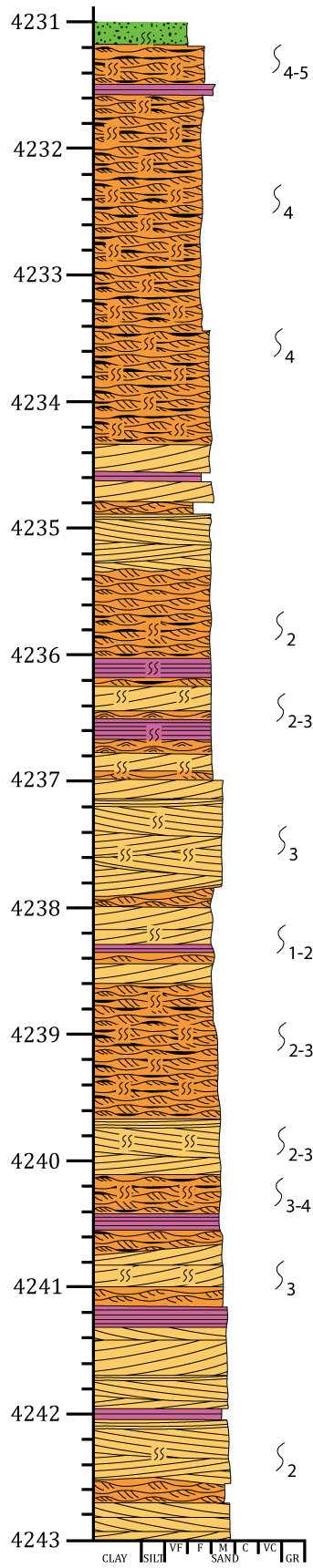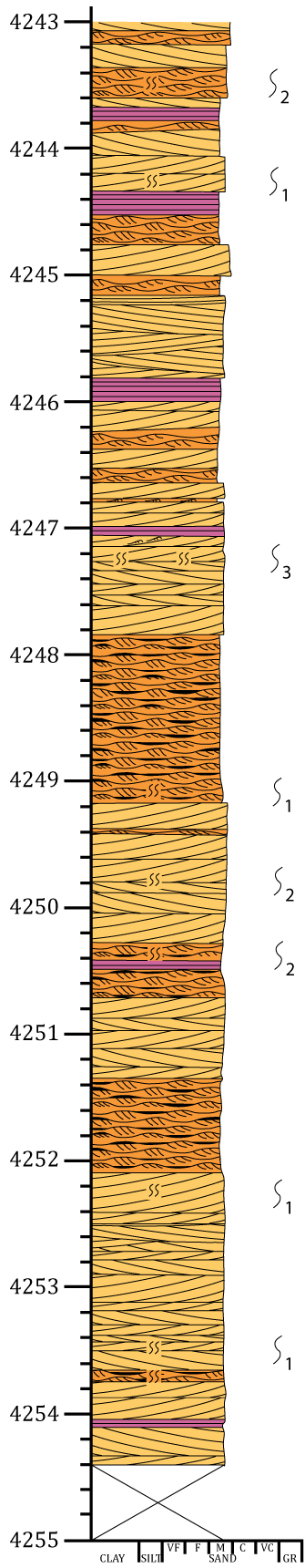
Well 6407/1-3

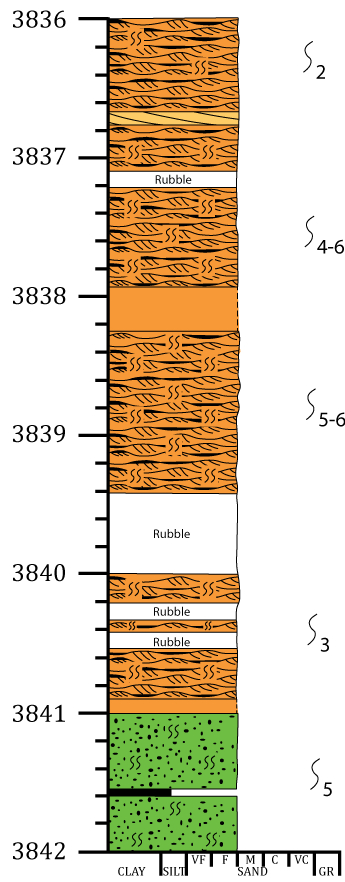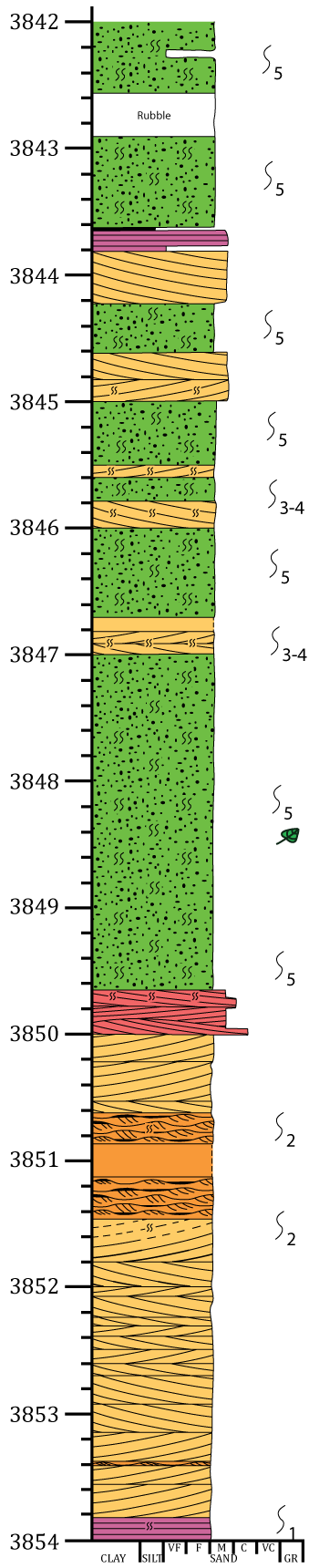Logging scale 1:20
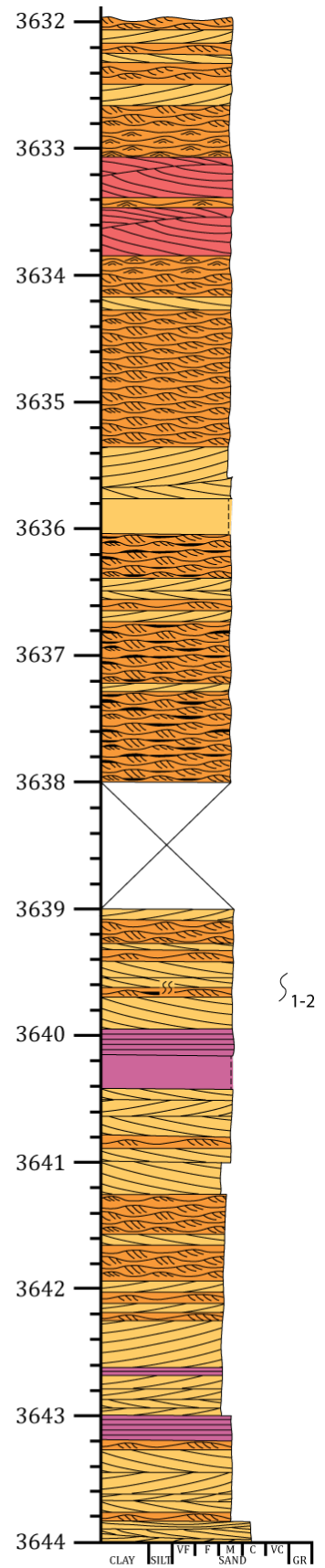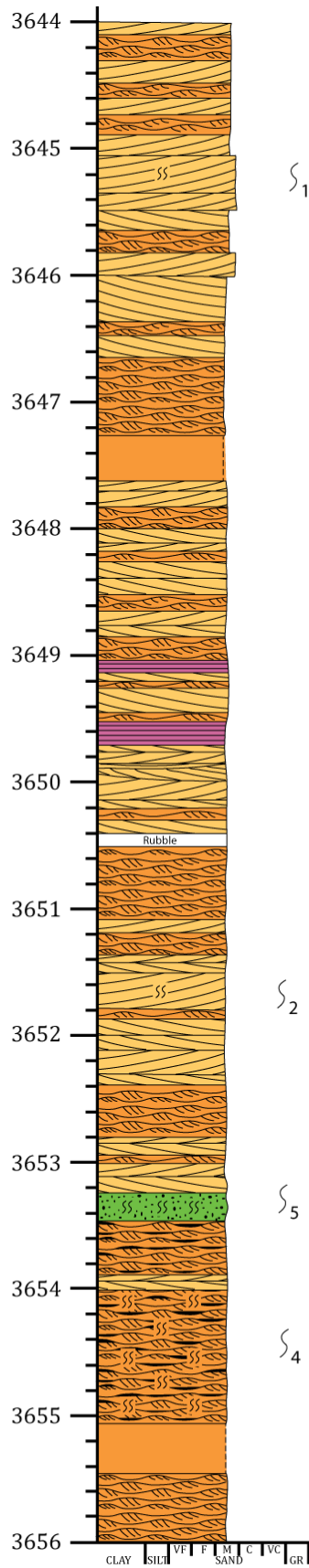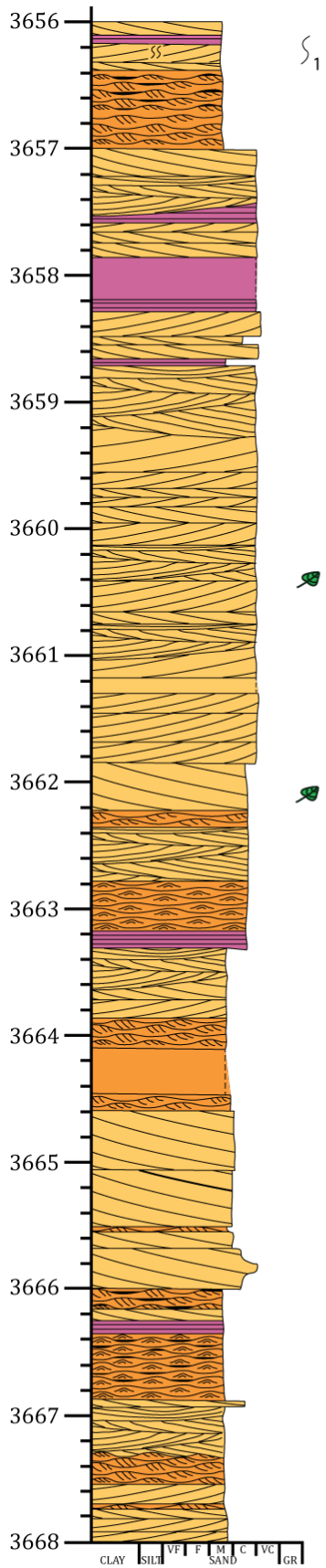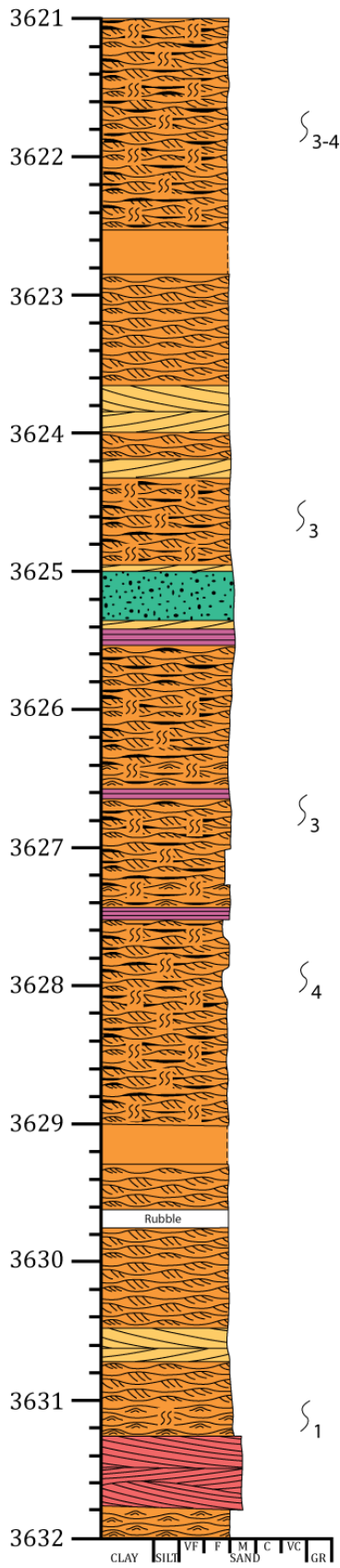
Well 6407/1-4

Logging scale 1:20
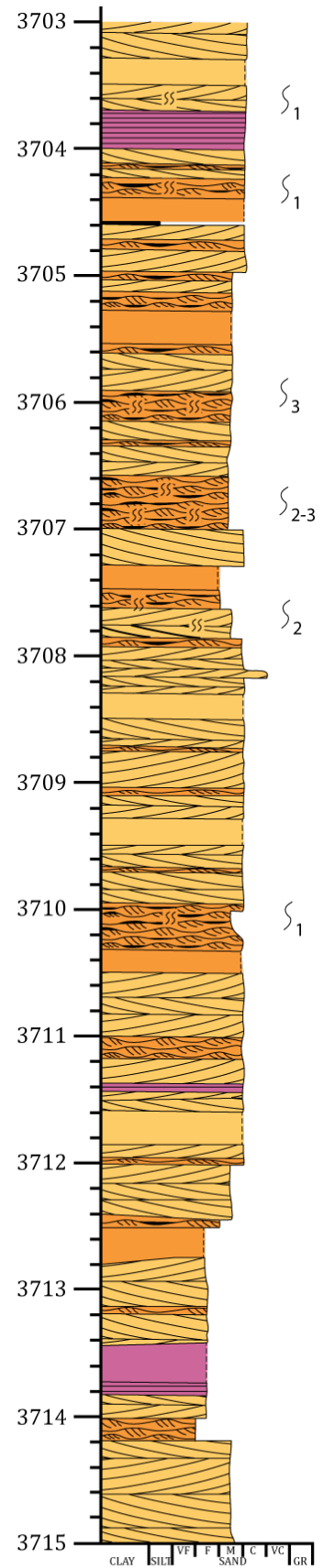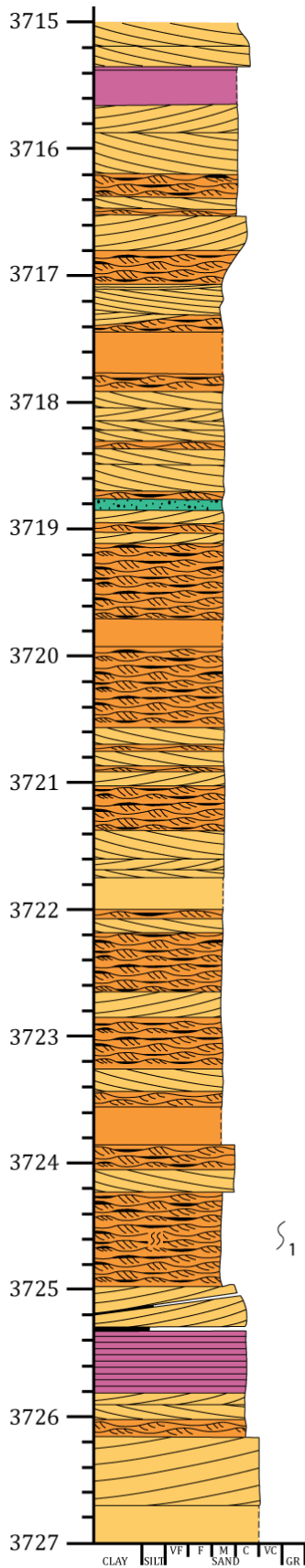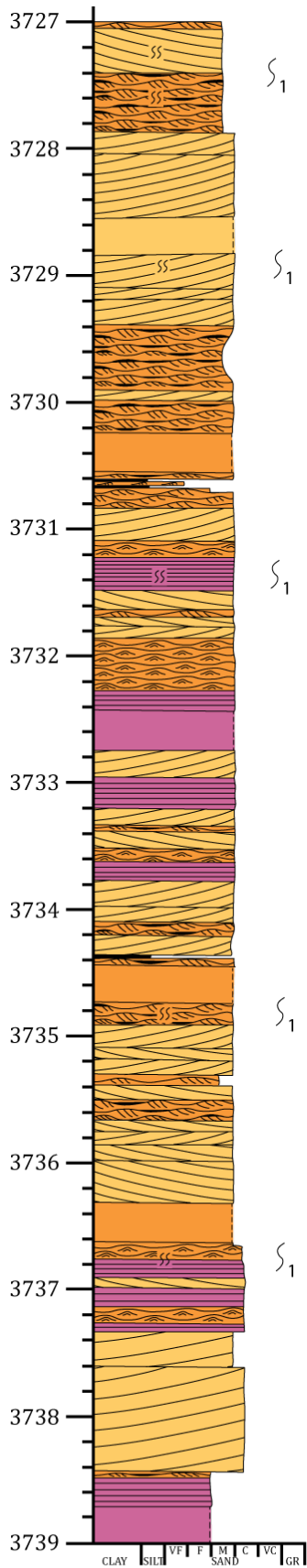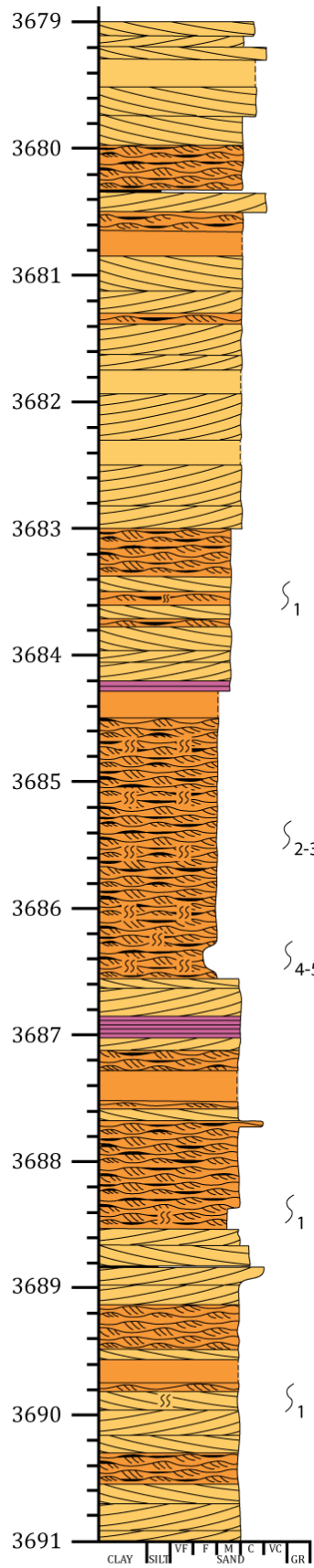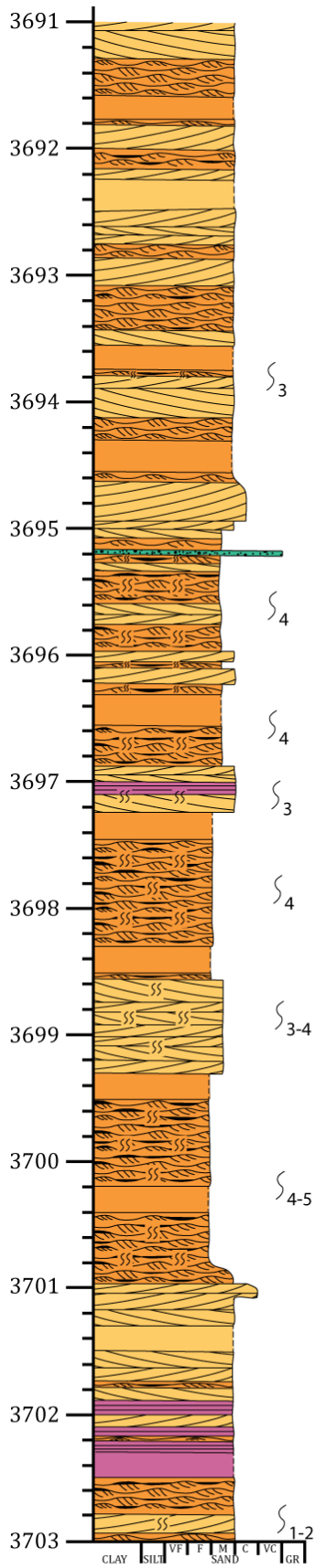
Well 6506/9-2 S

Logging scale 1:20
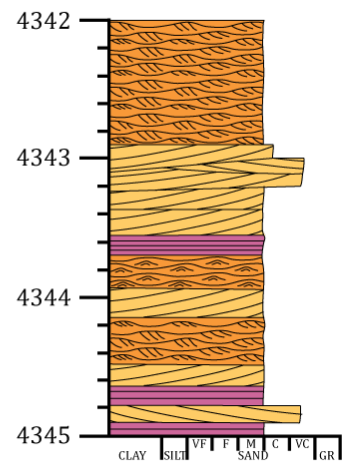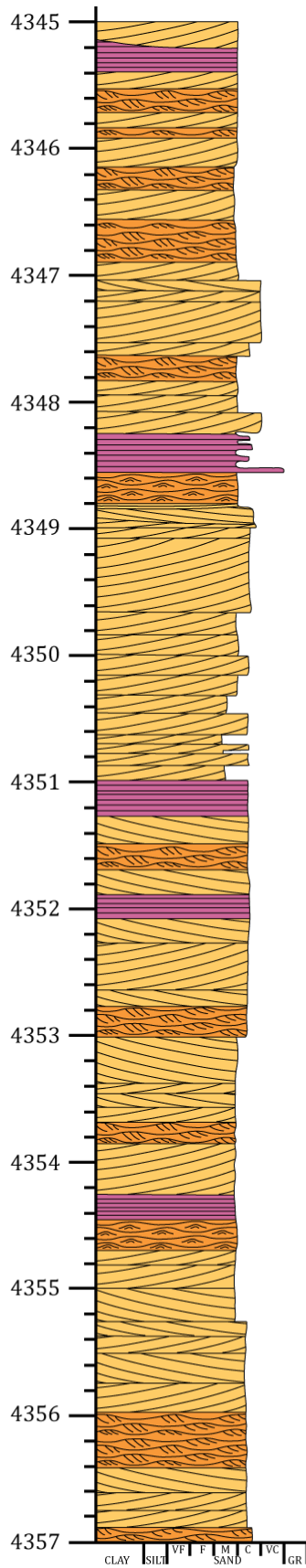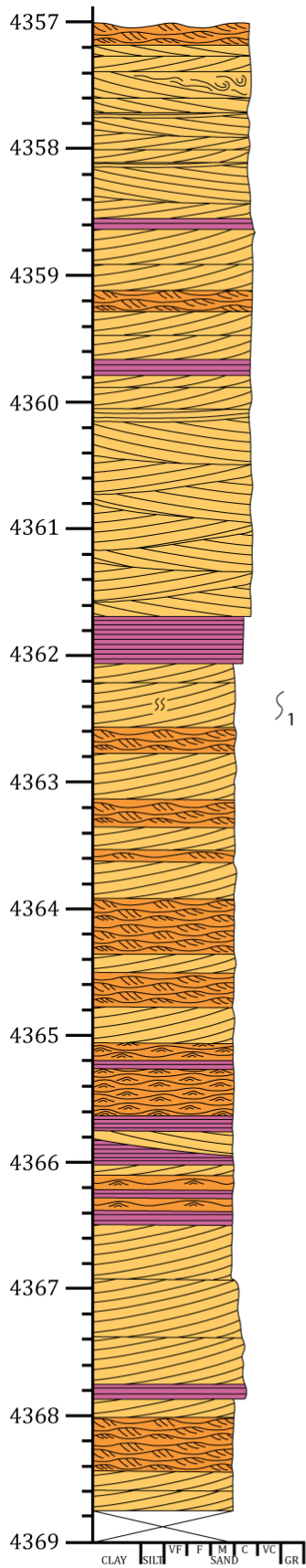
Well 6506/12-3

Logging scale 1:20

Base Garn
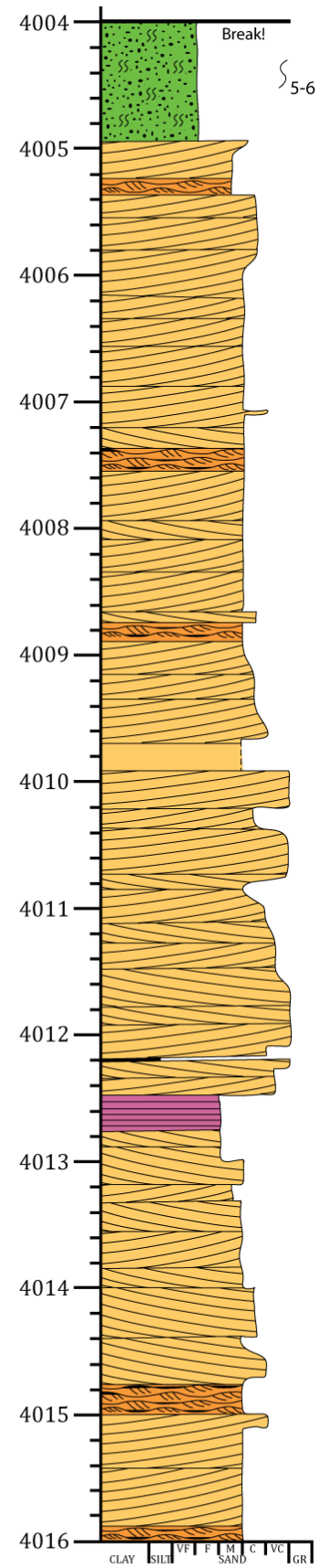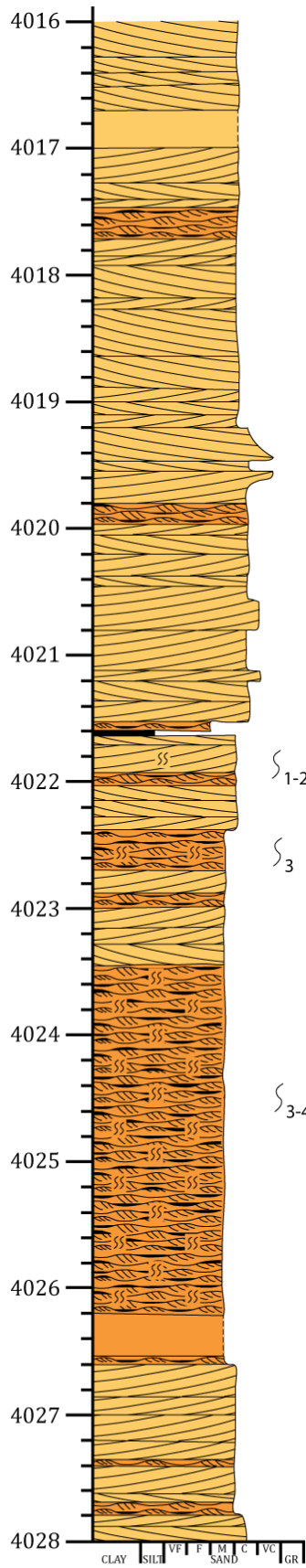Top Not
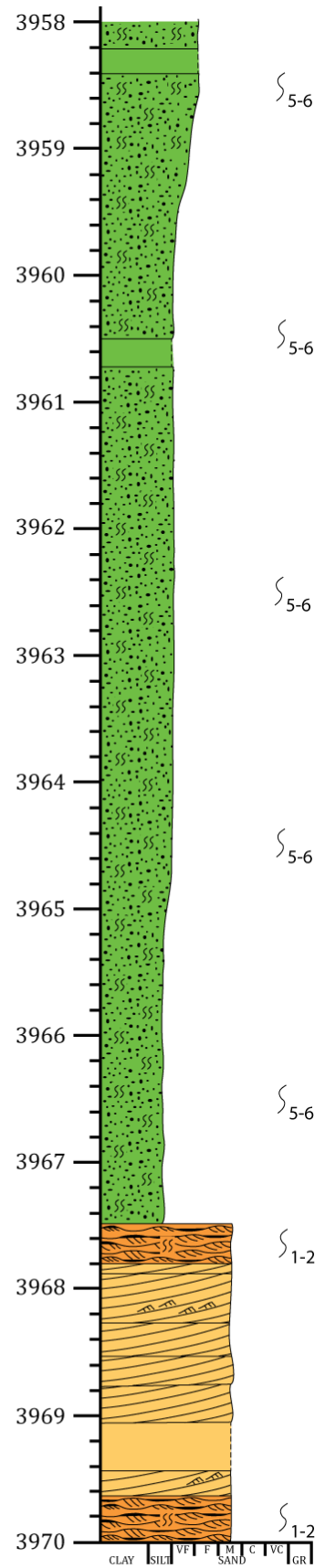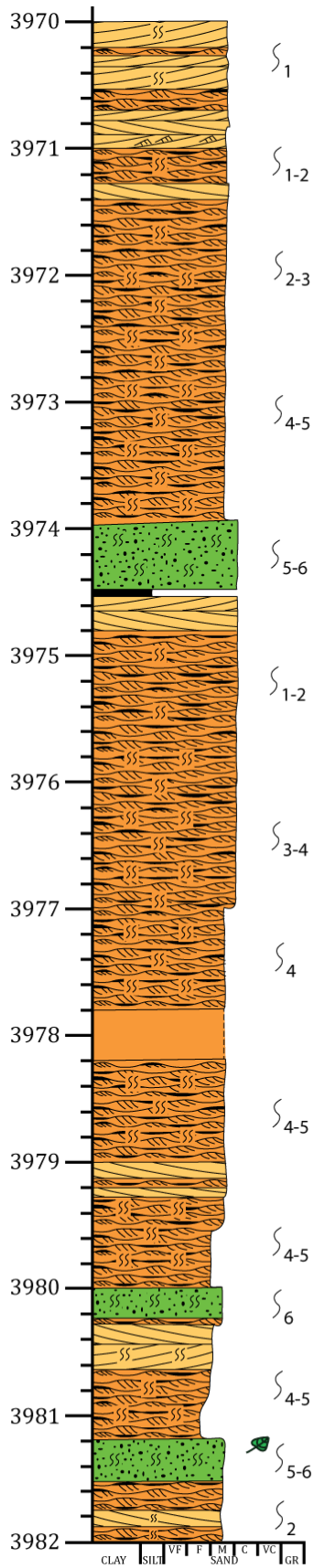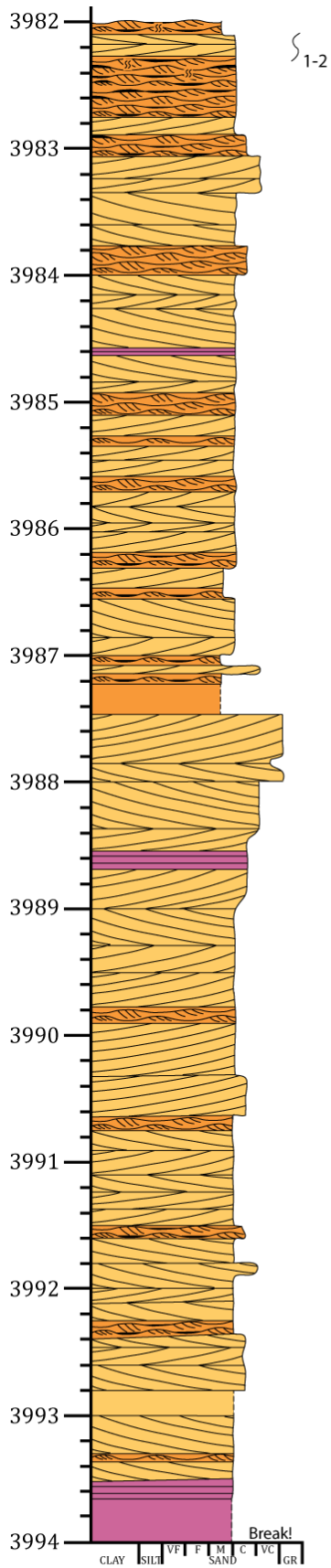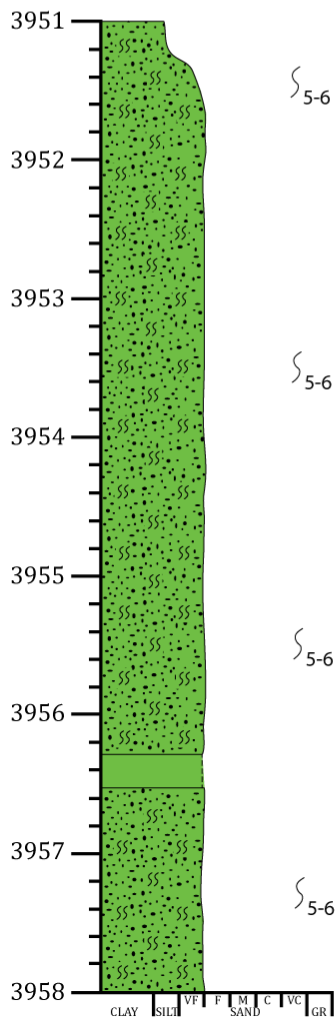
Rubble

Rubble

Rubble

0-4

CLAY SILT VF F M C VC GR
SAND

CLAY SILT VF F M C VC GR
SAND

CLAY SILT VF F M C VC GR
SAND

Left column (depth scale 3842–3854):

3842

5

Rubble

3843

5

3844

5

3845

5

5

3-4

3846

5

3847

3-4

3848

5

3849

5

5

3850

2

3851

2

3852

3853

3854   1

CLAY | SILT | VF | F | M | C | VC | SAND | GR

Right column (depth scale 3836–3842):

3836

2

3837

Rubble

3838   4-6

3839   5-6

Rubble

3840

Rubble

Rubble

3

3841

5

3842

CLAY | SILT | VF | F | M | C | VC | SAND | GR

103

Well 6506/12-5

Logging scale 1:20

3951

3952
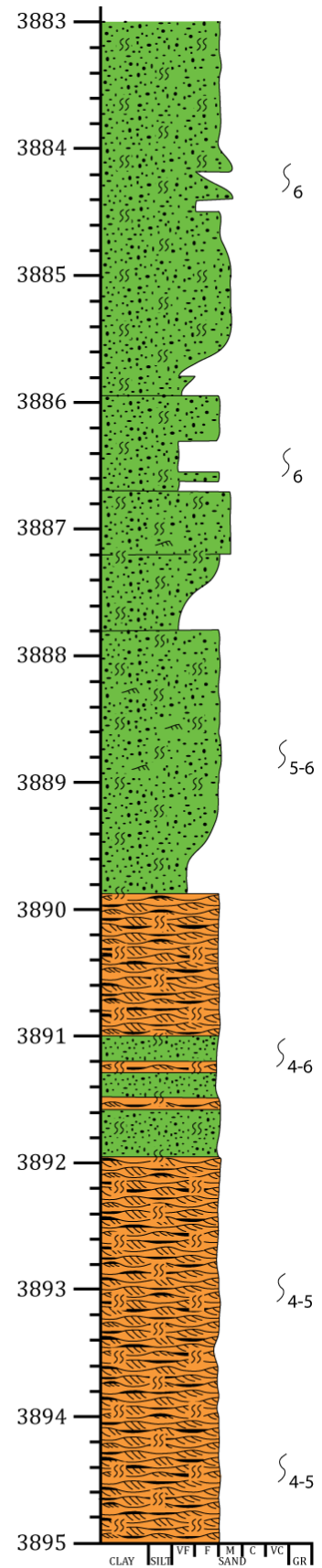
3953

3954

3955

3956

3957

3958

ζ_{5-6}

ζ_{5-6}

ζ_{5-6}

ζ_{5-6}

CLAY SILT VF F M C VC GR
SAND
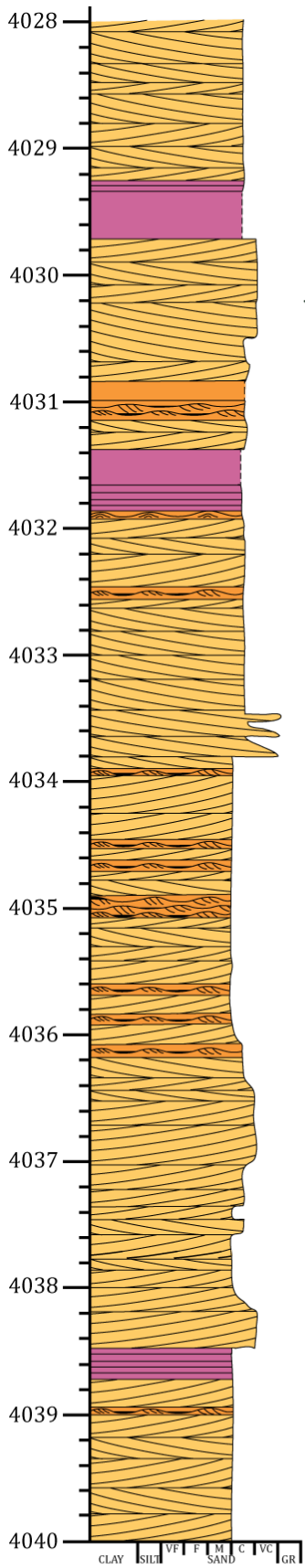
Well 6506/12-8

Logging scale 1:20

3907

3908

3909

3910

3911

3912

3913

3914

3915

3916

3917

Rubble

3918

3919

CLAY SILT VF F M C VC GR
SAND

⌇5

⌇4

3895

3896

3897

3898

3899

3900

3901

3902

3903

3904

3905

3906

3907

CLAY SILT VF F M C VC GR
SAND

⌇4-5

⌇5-6

⌇5-6

⌇5-6

⌇6

⌇3

⌇4

⌇4-5

⌇5

3883

3884

3885

3886

3887

3888

3889

3890

3891

3892

3893

3894

3895

CLAY SILT VF F M C VC GR
SAND

⌇6

⌇6

⌇5-6

⌇4-6

⌇4-5

⌇4-5

CLAY SILT VF F M C VC GR
SAND
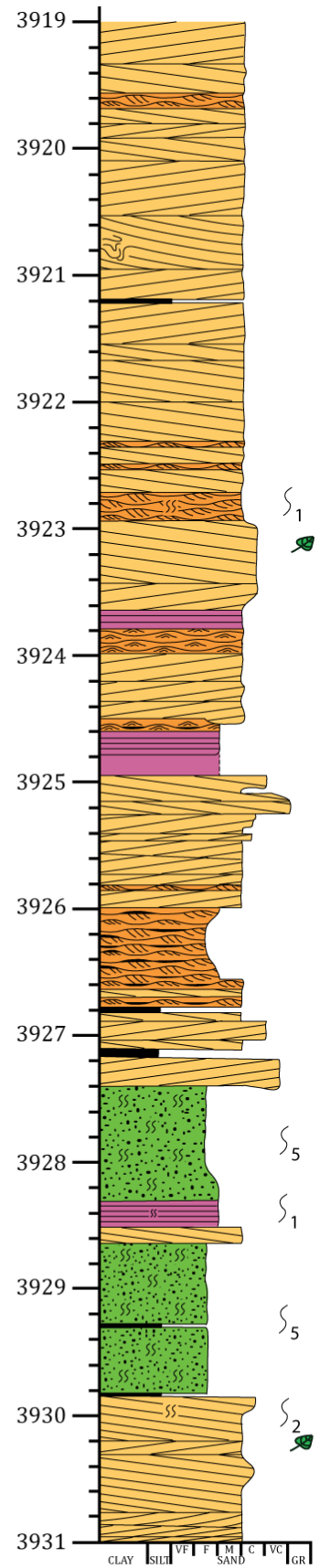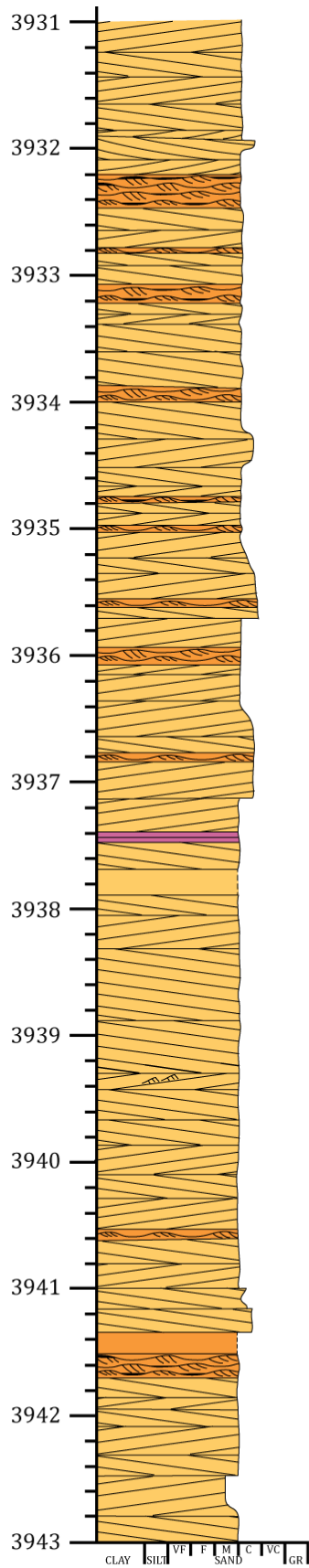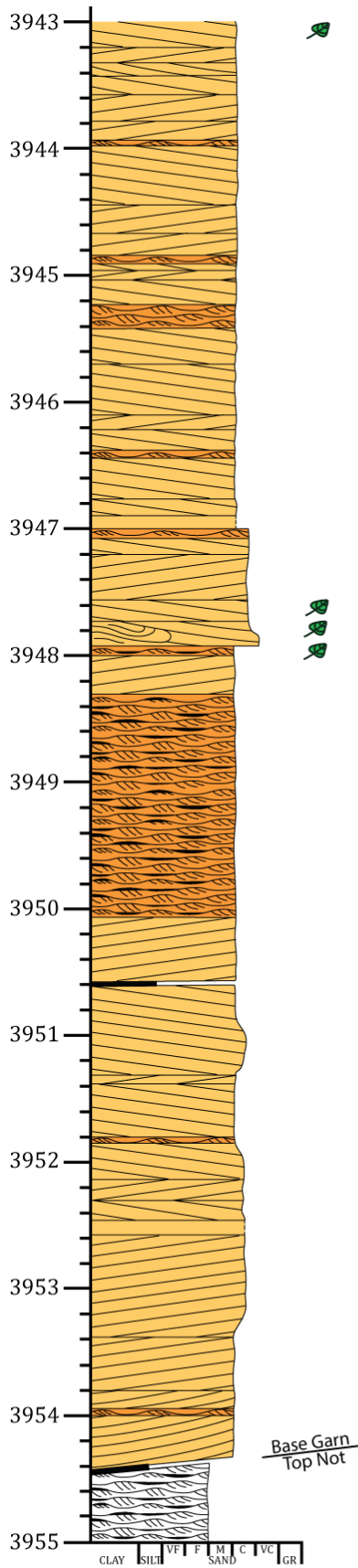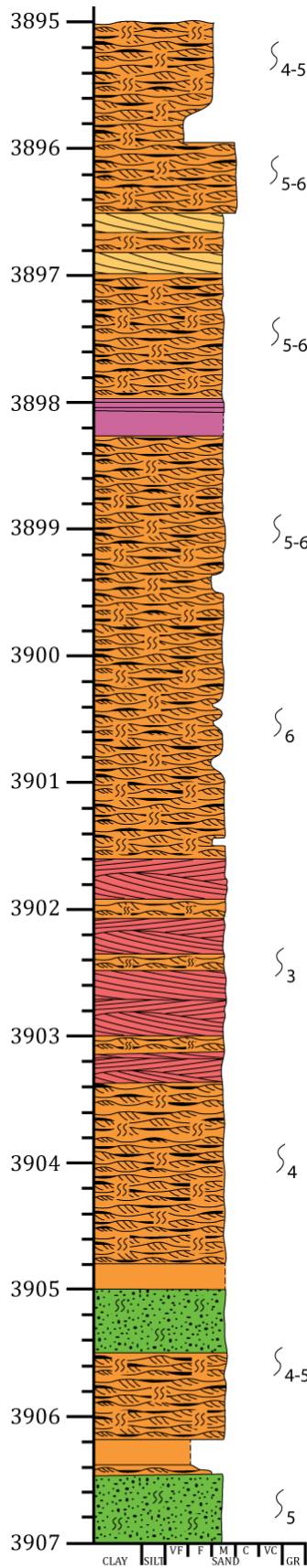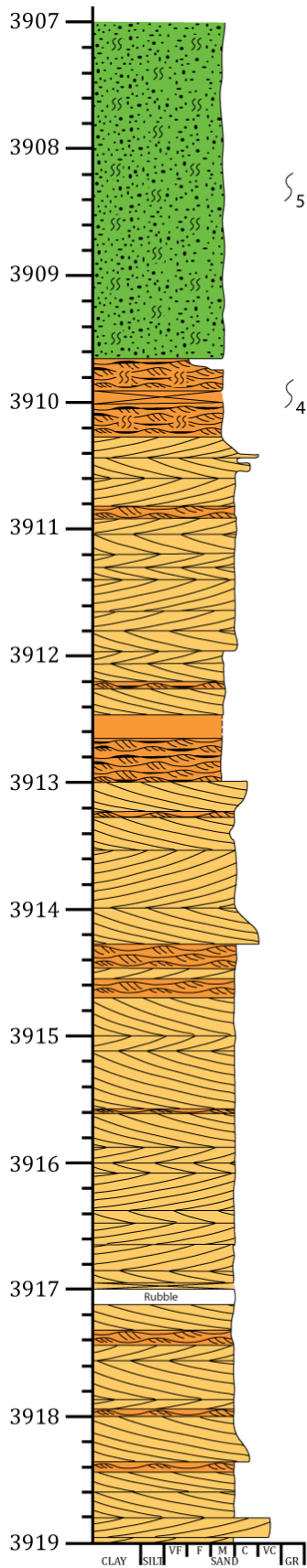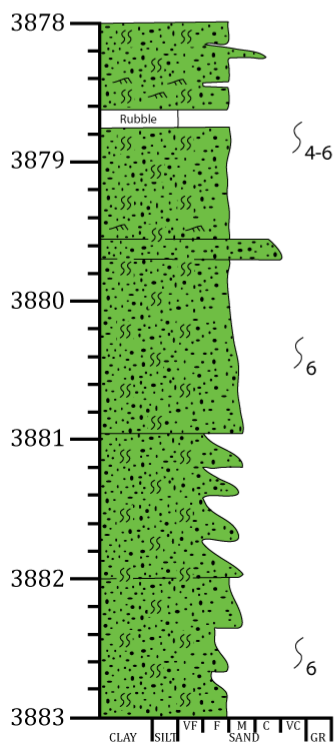
Well 6507/11-8

Logging Scale 1:20